INFLUENCE OF MIXING METHODS ON THE NO_X REDUCTION CAPABILITY AND ELECTRICAL PROPERTIES OF PHOTOCATALYTIC CEMENTITIOUS SYSTEMS

KARIŞTIRMA METOTLARININ FOTOKATALİTİK BAĞLAYICILI SİSTEMELERİN NO_X İNDİRGEME KABİLİYETİNE VE ELEKTRİKSEL ÖZELLİKLERİNE ETKİSİ

SAMED BAY

PROF. DR. MUSTAFA ŞAHMARAN
Supervisor

Submitted to
Graduate School of Science and Engineering of Hacettepe University
as a Partial Fulfillment to the Requirements
for be Award of the Degree of Master of Science
in Civil Engineering

2020

ABSTRACT

INFLUENCE OF MIXING METHODS ON THE NO_X REDUCTION CAPABILITY AND ELECTRICAL PROPERTIES OF PHOTOCATALYTIC CEMENTITIOUS SYSTEMS

Samed BAY

Master of Science, Department of Civil Engineering
Supervisor: Prof. Dr. Mustafa ŞAHMARAN
September 2020, 85 pages

Nitrogen Oxides (NO_x) are a group of highly reactive and hazardous gases encompassing compounds ranging from nitrous to nitric acid. Air pollution caused by nitrogen oxides that are emitted to the atmosphere by industrial corporations and vehicles has reached worrisome levels, especially in crowded cities. To eliminate the adverse effects of these gases, titanium dioxide (TiO_2) is used worldwide as a photocatalyst due to its high efficiency in oxidization of NO_x. Incorporating TiO_2 into cement-based composites gives them photocatalytic capability: uniform and stable dispersion of TiO_2 throughout the matrix is an indisputable requirement for improved photocatalytic efficiency. The main purpose of this study is to investigate the effects of different mixing techniques and surfactant materials on the dispersion of high dosage nano-TiO_2 particles (5% of total weight of binder materials) throughout cement-based materials, with the goal of producing cost-effective cementitious systems, more feasible mixing methods, and ensuring proper dispersion of nano-TiO_2. Five different mixing methods were proposed to achieve uniform distribution of the nano-TiO_2. They were each implemented using different mixing procedures, equipment and surfactants. The performance of each mixing method was evaluated based on photocatalytic performance, electrical impedance (EI), compressive strength and microstructural analysis. Test results showed evidence of the significantly positive effect of polyacrylic acid (PAA) on the dispersion of nano-TiO_2. In general, the highest dispersion occurred with ultrasonication and binary utilization of polycarboxylate ether-based plasticizer (PCE) and PAA. The EI test was a highly effective evaluation method for homogeneous distribution of conductive nano particles throughout the matrix. Results also showed a significant relationship between electrical performance and nitric oxide (NO) degradation of composites, and electrical properties of composites are able to provide a reliable estimate of the photocatalytic efficiency of them.

Keywords: Titanium dioxide (TiO_2), Photocatalytic activity, Cement-based systems, Mixing methods, Surfactant materials.

ÖZET

KARIŞTIRMA METOTLARININ FOTOKATALİTİK BAĞLAYICILI SİSTEMELERİN NO_X İNDİRGEME KABİLİYETİNE VE ELEKTRİKSEL ÖZELLİKLERİNE ETKİSİ

Samed BAY

Yüksek Lisans, İnşaat Mühendisliği Bölümü
Tez Danışmanı: Prof. Dr. Mustafa ŞAHMARAN
Eylül 2020, 85 sayfa

Toksik hava kirleticileri olarak kabul edilen nitrojen oksitler (NO_X), nitröz oksitten nitrik aside kadar değişen bileşikleri içeren yüksek derecede reaktif ve tehlikeli gazlar grubudur. Özellikle kalabalık şehirlerde sanayi kuruluşlarından ve araçlardan bu gazların salınımı ciddi seviyelere ulaşmıştır. Bu gazların olumsuz etkilerini ortadan kaldırmak için titanyum dioksit (TiO_2), genel olarak NO_x oksidasyonundaki yüksek etkinliği nedeniyle bir fotokatalizör olarak kullanılmaktadır. TiO_2'yi çimento esaslı kompozitlerde kullanmak, sisteme fotokatalitik yetenek kazandırır: TiO_2'nin matris içerisinde homojen ve kararlı dağılımı, gelişmiş fotokatalitik verimlilik için tartışılmaz bir gerekliliktir. Bu çalışmanın temel amacı uygun maliyetli çimentolu sistemlerin daha uygulanabilir karıştırma metotlarının ve TiO_2'nin uygun dağılımının sağlanması hedeflenerek çimento esaslı malzemelerde yüksek dozajlı nano-TiO_2(bağlayıcı malzemelerin toplam ağırlığının %5'i) dağılımı üzerinde farklı karıştırma teknikleri ve sürfaktan malzemelerin etkilerinin incelenmesidir. Nano-TiO_2'nin düzenli dağılımını sağlamak için beş farklı karıştırma yöntemi önerilmiştir. Söz konusu yöntemler farklı karıştırma prosedürleri, ekipman ve sürfaktan kullanılarak uygulandı. Her bir karıştırma yönteminin performansı, fotokatalitik performans, elektriksel dirençleri (EI), basınç dayanım ölçümleri ve mikroyapısal analize dayalı olarak değerlendirildi. Test sonuçları, poliakrilik asidin

(PAA) nano-TiO_2 dağılımı üzerindeki dikkat çekici olumlu etkisini açıkça göstermektedir. Genel olarak, en yüksek dağılım, ultrasonikasyon ve polikarboksilat eter bazlı akışkanlaştırıcı (PCE) ve PAA'nın birlikte kullanımıyla meydana gelmiştir. Elde edilen sonuçlar ışığında, EI testinin, matris boyunca iletken nanopartiküllerin homojen dağılımını belirlemede oldukça etkili bir değerlendirme yöntemi olduğu açıkça ifade edilebilir. Sonuçlar, ayrıca elektriksel performans ile kompozitlerin elektriksel özellikleri azot monoksitlerin (NO) oksidasyonu arasında önemli bir ilişkisini göstermiş ve kompozitlerin elektriksel özelliklerinin fotokatalitik verimliliklerinde güvenilir bir değerlendirme sağlayabilir.

Anahtar Kelimeler: Titanyum dioksit (TiO_2), Fotokatalitik aktivite, Çimento Bağlayıcılı Sistemler, Karışım Metotları, Sürfaktan Malzemeler.

ACKNOWLEDGEMENT

First of all, I offer my deepest gratitude to my valuable supervisor Prof. Mustafa Şahmaran who does not spare his help since the beginning of my dissertation study. I would also like to offer my great thanks to my colleagues who were with me and exchange ideas during my experimental studies, professors and, the jury members who participated in my thesis jury.

I owe thanks to TUBITAK for its financial support lent during my dissertation studies which were completed under Turkey's Scientific and Technological Research (TUBITAK) MAG-118M197 number research project.

Lastly, I would like to express my eternal gratitude to my family for their unwavering support, who helped me come to this day throughout my entire education life.

Samed BAY
September 2020, Ankara

TABLE OF CONTENTS

LIST OF FIGURE

LIST OF TABLE

SYMBOLS AND ABBREVIATIONS

Abbreviations

Å	Angstrom
m^2	Square meter
mm	Millimeter
cm	Centimeter
cm^2	Square Centimeter
MPa	Megapascal
mV	Milivolt
nm	Nanometer
µm	Micrometer
NO	Nitrogen Monoxide
NO_2	Nitrogen Dioxide
NO_x	Nitrogen Oxide
ppb	Parts Per Billion
ppm	Parts Per million
UV	Ultraviolet
eV	Electronvolt
SEM	Scanning Electron Microscopy
SO_2	Sulfur Dioxide
SO_3	Sulfur Trioxide
Al_2O_3	Aluminum oxide
ZnO	Zinc oxide
TiO_2	Titanium dioxide
SiO_2	Silicon dioxide
Fe_3O_4	Iron Oxide
E_{bg}	Band Gap
SiO_2	Silicon dioxide
Fe_3O_4	Iron Oxide
h^+_{VB}	Holes of Valence Band
e^-_{CB}	Electrons of Conduction Band
CT	Computed Tomograph

1. INTRODUCTION

Cement is one of the most used construction materials today. Cement production is a major environmental problem, and the main cause of CO_2 formation. During the cement production, it causes remarkable damage to the environment due to both intense energy consumption and carbon dioxide formed by calcination and combustion. It is considered that more than 7% of CO_2 emitted into the atmosphere originates from the cement industry worldwide (Sarker et al., 2013). It is considered that more than 7% of the CO_2 emitted into the atmosphere is produced by cement industries worldwide (Sarker et al., 2013). In order to produce 1 ton of cement, approximately 0.98 tons of CO_2 is released into the nature (Kapur et al., 2009). Despite this environmental damage, cement and concrete production of all countries have constantly increased in recent years.

According to the data of 2017 (Cembureau, 2017), our country is above the world average with an annual cement production of 82.8 million tons, with approximately 1-ton cement per person per year. In the light of these data, it can be said that concrete is the most used after water by people. With the rapid technological developments, increasing cement production day by day and these negative effects on the environment have become a major research subject.

Considering the cement production stage, it is evaluated that 95% of the total CO_2 emitted to the atmosphere occurs during the clinker production stage (Habert et al., 2010). Thanks to the use of environmentally friendly products instead of cement, products with better early and final performance can be produced and a reduction in CO_2 emission and energy consumption can be achieved. Especially in recent years, with the efforts to reduce the use of cement, environmentally friendly multi-functional cement-based composite production has also become the focus of research. In order to reduce energy use and CO_2 emission in cement and concrete:

- Reduction of energy and CO_2 emissions during clinker production
- Addition of inert filling materials to be used in concrete or cement
- Keeping the strength and durability of the concrete to be used at an optimum level

- Increasing the service life of the buildings and reducing the cement to be used in the buildings, are alternatives that should be considered (Schokker, 2010).

In addition to these, positive contributions to sustainability can be made with the effective use of some environmentally friendly products such as photocatalytic materials in cement and concrete. Thanks to the environmental regulations made in recent years, researchers have increased their studies on the development of new strategies on the reduction of volatile organic compounds, carbon monoxide, sulfur oxides and nitrogen oxides (NO_x) that harm human health. The main sources of NO_x emission, one of the most important of these pollutants, are factories and vehicles. Nitrogen oxides are highly reactive, colorless, odorless and water-insoluble gases that occur at high temperatures. Nitrogen oxides "NO_x" (NO and NO_2) are among the gases that are effective in the formation of ozone gases in the atmosphere and pose a threat to human health (Carp et al., 2004). These gases penetrate to the extreme points of the upper respiratory tract and have many serious negative effects on human health. Moreover, NO_x, together with SO_2 and SO_3, produces acid rain that can be harmful to vegetation, water and the built environment (Zivica and Bajza, 2001).

NO_x species, which are among the primary pollutants, affect humans especially through respiration and this situation affects people living in areas where motor vehicles are used. Low concentration NO_x species (< 50 ppm) emitted especially by motor vehicles cause symptoms such as cough, difficulty in breathing, sensitivity to light, insomnia. When exposed to high levels of NO_x species (> 100ppm), sudden burns, spasms, swelling of the upper respiratory tract tissues and oxygen reduction in body tissues may occur. For this reason, many international laws and regulations have been prepared and put into effect in order to control the amount of NO_x type gases in the atmosphere. It has been decided by the US Environmental Protection Agency (EPA, 2010) that NO_x emission values for the years 2008-2015 should be below 0.40 g / kW-h and sanctions have been imposed on this matter.

Investigations on nitrogen oxide values in the atmosphere for our country show that the situation has reached a worrying level, especially in our city centers. In evaluating the data related to this situation, it would be more correct to make an assessment based on the air quality index of the EPA official institution and by looking at the National Air Quality Index, which was created by adapting the national legislation and limit values. In this official report, which includes various air pollutants, it is seen that the limit value for NO_x in our country and the European Union is 30 µg / m^3 per year. It has been determined by the EPA that an hourly value for NO_2 should be at most 100 ppb (one in a billion) in order to increase the air quality standard (EPA, 2018). In this context, air quality standards in Japan and Europe also suggest certain restrictions. In line with these limitations, according to received data from the Republic of Turkey Environment and Urban Planning Ministry's Air Quality Monitoring Stations website (ÇŞB, 2020) of 01.07.19 - 01.07.20, for Ankara, the highest and average amounts of NO_x were measured as 831,8 µg / m^3 and 118,1 µg / m^3, respectively. For İstanbul highest 1754,2 µg / m^3, average 101,1 µg / m^3 NO_x values were measured for the same period (Fig. 1.1).

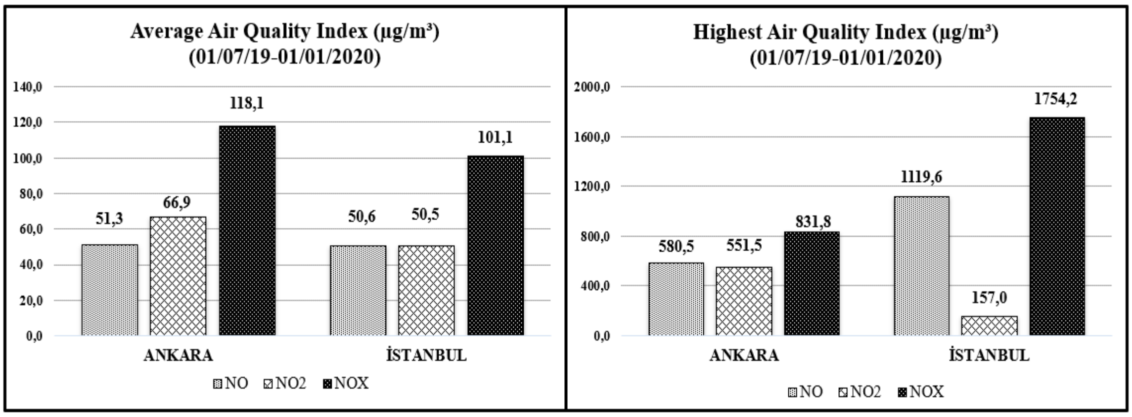

Figure 1.1 Annual highest and average NO_x values of Ankara and Istanbul measured between 01/07/2019 01/01/2020 (ÇŞB, 2018)

These data clearly show that NO_x emissions have reached levels that will adversely affect human health in our country due to the increasing urbanization. Although the steps that can be taken to reduce the gas emissions from vehicles and factories, which are the main sources of NO_x reaching critical levels in the atmosphere, are discussed worldwide, the increasing population and industrialization are the main obstacles to concrete steps to be taken. In addition to the main structural features of the basic construction materials used in the construction of the infrastructures located in the city centers where urbanization progress intensive, it is necessary to gain functions in different ways to reduce the air pollutants in the atmosphere. For these reasons, having additional functions of structural systems for reducing air pollution will make significant contributions to human health and the environment. New technologies are becoming necessary to reduce NO_x, especially in big cities.

In this context, sunlight, which has a major impact on achieving biological and environmental balance, has been used directly and indirectly in material and energy production until the early 1900s. However, considering the past century, the global overpopulation, the design of new materials, the excessive use of oil and nuclear power in the energy field have increased the distance between nature and societies. For this reason, there is enough research on using solar energy, especially in the field of civil engineering. Solar energy of approximately 5×10^{24} J reaches the Earth's surface every year. This energy is approximately 104 times the total energy consumption in the world. Considering this large resource and the need for a cleaner environment, combining solar energy with specially designed building materials is an important alternative opportunity in reducing air pollution. From this point of view, integrating photo-chemical materials into construction building materials can be an effective solution to the problems mentioned above. Considering the large surface areas of cement-based binder material applications used in buildings, the development of construction materials that use light energy can be an effective function to improve air quality. For this purpose, the use of photocatalytic materials is becoming widespread in the field of civil engineering to reduce air pollution. Photocatalysis is the enhancement in the rate of photoreaction by adding catalyst materials that complete the reaction without being consumed during the chemical reaction. This process, which accelerates the natural decomposition, can take place at room temperature. In addition, this process can convert organic pollutants into water and harmless substances without the need for any carrier gas. This technology also provides benefits in cleaning nitrogen oxides and other harmful compounds in the air (Martyanov and Klabunde, 2003; Nishikawa and Takahara, 2001). In addition, superhydrophilic (maximizing contact) and superhydrophobic (materials that spray water due to its nature, causing droplets) surfaces formed by photocatalytics have properties that facilitate self-cleaning of various contaminants with rain (Fujishima and Zhang, 2006).

Using nano-scale materials has become widespread in various industries over the last few decades due to their ability to improve the properties of conventional materials according to the needs of specific sectors. The abilities of nanomaterials are of particular interest to the construction sector and researchers, which is focused heavily on construction materials. This attention has subject to a number of studies into nanomaterial usage with cement-based composites, with the goal of producing more durable, high-performance and/or environmentally friendly composites. Including air purification capability to cement-based composites by using nanomaterials is one of the innovative approaches that allow them to absorb or transform deleterious particles (impurities) in the air. In this regard, researchers have increased their efforts to develop innovative composites containing nanomaterials to eliminate or reduce volatile organic compounds sustained in air such as carbon monoxide, sulfur oxides and nitrogen oxides (NO_x) (Tristantini and Mustikasari, 2011; Zhang et al. 2011; Kim et al., 2016; Çamurlu et al., 2012) which are dangerous for human health. NO_x gases are one of the most important pollutant gases and the biggest factor causing NO_x emissions are factories and vehicles.

Consequently, worldwide air quality; is an important issue affecting public health, economy, and environment. Especially in crowded cities, air pollution caused by nitrogen oxides released into the atmosphere from industrial enterprises and vehicles is at a worrisome level. High amounts of nitrogen oxides (NO_x) released into the atmosphere cause air pollution. Thanks to remarkable technological developments, such problems are reduced by using UV rays from solar energy and new solutions are tried to be produced for large surface areas of building materials. Considering that concrete is one of the most widely consumed material worldwide, it can be stated that one of the main ways to overcome the air pollution faced by modern societies is to develop existing basic building materials with innovative, functional and economic designs that will reduce the air pollution by binding them. For this reason, there is a need for a new generation of multi-functional cement-based composites with photocatalytic effect, which can offer applicable solutions to the aforementioned problems, different from traditional methods, and in which many parameters at different scales (micro and nano scales) are taken into account at the same time. Titanium dioxide (TiO_2), which is a semiconductor material as a type of photocatalytic material, exhibits strong oxidation capacity under UV lights, maintains its chemical stability when exposed to acidic, and some basic compounds, not being activated in the absence of UV lights and showing no toxic properties. All of these features have been brought the TiO_2 forefront in recent years in the construction industry.

(TiO_2) have frequently been used as a photocatalyst due to their high efficiency in oxidization of NO_x gases (Chen, 2008; Zhao and Yang, 2003). TiO_2 shows superior skill in the activation of photocatalytic reactions (Hager et al., 2000) and due to its chemical and photochemical stability, chemical inertness in the absence of ultraviolet (UV) irradiation, safety and cost-efficiency properties, and its non-toxicity in cement-based systems, it is a suitable photocatalyst (Zhao and Yang, 2003; Hüsken et al., 2009; Wang et al., 2007). The photocatalytic activity of semiconductor TiO_2 is highly dependent on the size, shape, type and phase of the material and changes in particle properties (Znaidi et al., 2001). Due to the high photocatalytic efficiency of nano-sized TiO_2 particles compared to larger size TiO_2 particles (Anpo et al. 1987; Cao et al., 1999; Cao et al., 2000; Gao and Zang, 2000; Ohama and Van Gemert, 2011; He et al., 2012), TiO_2 is generally used in cement-based composite at the nanoscale.

Since agglomeration of nanomaterials including nano-TiO_2 due to high surface interactions because of the particles' high surface area and energy is a general problem and quite strong attractive forces between nano-sized particles cause difficulties to disperse them homogeneously throughout the cement-based system (Kawashima et al., 2014), the use of nanomaterials is limited in cement-based composites (Tyson et al., 2011, Yazdanbakhsh et al., 2011; Sobolkina et al., 2012). Uniform and robust dispersion of nanoparticles is an indisputable requirement for them to be used in a healthy and effective way (Kawashima et al., 2014). In photocatalytic cement-based systems incorporating TiO_2, enabling the UV radiation to homogeneously and effectively, uniform distribution of TiO_2 particles (especially in nano-scale) along the surface of cement-based composites is one of the main goals to achieve optimum photocatalytic performance. Therefore, due to the reduction effect of agglomeration on photocatalytic activity (Lakshminarasimhan et al., 2008; Folli et al., 2010), proper dispersion of nano-TiO_2 prone to excessive agglomeration (Folli et al., 2009; Folli et al., 2010) is critically important in the production of cement-based composites with high photocatalytic activity. To uniformly disperse nanomaterials in an aqueous suspension, ultrasonication and incorporation of surfactants are common methods. Sato et al. (2008), investigated dispersion and agglomeration characteristics of nano and sub-micro scale TiO_2 particles in a suspension prepared by implementing three different mechanical dispersion agitations and using polyacrylic acid (PAA) with different average molecular weights as a polymer dispersant. They stated that the dispersion of nanoparticles in suspension is very important to completely benefit from the advantages of nanoparticles and ultrasonic irradiation is an efficient/effective method to disperse nanoparticles in aqueous suspensions. Othman et al. (2012), examined the effect of different parameters including ultrasonication amplitude and, type and utilization rate of dispersants on the dispersion and stability of photocatalytic nano TiO_2 particles in aqueous suspensions. They used two different dispersants which were PAA and ammonium polymethacrylate. They stated that increasing the ultrasonication amplitude has an improvement effect on the deagglomeration process and the stability of the suspensions. Yousefi et al. (2013), studied the effect of various parameters such as concentrations of nano-TiO_2 powder, type of dispersant (lime-saturated water solution and deionized water), mixing process, ultrasonication time on dispersion of TiO_2 particles incorporated into the cement paste. They found that the conventional mixing process causes high agglomeration of nano-TiO_2 and ultrasonication process is undeniable to disperse nano-TiO_2 throughout the cementitious system. They also stated that the utilization of saturated lime water provides improvement in photocatalytic degradation capability of nanoparticles alongside with convenient dispersion of nano-TiO_2 in cement paste. Sobolkina et al. (2012), studied the effects of sonication process with different implementation time and two different surfactants with different utilization rates, that are an anionic sodium dodecyl sulfate and a nonionic polyoxyethylene (23) lauryl ether, on the dispersion of carbon nanotubes (CNTs) in water and they aimed to improve the mechanical properties of cement paste by using aqueous dispersions of CNTs prepared with optimum sonication time and surfactant concentration they determined for appropriate dispersion of CNTs. Mendoza et al. (2013), investigated the effect of superplasticizer and $Ca(OH)_2$ on the dispersion stability of multi-walled CNTs for cement-based systems and stated that sonication process is an effective dispersion method for multi-walled CNTs and the use of a dispersing agent with the sonication process is necessary to ensure a greater degree of dispersion of particles for a longer duration. Alrekabi et al. (2016), investigated the dispersion of multi-walled CNTs in water under various sonication conditions to prepare homogeneous multi-walled CNTs suspension used for cementitious composites. They also used superplasticizer to achieve better dispersion of multi-walled CNTs. Saafi et al. (2013), also used superplasticizer as a surfactant and ultrasonication to ensure proper dispersion of multi-walled CNTs in a solution prepared for the production of geopolymeric nanocomposites. Nochaiya and Chaipanich (2011), examined the effect of the incorporation of multi-walled CNTs on the porosity and microstructure of cement-based systems. They used ultrasonication to ensure a homogeneous mixing. Zhang et al. (2012), and Zhang and Islam, (2012) also used ultrasonication and mechanical mixing to produce cement paste, mortar and concrete specimens incorporating nano-silica and stated that ultrasonication process provides better dispersion of nano-silica than mechanical mixing method. Therefore, several researchers have used ultrasonication and/or different surfactants to solve the agglomeration problem of nanoparticles and to improve the dispersion quality of different nanoparticles.

To improve clarifying and further evaluate their influence, more investigation is needed to better understand the mechanisms underlying the effect of mixing methods on photocatalytic activity and mechanical property of cement-based composites containing nano-TiO_2. The current experimental study was undertaken to address cost-effective, feasible mixing methods that will allow proper dispersion of nano TiO_2 and ensure it remains stable for a certain period during the fresh state of cement-based composites. Since, aggregates in mortar/concrete mixture may break down the nano-TiO_2 agglomerates, which result in better dispersion of nanoparticles throughout them compared to cement paste; due to comparatively quite larger particle size than nano-TiO_2 and cement, this study was undertaken by using only cement paste mixtures. For this purpose, five different mixing methods were used, with a wide literature review and past studies of the authors (Al-Dahawi et al., 2016) taken into account. These methods were based on three main mixing techniques using ultrasonication, a hand blender and a conventional cement mixer, and implemented with different mixing procedures and surfactant contents. Two surfactant materials were used: polycarboxylic ether-based superplasticizer (PCE) and polyacrylic acid (PAA). To compare mixing methods, in addition to evaluating photocatalytic performance, researchers studied compressive strength results and recorded electrical impedance results to determine the more successful mixing method in terms of dispersion of nano TiO_2 materials throughout the cement-based composites.

2. LITERATURE REVIEW

Considering the costs and damages in the use of cement, the researchers aimed to reduce this damage by replacing the cement with many different pozzolanic and nanomaterials. Different findings have been obtained by examining these materials in terms of strength, durability, economic and sustainability. Moreover, different properties have been integrated into the construction materials and multi-functional, innovative features have been included. Cementitious materials substituted with TiO_2 have been intended to gain in features such as air purification and self-cleaning. In other sections, the effects of nanomaterials on cementitious materials, properties of TiO_2, photocatalytic mechanism, and parameters that influential on mechanism will be explained in detail. Detailed information is given in the following sections related to such materials.

2.1. Historical Developments on Utilization of TiO_2 in Cement-based Composites

Nanomaterials are increasingly used in the field of construction materials (Teizer et al., 2011) and offer an important solution in improving the durability and mechanical properties of the structure along with its different age characteristics. In recent years, significant studies have been carried out on nanomaterials in the cement and concrete industry (Bjornstrom et al., 2004; Campillo et al., 2007). Substitution of nano-sized products to cement or concrete improves compressive, flexural strength and wear resistance. On the other hand, considering the energy consumption and environmental benefits, environmental damage can be reduced significantly by reducing the cement consumption.

Nanoparticles for the cement phases can have a nucleus effect, thus increasing cement hydration through its high reactivity. On the other hand, inert nano materials help reduce porosity by improving the interface and microstructure. The most important problem of nanomaterials used in cement and concrete is that they can be distributed effectively and homogeneously in the matrix. Although the use of nano materials has a positive effect on cement properties, scientists continue their researches for effective and homogeneous dispersion, cost, and effects on human health (Jo et al., 2007).

Photocatalytic materials can be used most commonly with concrete in the construction industry. By using photocatalytic materials in concretes with large surface areas, they will have an opportunity to improve air quality. When the photocatalytic material is exposed to light, it reacts as a liquid or a gas. Photocatalytic materials such as TiO_2 (titanium dioxide), ZnO (zinc oxide) and CdO (cadmium oxide) are frequently used due to their high efficiency in decomposing inorganic oxides (Chen et al., 2008). These materials decompose the pollutants with a little energy and turn them into harmless waste products instead of absorbing the pollution, which is one of the traditional air cleaning methods.

The photocatalytic materials such as titanium dioxide (TiO_2) have been investigated in the past 50 years, but the first studies date back to the 30s of the last century (Fujishima et al., 2008). Fujishima and Honda (Fujishima and Honda, 1972) discovered TiO_2 as a photocatalyst in 1972. For the past 20 years, the development of TiO_2 has progressed rapidly, and become very attractive in the construction materials with self-cleaning, air or water purification and antibacterial functions.

2.2. Titanium Dioxide (TiO_2)

2.2.1. Structure of TiO_2

The photocatalytic activity of the semiconductor TiO_2 depends on the changes in the size, shape, type and semiconductor particles of the material (Znaidi et al., 2001). Considering the place of this type of semiconductor particles in concrete applications, it will be very important to investigate the effect of different TiO_2 forms. TiO_2 was used in two different crystalline forms (anatase and rutile). Both anatase and rutile forms have Ti^{4+} centers in the crystal structure and TiO_6 octahedral chain bonds surrounded by six O^{2-} ions.

The unit cells of these crystals and the bond structure of atoms are shown in Figure 2.1 (Austin and Lim, 2008) and their bond angles are shown in Figure 2.2 (Diebold, 2003).

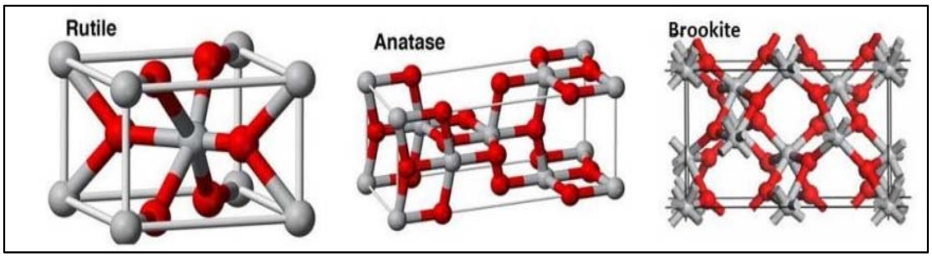

Figure 2.1 Bond structure of different crystallline forms of TiO_2 (Austin and Lim, 2008)

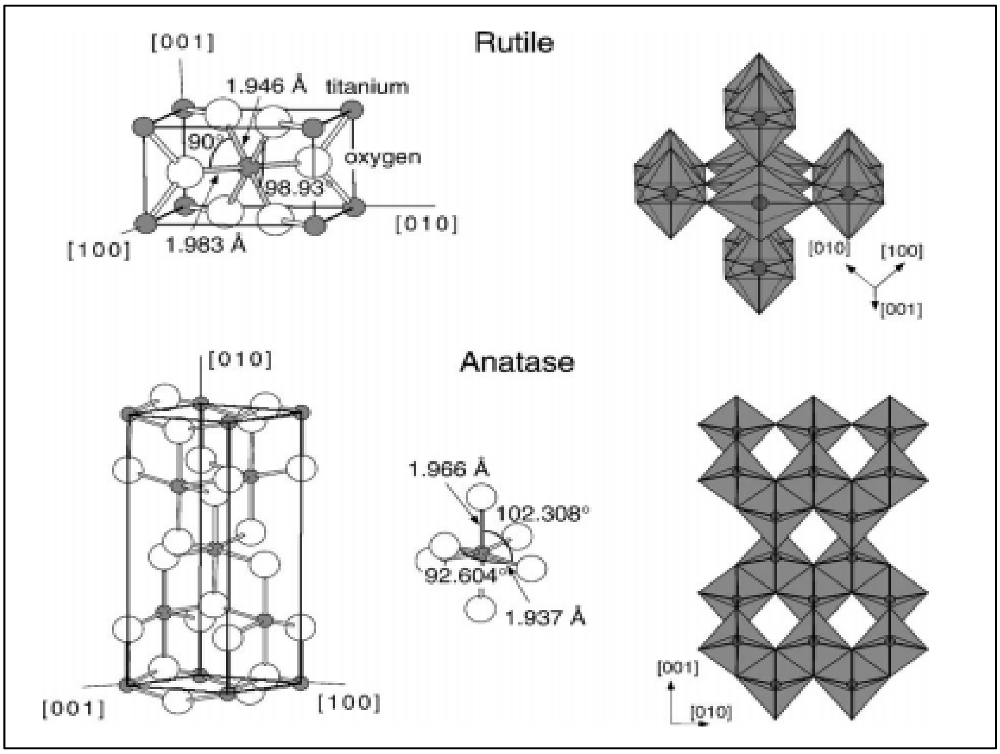

Figure 2.2 Bond angle of rutile and anatase (Diebold, 2003)

In recent years, studies show that TiO_2 in nano-size anatase form has better photocatalytic efficiency than nano-size rutile form TiO_2 (Hanson and Tikalsky, 2013). It is shown in Figure 2.2 that each Ti^{4+} ion in the crystal is surrounded by six O^{2-} ions. The length of the bond formed between Ti-Ti in the anatase form is 3.79 Å and 3.04 Å, which is larger than in the rutile form (3.57 Å and 2.96 Å). The bond length between Ti-O is 1.934 Å and 1.980 Å and it is shorter compared to rutile form (1.949 Å and 1.980 Å) (Diebold, 2003). This difference mentioned in the lattice structure of these forms causes different density and electronic band structure between the two forms of TiO_2 (rutile and anatase). This is shown as one of the reasons why the anatase form is more active than the rutile form. Some other basic properties of anatase and rutile forms are given in Table 2.1 (Hanaor and Sorrell, 2011).

Table 2.1 Basic properties of anatase and rutile form

Property	Rutile	Anatase
Crystallinity	Tetragonal	Tetragonal
Atoms per unit cell	2	4
Band gap (eV)	3.0	3.2
Solubility in water	Insoluble	Insoluble
Hardness (Mohs)	6-6.5	5.5-6
Bulk modulus (GPa)	206	183

The band gap energy (band gap; E_{bg}) of the semiconductor with the minimum light energy provides the electrical conductivity of the material. In other words, it is the minimum energy that allows the electron to be excited from the valence band to the conductivity band in order to form holes (h^+_{VB}) in the valence band of semiconductor particles exposed or excited. E_{bg} is 3.2 eV for anatase form and E_{bg} is 3.0 eV for rutile form. The UV that should be used for these values corresponds to the wavelength of 388 nm and 413 nm, respectively. It is seen as an advantage that the photocatalytic activity occurs in the visible region corresponding to 413 nm in the rutile form. However, crystal structure disorders in the rutile form are too much to be compared to anatase form. Therefore, less time remaining in the conductivity band of an excited electron causes the rutile form to not be preferred as an effective photocatalytic material (Schindler and Kunst, 1990). The more regular the crystal structure in TiO_2 forms, the better the photocatalytic activity.

2.2.2. Ultraviolet Rays

UV rays are divided into three categories, namely UV-a, UV-b and UV-c, because of their different characters and different effects on living things. UV-a is among the most common rays. The ozone layer allows these rays to pass. UV-b is quite dangerous. Most of these rays are blocked by the ozone layer. It constitutes 5% of UV rays. UV-c is the most dangerous rays for health. They are largely held in the ozone layer. UV-a ray, which can reach the atmosphere from the sun, has 315-400 nm, UV-b, which partially reaches the atmosphere, has a fill length of 280-315 nm, and UV-c light, which is absorbed in the ozone layer, has a wavelength of 200-280 nm. In Figure 2.3, the wavelength of various rays was given. Also band energies and wavelengths of some semiconductors were given in Table 2.3.

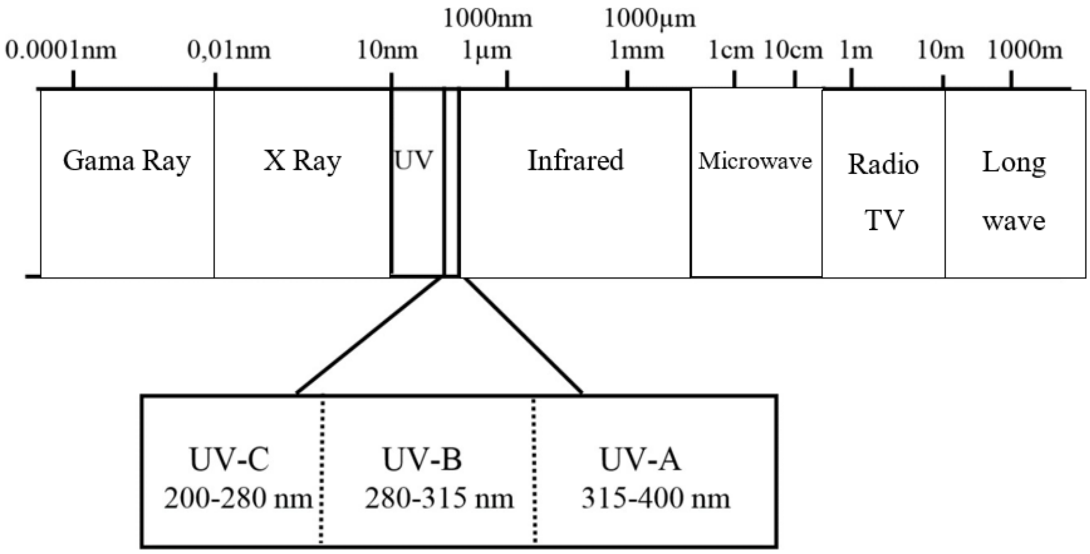

Figure 2.3 Wavelength change of different rays

Table 2.2 Band energies and wavelengths of some semiconductors

Photocatalytic Compounds	Wavelength(nm)	Limit of Band Energy (eV)
Titanium Dioxide-TiO_2 (rutile)	413	3.0
Titanium Dioxide – TiO_2 (anatase)	387	3.2
Zinc Oxide –ZnO	388	3.2
Zinc Sulphide– ZnS	335	3.6
Cadmium Sulphide – CdS	516	2.4
Hematite-Fe_2O_3	539	2.3
Tungsten Trioxide – WO_3	443	2.8

When the photocatalytic working principle of TiO_2 is examined, it will be seen that the energy provided by photons under light creates the electron holes in cases where the band gap of TiO_2 is equal to or greater than the amount of energy.

When the energy provided by the photons is equal to or greater than the band energy of the electrons, the electrons move from the valence band to the conduction band. Separated electrons cause oxidation-reduction reaction of existing substances.

2.2.3. Mechanism of NO_x Reduction

Studies have been shown that TiO_2 effectively oxidizes NO_x ($NO_x = NO + NO_2$) (Husken et al., 2009). In addition, TiO_2 is known to oxidize volatile organic compounds (VOC) that adversely affect air quality (Wang et al., 2007). In studies on TiO_2, although the anatase form has been shown to have a better photocatalytic effect, there are studies in the literature using only rutile form. In these studies, good results have been obtained against durability problems such as thermal degradation besides photocatalytic effect. (Fei et al., 2016). In another study, it was stated that the optimum anatase-rutile combination was found to achieve the best photocatalytic effect in cement-based systems (Demeestere et al., 2008; Su et al., 2011).

As one of the main reasons why the anatase form gives a more effective photocatalytic effect, it has been shown that the anatase form has a lower density than the rutile form and therefore TiO_2, which is substituted by weight instead of cement, has more surface area in this form (Melo et al., 2012). The order of photocatalytic reactions and the progress of the mechanism between the conduction and valence bands are given in Figure 2.4 and Figure 2.5, respectively. TiO_2 in reaction mechanisms summarized can be expressed as follows;

I. When the energy of the light sent on the material is equal to or greater than the electronic band gap value ($h\nu \geq Eg$), the material adsorbs the light. In this first stage of the photocatalytic reaction, with the help of photon from an energy source, a hole is formed in the valence band by providing electron movement from the valence band of TiO_2 to the conductivity band.

$$\mathrm{TiO_2} + h_v \rightarrow \mathrm{h^+} + \mathrm{e^-}$$

II. This formed hole (h^+) reacts with the electron to form an OH radical ($OH^\cdot$). The reduction of molecular oxygen (O_2) to superoxide anion (O_2^-) can be initiated by the power of the electrons which work as an inductor

$$\mathrm{H_2O} + \mathrm{h^+} \rightarrow \mathrm{H^+} + \cdot\mathrm{OH}$$

$$\mathrm{O_2} + \mathrm{e^-} \rightarrow \cdot\mathrm{O_2}^-$$

III. TiO_2 based photocatalytic removal reaction of the NO_x is mostly admitted as follows (Sugrañez et al, 2013):

$$\mathrm{TiO_2} + h_v \rightarrow \mathrm{h^+} + \mathrm{e^-}$$

$$\mathrm{O_2} + \mathrm{e^-} \rightarrow \cdot\mathrm{O_2}^-$$

$$H_2O + h^+ \rightarrow H^+ + \cdot OH$$

$$NO + \cdot OH \rightarrow HNO_2$$

$$NO + \cdot O_2^- \rightarrow NO_3^-$$

$$NO_2 + \cdot OH \rightarrow NO_3^- + H^+$$

$$HNO_2 + \cdot OH \rightarrow NO_2 + H_2O$$

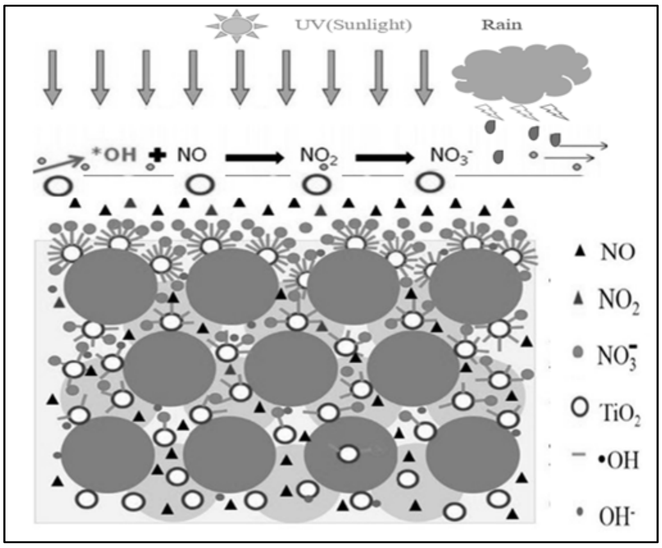

Figure 2.4 Photocatalytic reaction representation of TiO_2 (Xu et al. 2019)

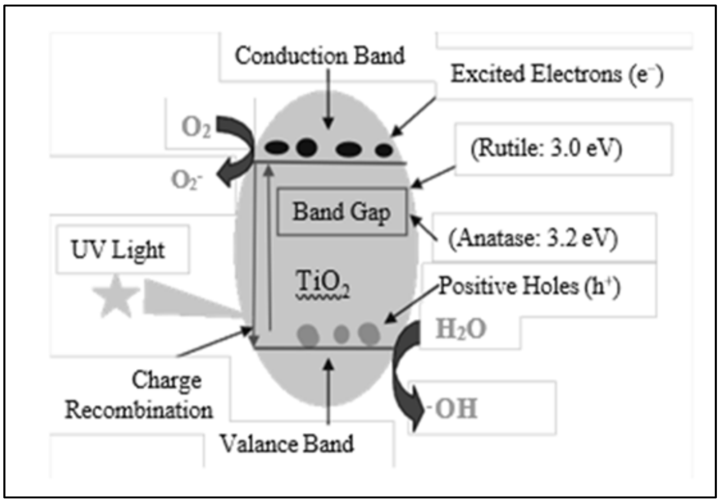

Figure 2.5 UV light TiO_2 photocatalysis mechanism

2.3. Factors Affecting Photocatalytic Activity

In photocatalytic reactions, light, movement of electrons, reaction products and TiO_2 forms play an important role. Therefore, environmental factors such as light, temperature, water and humidity and studies that can provide or change electron movement have been carried out. It was also examined how the size, amount, and form of TiO_2 that would provide photocatalytic properties changed the reactions. However, different results were obtained in these factors that would affect the photocatalytic property.

In some studies, it is stated that when the grain size of the photocatalyst is small, the e^-_{CB} and h^+_{VB} loads will be close to each other and these loads will have a high probability of recombination (Almquist and Biswas, 2002; Wang et al., 1997). The addition of metal ion to the TiO_2 substituted composites provides the appropriate potential change, resulting in reduction reactions on the photocatalyst surface. (Sayılkan et al., 2007). However, it has been stated that the addition of a high concentration of metal ions may cause the active areas on the surface to decrease and thus to decrease the photocatalytic activity (Sayılkan et al., 2007). The most important advantage of adding metal or ion at the appropriate concentration is that the semiconductor emits the light absorption spectrum from the UV region to a visible range in a wide range > 400 nm. As an example, it was found that the photocatalytic activity of TiO_2, which was synthesized by adding Sn^{4+} and Cr^{3+} at the beginning, was higher than that of pure TiO_2 without addition (Hung et al., 2007; Kemp and Mcintyre, 2006;). The same results were observed if niobium ion (Xie and Yuan, 2004), tungsten oxide (Li et al., 2001) and cobalt ion (Iwasaki et al., 2000) were added. While the energy level of one metal oxide is high, the energy level of the other may be small. By combining two or more semiconductors with different band energy levels and ensuring that the load carriers remain separate and stable, e^-_{CB} and h^+_{VB} can be re-combined. Electrons in the band with a low energy level if one of the semiconductors has a large band energy range and the other is small, passes to the valence band of the other semiconductor and from there to the conductivity band with the effect of light (Sayılkan et al., 2007).

The increase in the amount of absorbed photon during photocatalytic degradation likewise causes an increase in the degradation rate (Karunakaran and Senthilvelan, 2005; Qamar et al., 2006). It has been determined that the increase in pollution concentration up to a certain level increases the rate of photocatalysis disintegration. However, the increase in the concentration of impurity more than a certain level has been shown to cause a significant decrease in the photocatalysis reaction rate. (Kabra et al., 2004; Saquib, 2003).

Some researchers have examined the effect of pollution on photocatalytic reactions. The molecules that make up the pollution cause the light-active areas to be closed on the surface of the photocatalyst. Therefore, it prevents the formation of OH radicals that cause the pollutants to oxidize and decompose. In addition, with the increasing concentration of the molecules forming the pollution, a significant part of the light providing photocatalytic activity is absorbed by the polluting molecules. Therefore, pollution molecules on the photocatalyst surface prevent the formation of OH and O_2^- radicals. This causes the photocatalytic reaction rate to decrease (Jun et al., 2006). TiO_2 gains hydrophilic properties with UV from the sun. Hydrophilic property plays an important role in having a self-cleaning feature by easily removing the surface pollutants from the surface.

2.3.1. The Effect of TiO_2 Grain Size Distribution

As mentioned in the previous sections, the behavior of photocatalytic materials in composites, the realization of photocatalytic reactions seems to be directly related to the size of the photocatalytic surface. On the other hand, it is considered that it will contribute to the improvement of strength and durability in addition to photocatalytic effect by choosing the optimum grain size distribution in order to decrease porosity in concrete and cement. However, the study on the effect of TiO_2 with grain size distribution has not been found so far.

Different grain size distributions cause the compact structure of the composites to change. It is known that this change has an effect on cement dosage. This distribution is ignored in powder materials while the grain size distribution of the aggregates is considered. Without proper grain size distribution in powder materials, hydration products will not be able to fill all pores and an increase in porosity will occur. Application of the particle size distribution in powder materials will decrease the pores between particles and provide an improvement in strength / durability. Fuller and Thompson method has been used for a long time to determine the mixing rates of aggregates. In 1980, Funk implemented the minimum particle size. It has been stated that with this method, sufficient strength can be obtained with optimized aggregate and cement mixture (Johansen and Andersen, 1991). Most researchers working on aggregate gradation have developed their design according to an ideal aggregate grain size distribution curve. By using this method, it is aimed to increase the photocatalytic performance in addition to the mechanical property performances by determining the ideal particle size distribution and applying it to nano TiO_2.

2.3.2. The Effect of Metal Ion

The contact of the photocatalytic semiconductor with another phase creates a new charge distribution within the semiconductor. When charge carriers transfer between the semiconductor and the phase with which it comes into contact, the electronic band potential of the semiconductor may deteriorate in relation to the accumulation and / or depletion of charge in regions close to the surface. The bands can approach the upper surface as in n-type semiconductors or towards the lower surface as in p-type semiconductors. For example, on the TiO_2 surface, the oxygen gaps and Ti^{3+} regions with five coordination are formed by the removal of oxygen atoms. These regions act as powerful electron traps, causing the surface regions of the semiconductor to be negatively charged. In order to balance this effect, positively charged layers are formed in the semiconductor and the shifting of the electrical potential, thus the upward shift of the binding bonds, is ensured. Electrons, excited by a sufficient amount of radiation, move towards the catalyst surface to show activity while being excited from the valence band towards the conductivity band. As a result, by preventing e^-_{CB} and h^+_{VB} from coming together and mating, they cause a highly effective catalytic activity. This potential change can be changed significantly by the metal ion (usually metal salts) added to the surface (Wang et al., 2000). The addition of metal ion provides the appropriate potential change, resulting in reduction reactions on the photocatalyst surface. (Sayılkan et al., 2007).

As mentioned above, the addition of metal or ions to the photocatalytic product allows to increase the interface charge transfer, that is, the electron retention rate, which restricts the re-assembly of e^-_{CB} and h^+_{VB} during irradiation. In other words, this is a method that helps to reduce the imperfections within the crystal lattice of the semiconductor. The d-electron configuration of the added metal and the band energy gap level of TiO_2 play an important role in photocatalysis. These regions, where electron retention gradually increases, increase the redox potential of the semiconductor with the effect of the added metal ions, and increase the photocatalytic activity by increasing the duration of the charge carriers in the conductivity band of the excited electrons. The concentration of the added metal also causes a change in photocatalytic activity. In some studies, it has been stated that the addition of high concentrations of metal ions may cause a decrease in surface active areas and thus a decrease in photocatalytic activity (Sayılkan et al., 2007). The most important advantage of adding metal or ion at suitable concentration is that it spreads the light absorption spectrum of the semiconductor from the ultraviolet region to the visible region over a wide range of more than 400 nm. For example, it has been reported that the photocatalytic activity of TiO_2 synthesized by the addition of Sn^{4+} and Cr^{3+} in the visible region is higher than that of pure TiO_2 without addition (Hung et al., 2007; Kemp and Mcintyre, 2006; Venkatachalam et al., 2007). The same results were observed in the case of the addition of niobium ion (Xie and Yuan, 2004), tungsten oxide (Li et al., 2001) and cobalt ion (Iwasaki et al., 2000). While the band energy level of one metal oxide is high, another may be at the small band energy level or vice versa. By combining two or more semiconductors with different band energy levels, the reunification of e^-_{CB} and h^+_{VB} can be achieved by keeping the charge carriers separate and stable from each other. As seen in Figure 2.6, if the band energy gap of one of the semiconductors is large and the other is small, the electrons in the low energy band pass to the valence band of the other semiconductor and from there to the conductivity band immediately with the effect of light (Sayılkan et al., 2007). Thus, a positive gap is created in both semiconductors. Positive voids of a low band energy semiconductor behave as a strong oxidizer. On the other hand, since the conductivity band energy of the semiconductor with a low band energy gap is higher than the other, the excited electrons pass into the low energy conductivity band of the other semiconductor and this region takes part in the reduction reaction. As a result, the recombination of e^-_{CB} and h^+_{VB} is prevented and an increase in photocatalytic activity is provided. Oxides synthesized for photocatalytic activity are given in Table 2.3.

Table 2.3 Oxides synthesized for photocatalytic activity

Oxides Types	References
ZnO-ZnS	(Liao and Ho, 2005)
CdS-ZnS	(Ren et al., 2006)
SiO_2-TiO_2	(Oki et al., 2007; Sayılkan et al., 2007)
WO_3-WS_2	(Paola et al., 2000)
RuO_2-TiO_2	(Carneiro et al., 2005; Socha et al., 2006)
SnO_2-TiO_2	(Hou et al., 2007; Zakrzewska and Radecka, 2007)
ZrO_2-TiO_2	(Kan et al., 2007; Mishra, 2008)

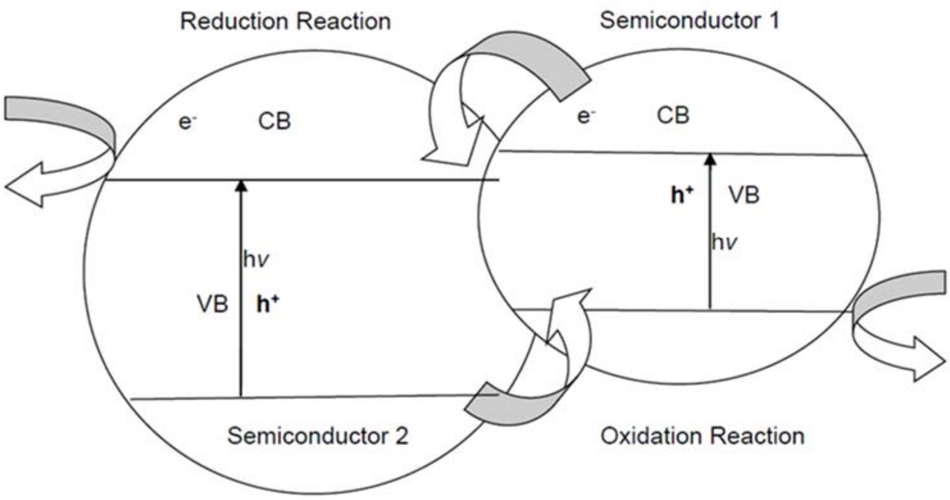

Figure 2.6 Charge transfer in a two semiconductor system (Sayılkan, 2007)

2.3.3. The Effect of Ray

To initiate photocatalytic activity, as described above, the photocatalyst must be excited with a ray equal to or greater than its band gap energy. The increase in the amount of photon absorbed during photocatalytic degradation causes an increase in the degradation rate (Karunakaran and Senthilvelan, 2005; Qamar et al., 2006). The photocatalytic reaction may vary depending on the type of photocatalyst to be used in the photocatalytic reaction and the ray irradiance used. When the photocatalyst surface is exposed to a ray of low irradiance, the reaction rate increases linearly with the irradiance of the ray (Curcó et al., 2002). At medium irradiance, the speed increases in proportion to the square of the ray irradiance (Xiao et al. 2007). When the ray irradiance is increased further, the observed effect is almost the same as with low ray irradiance. In other words, speed increases in direct proportion to the irradiance of the ray. If exposed to high light irradiance, it can cause the electron and gap pair to recombine. In this case, the speed will not increase at the desired rate. It has been found that when sunlight is used instead of ultraviolet ray as the exposed light source, the photocatalytic reaction rate increases for the first time and remains constant after a while (Ku et al., 2006). The reason for this is the changes in light irradiance over time.

2.3.4. The Effect of Temperature

Ambient temperature has a significant effect on the photocatalytic reactions of organic compounds. Generally, as the temperature increases, the speed of reunification of the electron-gap pairs on the photocatalyst surface increases. Since the reunion of the charge pairs and their reactions with the molecules in the environment are competitive reactions, high temperature reduces the photocatalytic activity by preventing the formation of redox reactions on the surface. It also increases the desorption rate of molecules adsorbed on the surface and reduces the amount of radicals formed (Fu et al., 1996).

2.3.5. The Effect of pH

One of the factors affecting the degradation reactions occurring on the surface of the photocatalytic material is the pH of the environment. By affecting the charge properties of the photocatalyst surface, it causes the surface characterization, the size of the aggregates formed, and the total surface area to change (Bahnemann et al., 2007). Charge exchange may occur on the TiO2 surface in acidic or basic environments.

$$\mathrm{TiOH} + \mathrm{H^+} \rightarrow \mathrm{TiOH_2}^+$$
$$\mathrm{TiOH} + \mathrm{OH^-} \rightarrow \mathrm{TiO^-} + \mathrm{H_2O}$$

Initiation reactions that occur on the surface have given above. TiO_2 surface will be charged positively in acidic environment (pH <6,9) and negatively charged in basic medium (pH> 6,9). The change of electric charges on the surface will affect the amount of radicals generated during degradation reactions and the amount of pollutants adsorbed on the photocatalyst surface. TiO_2 has higher oxidation activity at low pH values, but excessive H^+ at very low pH values can reduce the reaction rate (Sun et al., 2006).

2.3.6. The Effect of Pollution

The activity of the photocatalytic material also depends on the amount and type of pollution present in the ambient. It has been determined that the increase in the pollution concentration up to a certain level increases the rate of photocatalysis degradation. However, it has been observed that the increase in the pollution concentration above a certain level causes a significant decrease in the photocatalysis reaction rate. (Kabra et al., 2004; Saquib, 2003). It’s photocatalytic activity is related to OH radicals, which allow the semiconductor to break down by oxidizing contamination on its surface. When the concentration of the molecule constituting the pollution is above a certain value, the photocatalytic activity decreases. There are several possible reasons for this. First of all, the polluting molecules cause the photocatalyst's surface to be covered by the light active areas. Therefore, it prevents the formation of OH radicals that allow the degradation of impurities by oxidation. Another reason is that, with the increase in the concentration of pollution molecules in the environment, a significant portion of the UV rays, which provide the formation of photocatalytic activity, are absorbed more by the pollutant molecules than TiO_2 molecules, and the formation of OH and O^{2-} radicals, which cause the breakdown of pollution molecules on the photocatalyst surface, is prevented. This causes the photocatalytic reaction rate to decrease (Jun et al., 2006).

2.3.7. The Effect of Water and Humidity

Water molecules have a significant influence on the photocatalytic activity of the semiconductor. Water molecules in the photocatalytic environment are separated from the surface to form hydroxyl radicals that will act as oxidizers to the holes formed by the separation of oxygen atoms from the surface after the photocatalyst interacts with UV rays. Immediately afterwards, the degradation reaction of the impurity molecules absorbed on the photocatalyst surface occurs. In a reaction environment where there are no water molecules to be absorbed on the surface of the semiconductor, hydroxyl and / or peroxide radicals, which act as oxidizing molecules and play an important role in the transformation of pollution molecules into harmless products, will not be formed. Thus, the photocatalysis reaction will slow down. The hydrophilic properties of semiconductor surfaces play an important role in photocatalysis reactions, whether the semiconductor is used either as a particle or as a thin film. The formation of a hydrophilic surface is shown in Figure 2.7 below.

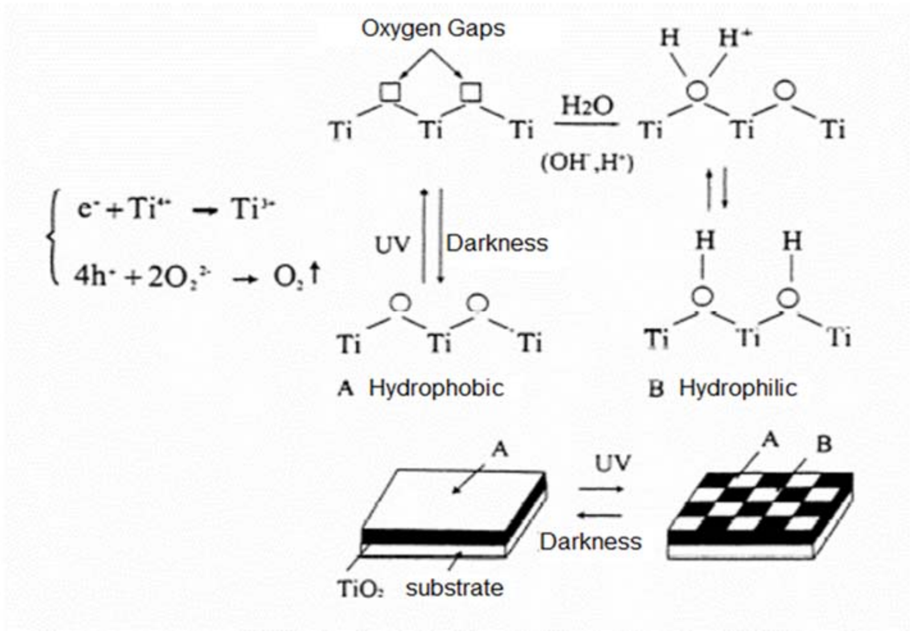

Figure 2.7 Formation of a hydrophilic semiconductor surface (Mardare et al., 2007)

Firstly, Ti^{4+} cations are reduced to Ti^{3+} position by electrons, while spaces (h^{+}_{VB}) oxidize oxide anions. After that, the oxygen atoms leave the surface and cause the formation of oxygen spaces. Water molecules bind to these spaces and cause the formation of hydroxyl ions that enable the surface to acquire hydrophilic properties. At this stage, when the surface is irradiated for a while, the contact angle of the surface with respect to the water approaches zero. Thus, water molecules spread on the surface in the form of a very thin film layer (Mardare et al., 2007). Whether the surface covered with a thin and transparent film layer has hydrophilic property can be understood by determining the contact angle between the surface of polar molecules such as water molecules dropped on the surface. As shown in Figure 2.8 below, the approach of the contact angle to zero degree indicates that the hydrophilic property of the surface increases.

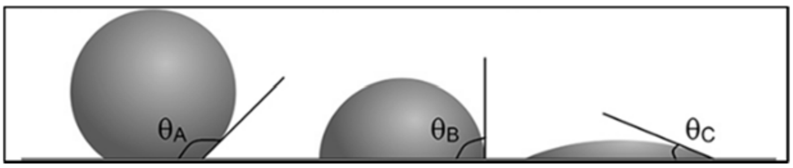

Figure 2.8 Contact angles on hydrophilic and hydrophobic surfaces (left) hydrophobic surface, (middle) partially wetting liquid, (right) hydrophilic surface

As mentioned before, the hydrophilic surface plays an important role in removing the contaminants from the environment by breaking easily and having self-cleaning feature. In order for any surface to gain "self-cleaning" feature with the effect of rays, attention should be paid to the following important processes:

• Keeping TiO_2 particles with high surface area and small crystal size,
• Preparation of TiO_2 solution in polar and / or apolar suspension,
• Modification of TiO_2 in the left with organic compounds,
• Homogeneous distribution of TiO_2 particles over the entire surface,
• Bringing super hydrophilic feature to the surface.

2.3.8. The Effect of Photocatalyzer Dosage

In photocatalytic reactions, it is important to determine the optimum amount of photocatalytic material in order to ensure that the photons coming to the semiconductor surface can be completely absorbed and to reduce the use of semiconductor in excess dosage. However, the optimum amount of pollution concentration of the environment is also an effective factor (Kabra et al., 2004). It is necessary to evaluate the effect of the photocatalyst ratio by considering the environments in which the photocatalytic reaction takes place. If the photocatalytic reaction is carried out in a suspension with catalyst and impurity molecules, changing the amount of photocatalyst changes the photocatalytic activity. However, the maximum utilization rate depends on the synthesis type of the photocatalyst, particle size, surface area, concentration and structure of the products to be broken down (Krýsa et al., 2004). Generally, the increase of photocatalyst up to a certain dosage in such environments causes the photocatalytic degradation / reaction rate to increase linearly. Photocatalytic reactions are slowed when the amount of photocatalyst exceeds a certain dosage. There are different reasons for this slowdown. For example, as the dosage of photocatalyst increases, semiconductor particles that become active by being stimulated by the effect of the beam sent into the suspension will be found in the system along with the particles in the ground state that do not interact. Particles in the ground state and excited may collide with each other before the photocatalytic reaction starts, causing the particles that undergo photocatalytic reaction, become inactive. Therefore, it is necessary to determine the optimum amount of photocatalyst (Chun et al., 2000). The situation is shown below.

$$\mathrm{TiO_2^*} + \mathrm{TiO_2} \rightarrow \mathrm{TiO_2^\#} + \mathrm{TiO_2}$$

In this equation, TiO_2* indicates the TiO_2 species that are active on the surface, and $TiO_2^{\#}$ indicates the TiO_2 species that have become inactive as a result of the collision of the particles (Asiltürk et al., 2006). In addition to this decomposition and precipitation of particles are also among the factors that negatively affect the reaction. If the photocatalytic reaction occurs on a surface in the form of a thin layer containing semiconductors, the composition of this layer and the ratio of semiconductors in the film layer play an important role in photocatalytic reactions. The increase in the solid semiconductor ratio in the film layer causes the surface to be activated on the coating surface to increase and thus the surface to gain hydrophilic feature. Due to this hydrophilic feature, the photocatalytic activity will increase with the increase in the dosage of radical products that act as oxidizing agents in the suspension medium. In addition, it is necessary to consider the effect of transition metal ions added to the semiconductor.

2.4. Research on Nano TiO_2 Used in Cement-based Composites

Titanium dioxide (TiO_2), which is an inert material, is used by substituting cement in different phases and sizes. The use of inert TiO_2, which is substituted for cement, in different sizes, forms and quantities, affects different age characteristics as well as NO_x reduction properties of the composite.

Products with self-cleaning properties are used in the paint, clothing and cement industries. It is frequently preferred in Europe and Japan as a coating material on roads, especially on building facades. NO_x reduction of Nano TiO_2 (Cassar, 2005; Husken et al., 2007), removing organic volatiles from its structure and the self-cleaning feature (Diamanti et al., 2008; Ruot et al., 2009) has been the focus of attention for most researchers. In addition to these features, it has been observed that Portland cement improves compressive, flexural strength and abrasion resistance of concrete (Li et al., 2006,) and accelerates hydration at an early age (Jayapalan et al., 2009). However, there were decreases in photocatalytic activity / efficiency and NO_x reduction due to carbonation (Lackhoff et al., 2003).

In some studies, it has been determined that nano-TiO_2 accelerates the hydration of Portland cement at an early age, (Jayapalan et al., 2010) and improves compressive, flexural strength (Li et al., 2007). Degussa P25, which has approximately 80% anatase and 20% rutile form content, has been used in these studies and has been found to be activated in many photocatalytic reaction systems. (Li et al., 2016; Ma et al., 2016; Wang et al., 2016; Yousefi et al., 2013). According to the results in photocatalytic activity, it can be seen that the desired efficiency can be increased by using rutile and anatase forms in combination (Ohtani et al., 2010). In addition, nano TiO_2 improves reaction efficiency positively because it can easily transfer current from its surface (Carp et al., 2004). Studies on the physical properties of TiO_2 used in composites in the literature are shown in Tables 2.4 and 2.5.

Table 2.4 Physical properties of nano TiO_2 substituted cement binder composites

Purity/Form	Specific Surface Area (m^2/g)	Average Particle Size (nm)	References
99.9/-	150±12	15±3	Nazari and Riahi, 2011d
99.9/-	58.8	21	Chen et. al., 2011
99.9/-	150±12	15±3	Nazari and Riahi, 2011b
-/-	-	10-25	Shekari and Razzaghi, 2011
99.5/-	50±15	21	Lee et. al., 2013
97.0/Anatase	45-55	20-30	Lee et. al., 2013
-	-	60-75	Feng et. al., 2013
99.9/-	165±17	25±5	Jalal et. al., 2013
99.9/-	165±17	25±5	Jalal et. al., 2013
99.9/Anatase	240	15	Noorvand et. al., 2013
99.8/-	260	15	Salemi et. al., 2014
-	50	-	Ma et. al., 2015
-	-	20-100	Yang et. al., 2015
-	-	25	Zhang et. al., 2015
99.5/-	-	10-20	Rahim et. al., 2016
99.9	150	10	Li et. al., 2017
96/Rutile	-	20	Han et. al., 2017
99.9/-	20-30	10-20	Salman et. al., 2017

Table 2.5 Studies on cementitious composites containing TiO_2

Mixture content	Mold size/Test (mm)	Curing Condition	References
0.95W+ NT C+S 0.05W	50x50x50 (Compressive) 40x40x160 (Bending)	Water/23± °C	Salman et. al., 2017
W+NT+C	3x4x33 (3 point bending) 13φx25 (compressive)	Climatic cabinet ambient temperature	Feng et. al., 2013
W+NT+SP+SF C+FA S	40x40x160 (bending) 40x40x40 (compressive)	Water/20±1 °C	Li et. al., 2017
G+W	100x100x100 (compressive) 100φx200 (durability)	-	Rahim and Nair, 2016
W+SP+NT C+W	100x100x100 (compressive)	Ambient/20 °C	Salemi et. al., 2014
W+SP+NT Coarse Agg+S+C W+NT+SP S+C+0.75 (W+NT+SP) G+0.25 (W+NT+SP)	100x100x100 (compressive) 50x50x200 (bending)	-	Nazari and Riahi, 2011c
0.75W+NT+0.25 SP S+C	50x50x200 (bending)	Ambient/20 °C	Nazari and Riahi, 2011d
W+NT+SP C+FA+S	40x40x160 (bending) 40x40x40 (compressive)	Water/20± 1 °C	Han et. al., 2017
C+NT+S+G W	50x50x200 (bending)	Water/20 °C	Nazari and Riahi, 2011b

Mixture content	Mold size/Test (mm)	Curing Condition	References
C+W+NT	40x40x40 (compressive)	Climatic cabinet 25 °C, %95 humidity	Chen et. al., 2011
C+NT+S+G ½W+SP ½W+RHA	150x150x150 (compressive, RCPT) 200x50x50 (bending)	Water/20 °C	Jalal et. al., 2013
C+NT W+S+G	150x150x150 (compressive) 100x100x100 (water permeability)	Climatic cabinet /21± 2 °C, %95 humidity	Mohseni et. al., 2016
C+RHA 0.9W+NT S 0.1W+SP	50x50x50 (compressive, electrical resistivity)	Water/23± 3 °C	Mohseni et. al., 2015

Note: SP: Superplasticizers, **C:** Cement, **W:** Water, **S:** Sand, **G:** Aggregates, **BRHA:** Black Rice Husk Ash, **GGBFS:** Ground Granulated Blast Furnace Slag, **NT:**Nano Titanium Dioxide **RHA:** Rice Husk Ash

In a study examining the effect of nano-sized TiO_2 on the permeability, thermal and mechanical properties of self-settling high strength concrete (Nazari and Riahi, 2010a), compressive, tensile and bending test results were increased in case of TiO_2 substitution up to 4% of the binder weight. When the 90-day strength test results were examined, 50.1 MPa for compressive, 2.9 MPa for tensile and 6.3 MPa for bending were recorded as maximum strength results. It is understood that this increase in strength is due to the formation of more hydrate products in TiO_2 substituted state. In addition, nano-sized TiO_2 increased the water permeability of the samples under 7 and 28 days curing conditions. Up to 4% TiO_2 replacement rate, the time of the first peak in isothermal calorimeter is shortened. This is related to the rapid formation of hydration products. Thermogravimetric analysis showed that the weight loss of the samples increased up to 4% TiO_2 substitution rate. XRD results also support this situation. Nanosize TiO_2 substitution developed the pore structure of the self-settling concrete. (Nazari and Riahi, 2010a).

In a study investigating the effect of nanoscale particles on the durability and mechanical properties of high performance concrete (Shekari and Razzaghi, 2011), 1.5% by weight of the binder material nanoparticles (Nano-Fe_3O_4 (NF), Nano-ZrO_2 (NZ), Nano TiO_2 (NT) and Nano-Al_2O_3 (NA)) were used. While the highest compressive strength (119.0 MPa) was obtained in the mixture using nano Fe_3O_4, 113.3 MPa compressive strength was obtained in the mixture where nano TiO_2 was used. All of the nanoparticles analyzed increased the mechanical and durability properties of high performance concrete and the best results were obtained in the nano Al_2O_3 substituted sample (Shekari and Razzaghi, 2011).

In a study examining the hydration and properties of nano TiO_2-substituted cement-based composites (Chen et al. 2012), samples were prepared in mortar and paste phase by substituting TiO_2 at 0-5-10%. In the case of TiO_2 substitution in nano size, the peak value of the hydration heat was obtained in a shorter time. In addition, an increase in the peak value was observed if the replacement rate increased from 5% to 10%. Although there was not a huge increase in total hydration temperature, an increase in total hydration temperature was observed as TiO_2 replacement rate increased. Nucleation has occurred due to the accumulation of hydration products around the TiO_2 particles. Degussa P25, which also has particles of smaller size than anatase, has more surface area and accelerated the hydration reaction since it will provide more space for the accumulation of hydration products. Nano TiO_2 dosage significantly increased the amount of bound water, especially during the early curing times, causing the hydration reaction to accelerate. It was determined that TiO_2 which is an inert material does not have pozzolanic activity. In addition, it was observed in this study that the need for water would increase with the reduction of Nano TiO_2 particles.

In a study investigating the microstructure and mechanical properties of nano TiO_2-substituted cement paste (Feng et al. 2013), samples were prepared with 0.9% TiO_2 substitution of cement weight. While the average bending strength of 28 days in samples prepared with cement was 11.78 MPa, the average bending strength of samples obtained with 0.9% TiO_2 substitution of cement weight was measured as 13.68 MPa. So, an increase of 16.12% has been achieved. Similar results were obtained in compressive strength, while the average compressive strength in samples prepared with cement was 57.37 MPa, while the average compressive strength was measured as 65.49 MPa in samples obtained with 0.9% TiO_2 substitution of cement weight. In other words, an increase of 14.15% has been achieved. Nano TiO_2 particles with microstructural properties have formed a dense structure by filling the gaps between the cement grains (Feng et al. 2013).

Investigating the effects of nano-sized TiO_2 on the properties of cement-based materials, Lee and other authors found that the nano TiO_2 (P25) substitution accelerated hydration reactions at an early age (Lee et. Al. 2013). The degree of this acceleration increased at higher dosages (10% TiO_2 substitution provided a 46% increase in the degree of hydration at 12 hours.). On the other hand, in the case of 10% P25 substitution, the shrinkage increased by 53%, which is directly related to the increasing degree of hydration. It has increased the degree of hydration more than anatase due to the fact that P25 can be dispersed more into the mixture. When 0.40 is used as water / cement ratio in the composites, it increases the compressive diffusion in the substitution conditions up to 10% of the cement weight where P25 is used.

In a study examining the strength and durability properties of nano TiO_2 substituted cement-based materials (Ma et al., 2015), the tensile strength of the nano TiO_2 substituted sample increased by 65% compared to the control sample and increased bending strength by 61.9%. However, a decrease in strength was observed in higher substitution rates (4-5%). The reasons for the increase of this change in cement-based material were determined as the nucleation effect and the change of the crystal structure of $Ca(OH)_2$ (Ma et al., 2015).

Zhang et al. (2015) examined the effect of nano TiO_2 substitution on hydration reactions and drying shrinkage of cement-based materials. As in the similar studies mentioned above, in the case of TiO_2 substitution, the total pore volume decreased and the hydration rate increased. In connection with these reasons, an increase in compressive strength was observed. The mortar had a denser structure, therefore drying shrinkage was also reduced with TiO_2 substitution. The increase of hydrophilic property of the composite and the decrease of pores was shown as the reasons for this situation. (Zhang et al., 2015) With the substitution of TiO_2, which has smaller dimensions than the other two nanoparticles, concrete has formed in a denser structure. It was also determined that TiO_2 substituted mixtures are more resistant to acidic and salt-containing environments (Rahim and Nair, 2016). In a study conducted by Salman et al. (2017), the effect of nano TiO_2 substitution on the compressive and flexural strength of cement mortars was examined. The addition of nanoparticles up to 0.75% of the cement weight has increased compressive and flexural strength. As in similar studies, nano TiO_2 substitution reduced $Ca(OH)_2$ and crystal sizes. In addition, the increase in the replacement rate up to 1.75% was found almost at the same level with the control sample in mechanical properties. (Salman et al., 2017).

2.5. The Existing Standards of NO_x Degradation

Dynamic and static tests are generally used to determine NO_x conversion efficiency. In the dynamic method, the NO or NO_x gas touches the surface of the samples at a constant flow rate, and the NO_x concentration is continuously measured in real real-time. In a static test, a certain amount of NO gas is given to an environment where the sample is located, and it is circulated as a closed circuit in the reaction chamber (Maggos et al., 2007b).

There are 3 different dynamic test standards on the basis of the most widely used in the literature on NOx reduction. These are Japan's JIS R 1701-1, Italy's UNI 11247 and ISO 22197-1 standards. The measurement and evaluation methods of these standards are explained below.

2.5.1. JIS R 1701 -1 Standard

The JIS R 1701-1 standard from 2004 is a standard method for cement-based materials based on nitric oxide (NO) removal to determine the air cleaning performance of photocatalytic materials. In this method, gas flow (NO) is provided from a reactor where samples are placed and UV ray is sent to the sample from the top of a transparent reactor (Figure 2.9). The NO gas delivered to the system at a certain concentration and speed is measured with a chemical NO_x analyzer at the exit of the reactor. After the photocatalytic test, the separation test is performed on the test to measure the nitrate (NO^{3-}) and nitrite (NO^{2-}) ions produced during the reaction. With this test, changes in the NO gas supplied to the system enable the nitrogen oxide-nitrogen oxide (NO_x) reduction test results to be evaluated.

In the JIS standard, with a permanent flow of reactant gas (dynamic method), it flows to the surfaces of the sample to be tested, and the reactant and gas concentration are continuously measured by a chemistry NOx analyzer. NO gas at a concentration of 1 ppm is used in the test. During the test, the gas flow rate should be 3.0 L / min, relative humidity 50% and ambient temperature 25.0 °C ± 2.5 °C. In the system, a UV lamp with a wavelength of 300 nm to 400 nm is used as the UV light source and the radiation on the sample surface must be 10 W / m^2. The dimensions of the photocatalytic sample to be tested are in the form of a flat plate 49.5 mm ± 0.5 mm wide and 99.5 mm ± 0.5 mm long. The distance between the sample surface and the top plate of the reactor cabinet should be 5 mm. For the adsorption process, the gas must be tested under dark environment before UV light illumination until the concentration of NOx exceeds 90% of the desired concentration before UV light illumination. UV irradiation is continued for 5 hours for the photocatalytic reaction. The experiment can be completed if the NOx concentration remains constant before this period. The samples are exposed to gases and the photocatalytic conversion is measured according to the following equation using an integral of the difference between the inlet and outlet concentration of the gas.

$$\eta_{ads} = Q_{ads} = (f/22{,}4)\ x \left\{ \int_0^T ([NO_X]_i - [NO_X]_O)dt \right\}$$

f	Conversion of air flow rate to standard (0 ^{0}C and 101.3 kPa)
$\eta_{ads} = Q_{ads}$	Gas adsorbed by the test sample (µmol)
$[NO_X]_i$	Input concentration of NO_x gas (µl / 1 or ppm)
$[NO_X]_O$	Output concentration of NO_x gas (µl / 1 or ppm)
T	Time

The NO_x conversion efficiency of the test sample is verified by detecting the nitrate (NO_3^-) and nitrite (NO_2^-) ion produced in the test sample.

This standard also allows the determination of the decomposition of nitrate and nitrite ions produced during the test. Using the sets of equations, the amount of NO_x lost and formed, and the amount of NO_x absorbed and not absorbed can be calculated with the test sample.

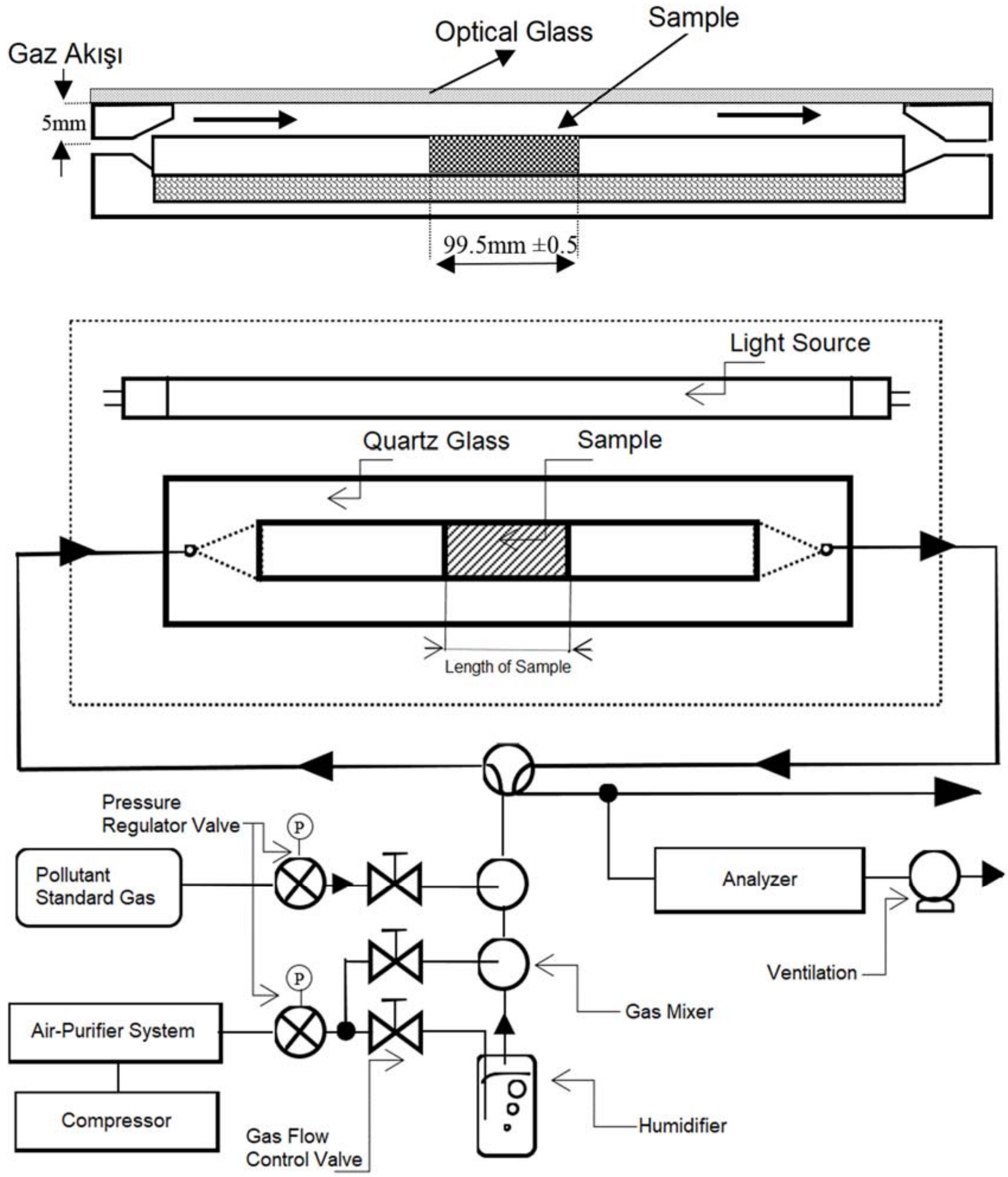

Figure 2.9 Scheme of test equipment for evaluating air purification performance (JIS R 1701–1:2004)

2.5.2. ISO 22197-1:2016 Standard

The ISO 22197-1 standard is a standard obtained by taking into account the JIS R 1701-1 standard. The photo-reactor system includes an airtight stainless steel box with glass on top (**Figure 2.10**). The glass on the sample, which has a surface area of 0.0929 m^2 (1 ft^2), allows UV light to be stored by passing through the sample surface. There is a 5 mm (0.20 inch) gap between the bottom of the glass and the top of the sample. Air containing NO_x is delivered to the sample section at a flow rate of 3 L / min at 1.0 ± 0.1 ppm. The NO_x analyzer tests the NO_x contamination concentrations from the waste gas line passing through the sample surface. When testing materials containing TiO_2, UV light sources have an average capacity of 13 W/m^2. During the experiment, the relative humidity of the environment is 50% and its temperature is kept at 25 ° C. During the test, NOx concentration, gas flow rate, relative humidity and temperature values are kept within the specified range. In the ISO 22197 standard, it is clearly stated that the UV light intensity value should be 10 ± 0.50 W/m^2. However, in order to test the UV effect, the concentration of the UV light can be reached to the sample surface at 1300, 950, 700, 550, 350 and 150 ± 50 $\mu W / cm^2$ average values. UV rays vary widely depending on seasonal conditions, time of day, weather conditions, and shading. While the average UV light reaching a place exposed to the sun on a summer day was determined to be at most 1300 $\mu W/cm^2$, it was determined to be 150 $\mu W/cm^2$ in a shady environment in spring or autumn. In this test method, the test is done for 5 hours. For the first and last 30 minutes, the UV light source is turned off to ensure the system stabilizes. In the 30th minute, the UV light source is turned on and the system continues to measure for 60 minutes. The mean concentration is evaluated between the first and last 30 minutes of the test. The average reduced NO_x concentration is found by taking the average value in 60 minutes from the 30th minute when the UV light source is on to the last 30 minutes. In case the output concentration in the NO_x analyzer becomes stable, the experiment can be terminated before 5 hours. The photocatalytic efficiency can be determined for each sample using the following equation.

$$Photocatalytic\ Effect(\%) = \frac{Concentration_{initial} - Concentration_{induced}}{Concentration_{initial}}$$

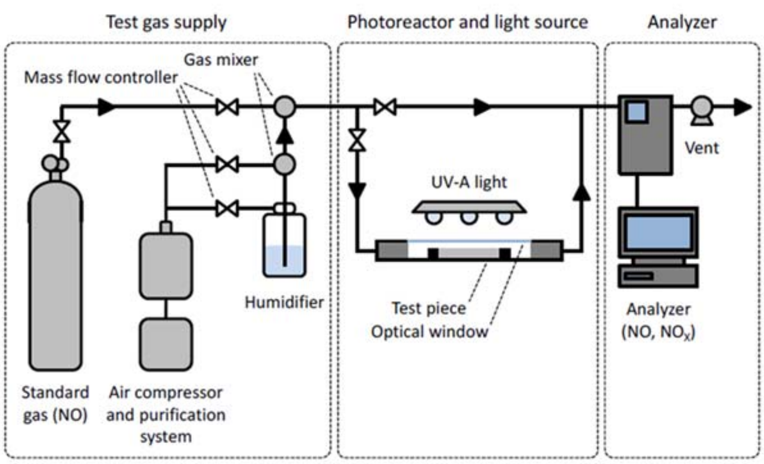

Figure 2.10 Schematic representation of ISO 22197-1 test equipment

2.5.3. UNI 11247 Standard

The UNI 11247 standard was developed by the Italian Standards Organization (UNI) to determine the reduction of photocatalytic inorganic materials and nitrogen dioxides (Figure 2.11). This test is a "dynamic" method with a continuous flow of NO_x gas, similar to JIS R 1701-1 and ISO 22197-1 tests. The concentration of gases is different from previous tests. A total of 0,55 ppm NO_x gas consisting of 0,15 ppm NO_2 (Nitrogen dioxide) and 0,40 ppm NO (Nitrogen monoxide) is used. The UV ray intensity is 20 W/ m^2 at the sample surface, which is twice the JIS / ISO value. Gas flow is tested for 1 hour. With a NO_x concentration of 0,55 ppm, 0,15 ppm NO2 and 0,40 ppm NO, gas flow occurs at a flow rate of 3 L / min. Other parameters used are similar to the ISO and JIS standard tests described above.

One of the important differences that distinguishes the UNI 11247 standard from the other two standards is the combination of NO and NO_2 of the gas used in the test. The advantage of using mixed gas is that it reflects the actual environmental condition, so the results of the photocatalytic effect can be used to estimate how it works under real environmental conditions. The conversion of NO and NO_2 to each other under photocatalytic reaction is also an important consideration. However, due to the conversion of NO and NO_2 to each other, analytical work may not always be suitable for investigating the detailed oxidation mechanism. In photocatalytic reactions, it may take more than one hour for gases to stabilize in a sample exposed to NO_x gas. Therefore, the short-term UNI 11247 test may not be suitable for some materials.

Another difference of this standard from JIS and ISO standards is that it is specially prepared for cement-based materials. With this customized method, it can be used more than JIS / ISO standards. The results of the UNI standard method are calculated as percentage NO_x reduction. In addition, photocatalytic activity can be calculated from the gas concentration measurement. This is a more practical method than measuring the amount of product (nitrate and nitrite ions) removed by photocatalysis.

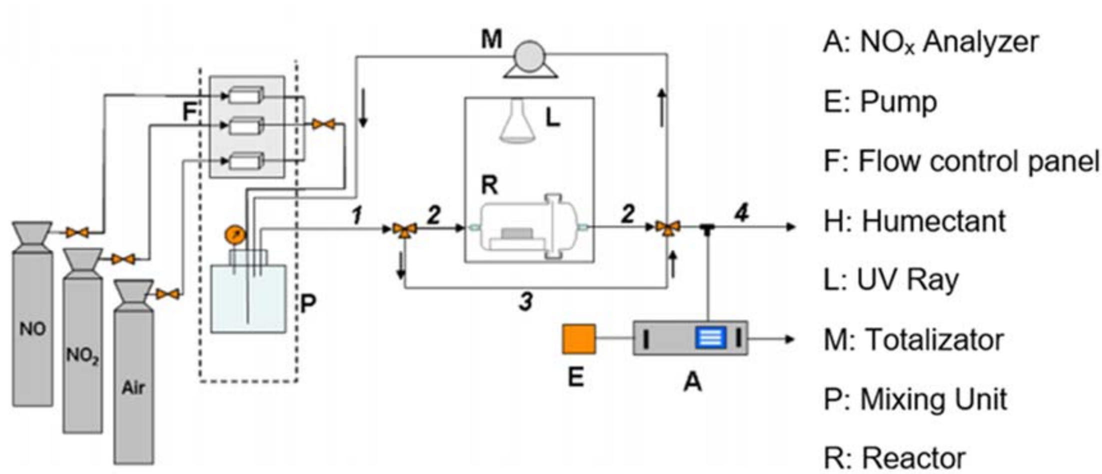

Figure 2.11 Schematic representation of UNI 11247 test equipment

The photocatalytic property and standards used in the determination of NOx reduction, explained in detail above, are shown comparatively in Table 2.6 below.

Table 2.6. Comparison of NO_x reduction standards

		ISO 22197-1	JIS R 1701-1	UNI 11247
Test Parameters	Gas	NO	NO	NO and NO_2
	Gas Concentration	1000 ppb	1000 ppb	400 ppb NO + 150 ppb NO_2
	Gas Flow Rate (L/min)	3	3	3
	Testing Time	5 Hours	5 Hours	1 Hours
	UV Irradiance (W/m^2)	10	10	20
Specimen Properties	Specimen Surface Area (cm^2)	49.25	49.25	65
Analysis Parameters		η_{ads} (pollutant gas absorbed)	η_{ads} (pollutant gas absorbed)	NO_x reduction percentage

2.5.4. Other Test Methods

In addition to the standards mentioned above, there are some methods applied in terms of photocatalytic property comparison (Table 2.7).

Table 2.7 Overview of international standards related to TiO_2 photocatalysis as of 2008

Performance attributes	Principle of test method	Japanese and Italian Standard
Air purification effect	Nitric oxide removal ISO 22197–1:2007 (International)	JIS R 1701–1:2004
		UNI 1247:2007
	Removal Volatile Organic Compound	UNI 11238–1:2007
		11238–2:2007
	Acetaldehyde removal	JIS R 1701–2: 2008
	Toluene removal	JIS R 1701–3: 2008
Water purification effect	Active oxygen-forming	JIS R 1704:2007
Self-cleaning effect	Water contact angle change	JIS R 1703–1:2007
	Methylene blue decomposition	JIS R 1703–2:2007
	Rhodamine	UNI 11259:2008
Biocidal effect	Antibacterial activity	JIS R 1702:2006
	Antifungal activity	JIS R 1705:2008
-	Light source for test under UV irradiation	JIS R 1709:2007

3. MATERIALS AND METHODOLOGY

Materials and methods used in the design of photocatalytic composites are described in this section.

3.1. Materials Used in Experimental Studies

3.1.1. Cement

The CEM I 52,5 R White Portland cement (WPC) complying with ASTM C150 was used as the main binder material for all mixtures. Physical properties and chemical composition of WPC are given in Table 3.1. The selected cement complies with TS EN-197-1 (2012) and ASTM C150 (2007) cement standards.

Table 3.1 Chemical composition and physical properties of CEM I 52,5 R WPC

Chemical Composition, %							Physical Properties	
SiO_2	Al_2O_3	Fe_2O_3	CaO	MgO	SO_3	Loss of ignition	Density (g/cm^3)	Specific surface, Blaine (cm^2/g)
21.39	3.37	4.89	62.6	2.39	4.55	3.1	3.15	4650

3.1.2. Titanium Dioxide (TiO_2)

In the study, anatase form of TiO_2 was used with nano particle sizes as nano (10-20 nm) TiO_2 powder used in this study was characterized by using scanning electron microscope (SEM) (Tescan GAIA 3 FIB-SEM operated at 3.0 kV) and X-Ray diffraction measurement (XRD) (Rigaku Ultima-IV diffractometer at 40 kV, within a scan range of 2θ=5–55° and 30 mA with Cu-Kα (λ=1.5405Å) radiation.). To avoid any misleading results, a true representative sample of powder, weighing a few grams, was taken from the core of the powder batch of nano anatase TiO_2 and was dried overnight in an oven before testing. The SEM micrograph image and XRD pattern of the nano-sized anatase form of TiO_2 are shown in Figure 3.1. Considerably small size and extremely rough surface morphology of the nano-TiO_2 particles can be seen from Figure 3.1a and the diffraction peak value of 25.4°, that can be seen from Figure 3.1b, validated the anatase phase/structure of TiO_2 used in this study (Ba-Abbad et al., 2012; Theivasanthi and Alagar, 2013).

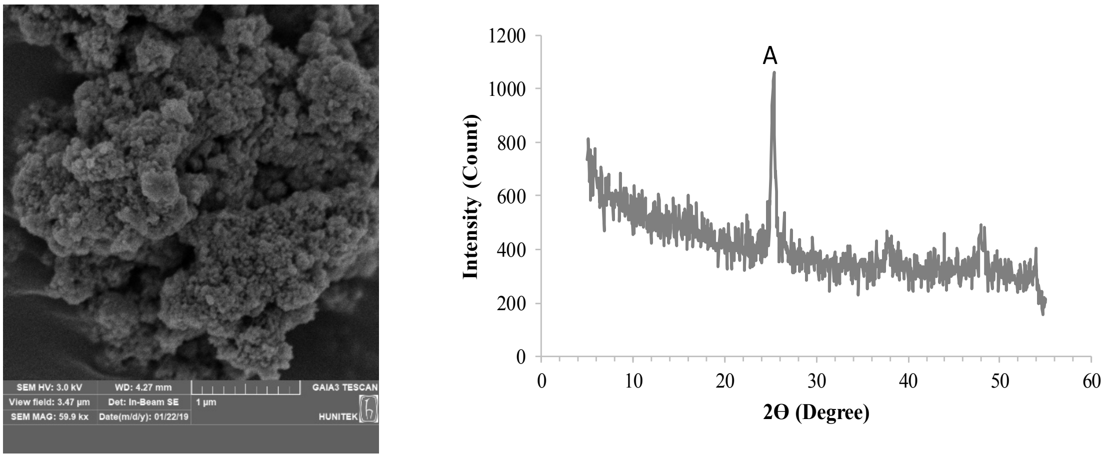

a) b)

Figure 3.1 a) SEM micrograph, b) XRD analysis of nano-sized anatase TiO_2

Digital camera, SEM image and EDX analysis of nano anatase form (NA) used in experimental studies are shown in Figures 3.2.,

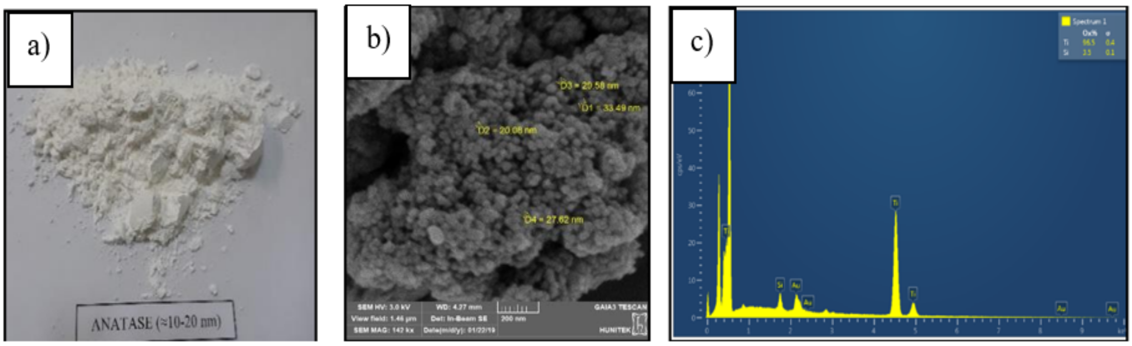

Figure 3.2 a) Nano anatase TiO_2 digital camera image, b) SEM image, c)EDX analysis

The grain size analysis of nano particle size TiO_2's were analyzed by using nanosizer in Abdullah Gül University Civil Engineering Laboratory. In addition, grain and chemical characterizations of the TiO_2 used were obtained by using multi-point BET surface areas and XRF analysis. The grain size, physical and chemical properties of TiO_2 are shown in Table 3.2.

Table 3.2 Physical properties of Nano Anatase TiO_2

Physical Properties	Type
	Nano Anatase TiO_2
Purity (%)	99.86
BET* (m^2/g)	79.6
Density (gr/cm^3)	3.55
Average Grain Size	10-20 nm
Maximum Grain Size	50 nm
Minimum Grain Size	10 nm

BET: Brunauer–Emmett–Teller surface area

3.1.3. Surfactant Materials

Two different surfactant materials including superplasticizer satisfying minimum requirements of ASTM-C494/C494M standard and polyacrylic acid were used to ensure homogeneity of mixtures and better dispersion of nano TiO_2 powders. Polycarboxylic ether-based superplasticizer (PCE) manufactured by BASF Construction Chemicals with MasterGlenium 51 commercial name were used to disperse TiO_2 powders easily. The superplasticizer is in a liquid form contains 40% solid material and its specific gravity was 1,1. Polyacrylic acid (PAA) consisting of polyphosphates and amino carboxylate manufactured by Acar Chemicals were used to control particle surface charges with its polyelectrolyte dispersant feature.

3.2. Methods Used in Experimental Studies

3.2.1. Determination of Suitable Mixing Parameters for TiO_2 Dispersion

Due to the agglomeration and sedimentation problem of TiO_2 in a suspension and consequently in a fresh cement-based mixture, different innovative mixing methods were used in addition to the mixing methods used in the literature (Mendoza et al., 2013; Saafi et al., 2013; Kim et al., 2014; Al-Dahawi et al., 2016). In total, 5 different mixing methods were implemented to disperse TiO_2 powders in cement-based mixtures. Vibra-Cell ultrasonic mixer with a 25 mm probe diameter that can be operated for different amplitudes (0-100%) and energy levels (0-9999 Joule), high-speed hand blender and conventional cement mixer were tested to obtain the feasible and cost-effective mixing method which also provide the better dispersion of TiO_2 (Figure 3.3).

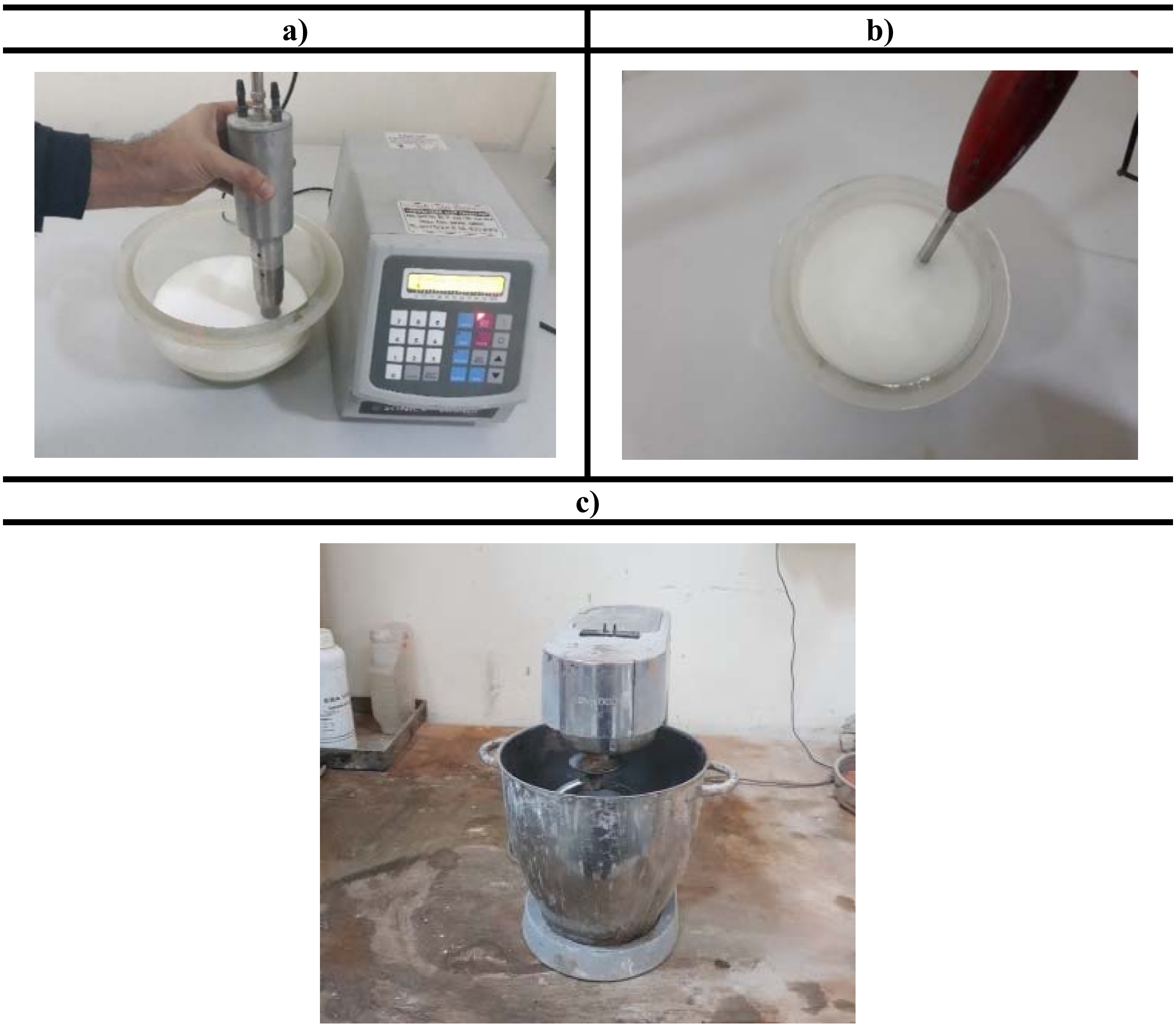

Figure 3.3 a) Ultrasonic mixer, b) High-speed hand blender, c) Conventional cement mixer

Optimum amplitude and energy value of the ultrasonic mixing process for more homogeneous dispersion of nano-TiO_2 were determined by comparing the duration of suspense for nano TiO_2 particles in the solution. The influence of ultrasonic mixer amplitude value on the zeta potential of suspension was investigated. For this purpose, the ingredients of the solutions were determined based on the nano TiO_2 and water content of a reference mixture with water-to-binder ratio of 0.33 containing different percentages of nano TiO_2 by total weight of binder materials. Therefore, 140 ml water and 20 gr nano-TiO_2 were mixed for 10 minutes with different amplitude values and constant 1100 J energy inputs. The zeta potential values of the suspensions for different amplitude values were shown in Figure 3.4. Zeta potential results of suspensions clearly increased negatively with the increase of amplitudes of ultrasonication. This means that high amplitude values provide a significant dispersion of TiO_2 particles leading to increase in suspension stability as a result of more repulsive force application of nanoparticles on each other.

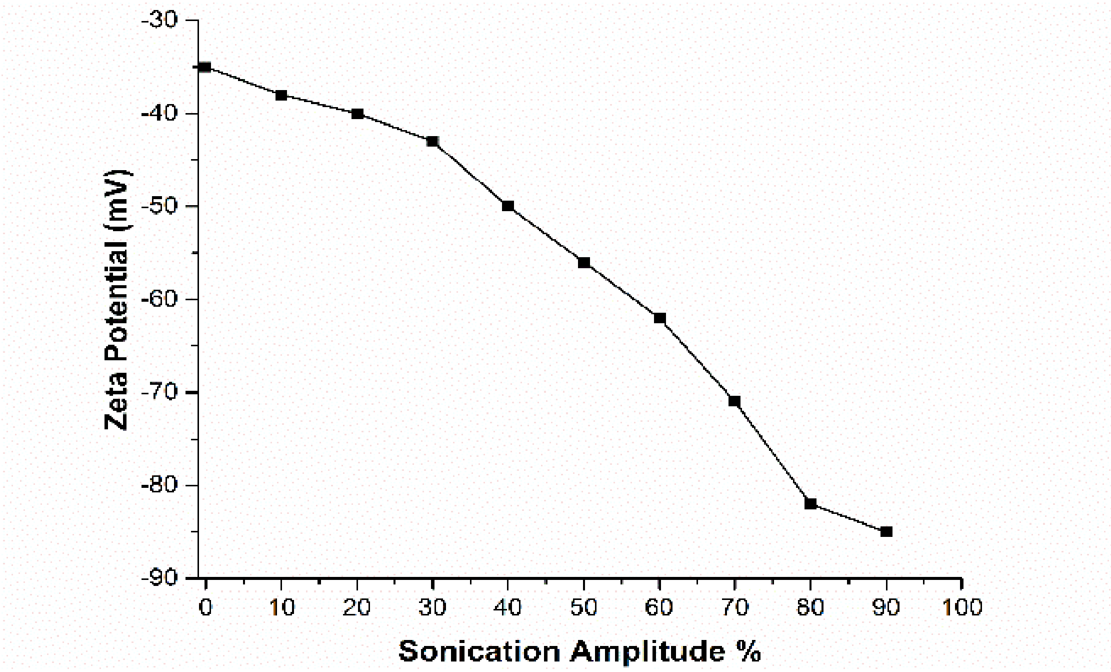

Figure 3.4 The influence of amplitude modification on zeta potential (mV) of suspensions

After the investigation about the effect of different amplitude values on the zeta potential measurement, the combined effect of the implementation of sonication with different amplitude and energy input on suspension stability was examined with same solution composition and mixing time used before. The amplitude and energy input values used in the experiment were given in Table 3.3.

Table 3.3 List of amplitude and energy input values of ultrasonic mixer used for mixing process

Label	Amplitude (%)	Energy (J)
D-1	40	1000 J
D-2	80	1000 J
D-3	40	1900 J
D-4	80	1900 J
D-5	40	4000 J
D-6	80	4000 J

The solutions prepared with given mixing parameters were stored under the same environmental condition and were observed during the suspension period. The suspense states of solutions for different periods were shown in Figure 3.5, respectively.

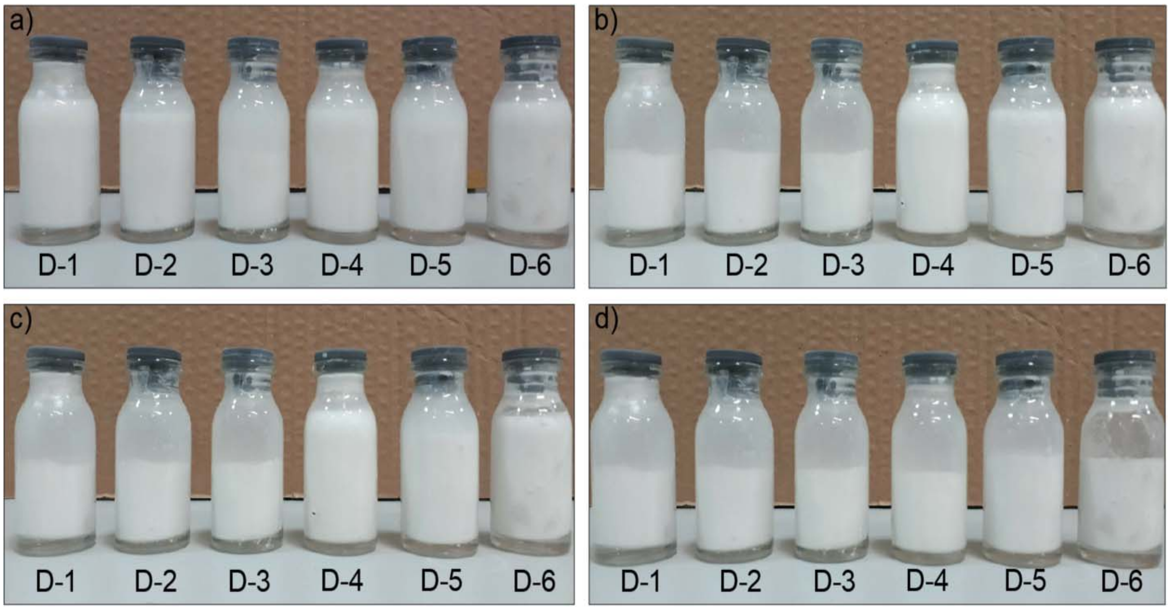

Figure 3.5 The dispersion states of nano TiO_2 for different periods a) 15 minutes, b) 30 minutes, c) 1 hour, d) 2 hours

Increment of amplitude and energy input values caused a remarkable increase in the duration of suspension. Nano-TiO_2 particles completely precipitated for the D-1 and D-3 solutions in the first 30 minutes. However, this was not the case for D-5 mixed with ultrasonication by using the same amplitude value with them. Due to high energy input of D-5, the nano-TiO_2 did not completely collapse even after 1 hour. Although nano TiO_2 particles of D-2 solution collapsed in 30 minutes with the amplitude of 80%, D-4 and D-6 did not show any precipitation in 1-hour period. In line with all these observations, D-4 solution were selected to be used in later stages of the study due to sufficient performance for the duration of suspense with optimum energy inputs for ultrasonic mixing process.

In the current study, the effect of the utilization rates of surfactant materials on the zeta potential of suspension was also investigated. To this end, the ultrasonic mixer was used with 40% amplitude and 1100 J energy input. Solutions were prepared as previously described. So, 140 ml water, 20 gr nano-TiO_2 and relevant surfactant materials were mixed for 10 minutes.

The effect of PCE on the zeta potential of suspension was studied with utilization rates of 0.5%, 1%, 1.5% and 2% by total weight of binder materials. The effect of PCE as a surfactant material on the zeta potential of suspensions can be seen from Figure 3.6. According to this graph, zeta potential value increased negatively up to 1.5% utilization rate of PCE and reached its maximum value as -55mV. When the utilization rate of PCE exceeded 1.5%, a negative decrease started from this point in the zeta potential value. Therefore, it can be said that the optimum utilization rate for superplasticizer regarding zeta potential can be determined as 1.5%. The suspensions including PAA up to 4% of binder materials by weight were also prepared in order to evaluate the effect of PAA on the zeta potential of suspensions. Zeta potential value increased negatively up to 2.0% utilization rate of PAA and reached its maximum value as -65mV. A negative decrease for zeta potential started beyond this point (Figure 3.6). In the case of binary utilization of PAA and PCE with an equal rate, zeta potential value increased negatively up to 2.0% total utilization rate of PAA and PCE (1%+1%) and reached its maximum value as -62mV. A negative decrease in the zeta potential value started beyond this point (Figure 3.6).

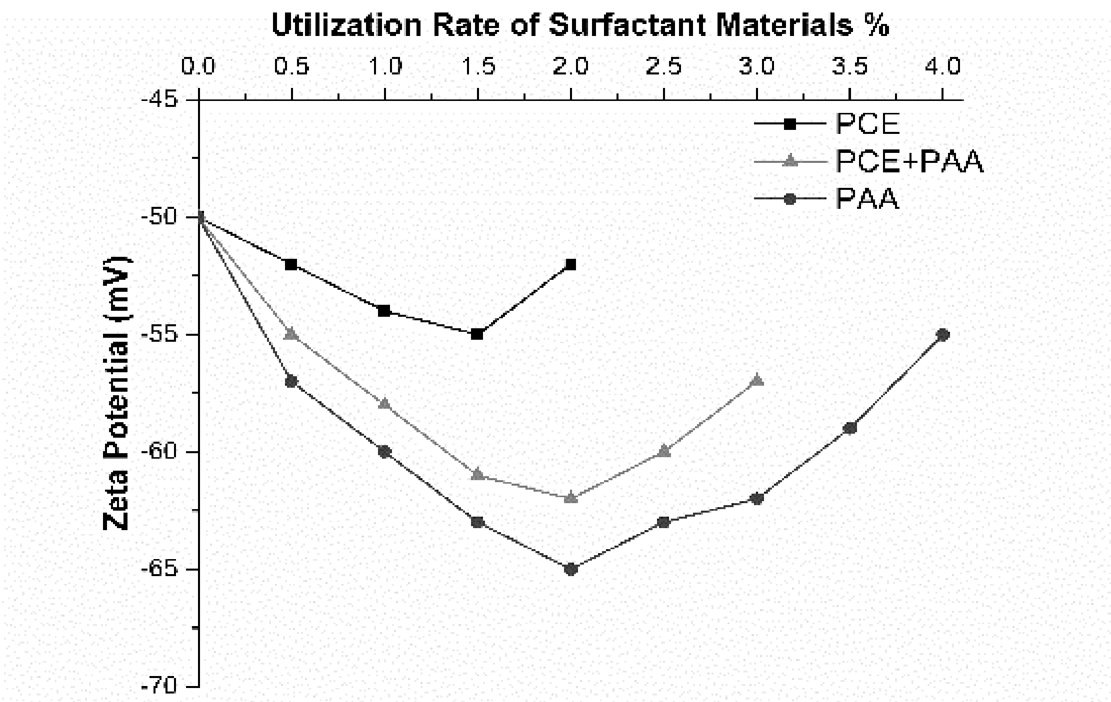

Figure 3.6 The effect of the utilization rate of surfactant materials on zeta potential of suspension

After the evaluation of zeta potential measurement values according to surfactant material content of suspensions, the solutions with the same composition and mixing time used for zeta potential measurements were prepared by using different proportions of the surfactant materials. Although solutions made with surfactant materials required relatively higher dosages to achieve optimum zeta potential values, it can be ensured by using surfactant materials at lower rates that can provide a sufficient time period to sustain dispersion of the TiO_2 until the beginning of the initial setting time of the concrete. Because it can be provided that keeping TiO_2 particles as scattered due to the beginning of concrete hardening. According to the studies of Alqedra et al. (2014) and Majekodunmi and Deb, (2007) in case of use of PAA more than a certain level, it has a negative effect on the strength of concrete. In addition, the increase in surfactant utilization rate in concrete causes less compressive strength and elastic modulus compared to nonsurfactant concrete (Kim et al., 2010). Therefore, it should be taken into consideration what kind of changes occurs in the hydration process and mechanical properties of cement-based composites for high utilization rates. There is also an extra cost for concrete production incurred by the use of surfactant materials. Taking all these into consideration, the utilization rates of surfactant material that can be seen from Table 3.4 determined without endangering sufficient period for dispersion of TiO_2. The prepared solutions were stored under the same environment condition and the precipitation state of TiO_2 particles was observed for different periods. The precipitation state of solutions for different periods are displayed in Figure 3.7, respectively.

Table 3.4 Utilization rates of surfactant materials (% by total weight of binder materials)

Label	Super Plasticizer (%)	Polyacrylic Acid (%)
S-1	-	-
S-2	0.5	-
S-3	0.5	0.5
S-4	-	0.5
S-5	1	-
S-6	-	1
S-7	1	1

Figure 3.7 The dispersion states of nano TiO_2 for different periods a) 2 hours, b) 1 month, c) 3 months, d) 6 months

3.2.2. Dispersion Methods of TiO_2 Solution

New methods in the light of preliminary studies explained before to obtain a homogenous mixture have been tried to determine their availability on the dispersion of TiO_2 within the cement matrices. In total, five mixing methods were proposed to enhance the dispersion of nano TiO_2 and improve photocatalytic performance without endangering the mechanical properties of the produced cement-based matrixes.

1st mixing method: This method was used for the preparation of reference specimens and formed as a modification of the standard mortar mixing method specified in TS EN 196-1 utilized for the paste phase. According to this method, the following steps were performed: All dry raw materials (TiO_2 and WPC) were mixed in a 5-liter-capacity conventional cement mixer at 100 rpm for 10 minutes. Mixing water was added into the raw materials over 30 s while mixing was in progress at 100 rpm. Then, the speed of mixing was increased to 300 rpm and all the PCE (1%) was added to the mixer over 30 s. Finally, all these materials were mixed for an additional 10 minutes at 300 rpm (Musso et al., 2009).

2nd mixing method: In this method, the TiO_2 and PCE (1%) were added to the mixing water and ultrasonication was applied for 10 min with 80% amplitude and 1900 J energy inputs.

After ultrasonication process, this suspension was slowly added to the WPC in the 5-liter-capacity conventional cement mixer operating at 100 rpm over 30 s. Then, the speed of mixing was increased to 300 rpm and mixing was continued for additional 10 minutes at 300 rpm (Moore et al., 2003; Saafi et al., 2013; Sobolkina et al., 2012).

3rd mixing method: TiO_2, PCE (1%) and all of the mixing water were mixed by using a hand blender for 10 min at 3000 rpm. After that, this suspension was slowly added to the WPC in the 5-liter-capacity conventional cement mixer operating at 100 rpm over 30 s. Then, the speed of mixing was increased to 300 rpm and mixing process of all these ingredients (WPC, TiO_2, water and PCE) was continued for additional 10 minutes at 300 rpm.

4th mixing method: In this method, it was intended that the evaluation of the effect of PAA on the dispersion of TiO_2 particles in the cement-based composites. Therefore, PAA was used alone by 0.5% of the total weight of binder materials. TiO_2 and all of the mixing water were mixed for 10 min by using ultrasonic mixer with 80% amplitude and 1900 J energy inputs. PAA was slowly added to this mixture during ultrasonication process. At the end of this, the suspension was slowly added to the WPC in the 5-liter-capacity conventional cement mixer operating at 100 rpm over 30 s. Finally, the speed of mixing was increased to 300 rpm and all of these ingredients (WPC, TiO_2, water and PAA) were mixed for additional 10 minutes at 300 rpm.

5th mixing method: Binary of PAA and PCE (0.5%+0.5% of the total weight of binder materials) were used to evaluate combined effect of them on the dispersion of nano TiO_2 particles in the cement-based composites. All of the ingredients except WPC were mixed for 10 min with the help of using ultrasonic mixer with 80% amplitude and 1900 J energy inputs. The suspension obtained at the end of ultrasonication process was slowly added to the WPC in the conventional cement mixer operating at 100 rpm over 30 s. As the final step, the mixing speed was set to 300 rpm and mixing of all materials (WPC, TiO_2, water, PCE and PAA) were continued for additional 10 minutes at 300 rpm.

3.2.3. Specimen Preparation and Testing

In the current study, specimens were manufactured to assess the performance of different mixing methods using TiO_2 at nanoscale by measuring photocatalytic performance, electrical impedance and compressive strength. In this context, the mixtures prepared with different mixing methods were poured into the oiled molds and cured at laboratory environment for 24 hours. After 24 hours initial curing, specimens were de-molded and further cured in water at room temperature (23 ± 1) until the time of testing. At the day of testing, the specimens were taken out of the water, wiped and surface dried.

3.2.4. Compressive Strength

Compressive strength test was conducted on cubic specimens with a dimension of 50 mm by following the ASTM C109 standard. The tests were performed at 7 and 28 days under uniaxial loading a rate 0.9 kN/s. For each mixing method, six replicates were tested for each curing age and results were averaged.

3.2.5. Electrical Impedance (EI) Test

For EI measurements of cement-based composites, two Ø100×50 mm cylindrical specimens were prepared using each mixing method. Ø100×50 mm cylinder specimens were extracted from the larger cylinders with a diamond blade. Considering the possibility of inaccuracy in EI measurements due to troweled and/or molded surface conditions, the top and bottom ~1 cm of each cut specimen were not used to determine electrical property. Consequently, for each mixing method, six Ø100×50 mm-cylindrical pieces were used for EI tests at 7, 28 and 90 days (Figure 3.8a) and results were averaged.

A 2-probe electrical resistivity meter – which gives impedance results using alternating current (AC) impedance, works with frequencies from 1 Hz to 30 kHz and detects the phase angle between 0° and 180° – was used to measure EI (Figure 3.8b). According to Hou (2008), polarization effect can be eliminated with a frequency of at least 1 kHz AC current application, therefore a 1 kHz operating frequency was chosen for this study. In this configuration, cylindrical specimens were placed between two parallel plate electrodes, with wet sponges 10 mm high and 150 mm in diameter used to ensure adequate electrical contact between the specimen and electrodes. Sponges were each saturated with the same amount of water to eliminate any deflection of the EI measurement results.

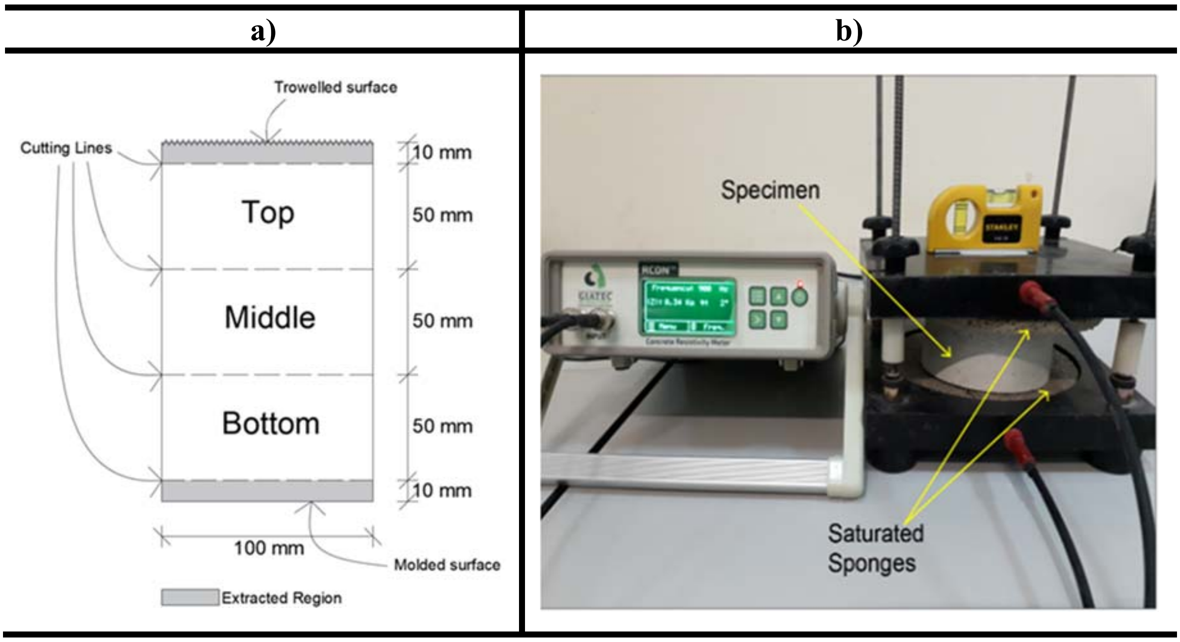

Figure 3.8 a) Specimen preparation, b) Concrete resistivity meter and testing of a specimen

3.2.6. Tomography Imaging and SEM Characterization

The dispersion of nano-TiO_2 particles throughout the matrix was also evaluated using a computed tomography device (CT) for non-destructive testing of Ø18×20 mm cylindrical specimens (Figure 3.9). Cross-section images from the CT scan were pre-treated for the nano-TiO_2 particles to be clearly visible. SEM/EDX (Energy-dispersive X-ray spectroscopy) mapping images, which identify the elemental composition of the analyzed specimen and show distribution states of chemical elements via elemental mapping by using representative colors of each certain element, were also used to observe the dispersion and/or agglomeration of the nano-TiO_2 particles in the matrix. Small portion of specimens taken from tested cubic specimens under compressive strength test were oven-dried overnight and their SEM-EDX mapping images were captured.

a)

b)

Figure 3.9 a) Computed Tomography Device, b) Test Specimens

3.2.7. Photocatalytic Efficiency

In this study, photocatalytic efficiency of the specimens was measured by using dynamic test method. According to this method, NO or both of NO and NO_2 gases flow at a constant rate and are in contact with the surface of the specimens. The NO_x concentration is continuously measured in real time to compare the input and output concentration of gases associated with photocatalytic degradation (Cassar et al., 2007; Jalayapan et al., 2015). The testing parameters are summarized in Table 3.5.

Table 3.5 Testing parameters used in this study

Testing Parameters	
Type of Gas	NO
Gas Concentration (ppb)	1000±50
Gas Flow Rate (L/min)	3
Test Duration (Min)	30
UV Light Intensity (W/m^2)	10
Specimen Surface Area (cm^2)	50±1
Analyze Method	NO_x degradation %

The photocatalytic activity measurement system that used to determine NO degradation capability of specimens, was given in Figure 3.10 and schematized in Figure 3.11.

Photocatalytic performance was determined according to the degradation of NO gas applied to the surface of 50×50×100 mm^3 test specimens while the UV light source was on. A flow of 1000 ± 50 ppb (particle per billion) of NO gas was maintained at a rate of 3.0 l/min from a 5 mm distance, between the 50 ± 1 cm^2 specimen surface and quartz glass, which is permeable to UV light. Specimens were illuminated with two Osram brand 18W UV-a blue lamps and one Philips brand 36 w (UVA-1) white lamp. The light irradiance was adjusted to 10 W/m^2 by a light intensity controller and was kept between 350 and 450 nm. NO gas, regulated in terms of flow rate and concentration, was moistened about 50-60% in the humidifying bottle before contacting the specimen surface. The NO gas used in the experiments was diluted from 100 ppm to 1 ppm using dry air. The NO gas supplied for the system at 1 bar pressure was continuously measured using the Thermo Scientific Model 42i NO_x analyzer. The flow rate was set and fixed to 3.0 l/min during the test and the initial concentration of NO gas from the NO_x analyzer was checked to ensure flow concentration of 1 ppm.

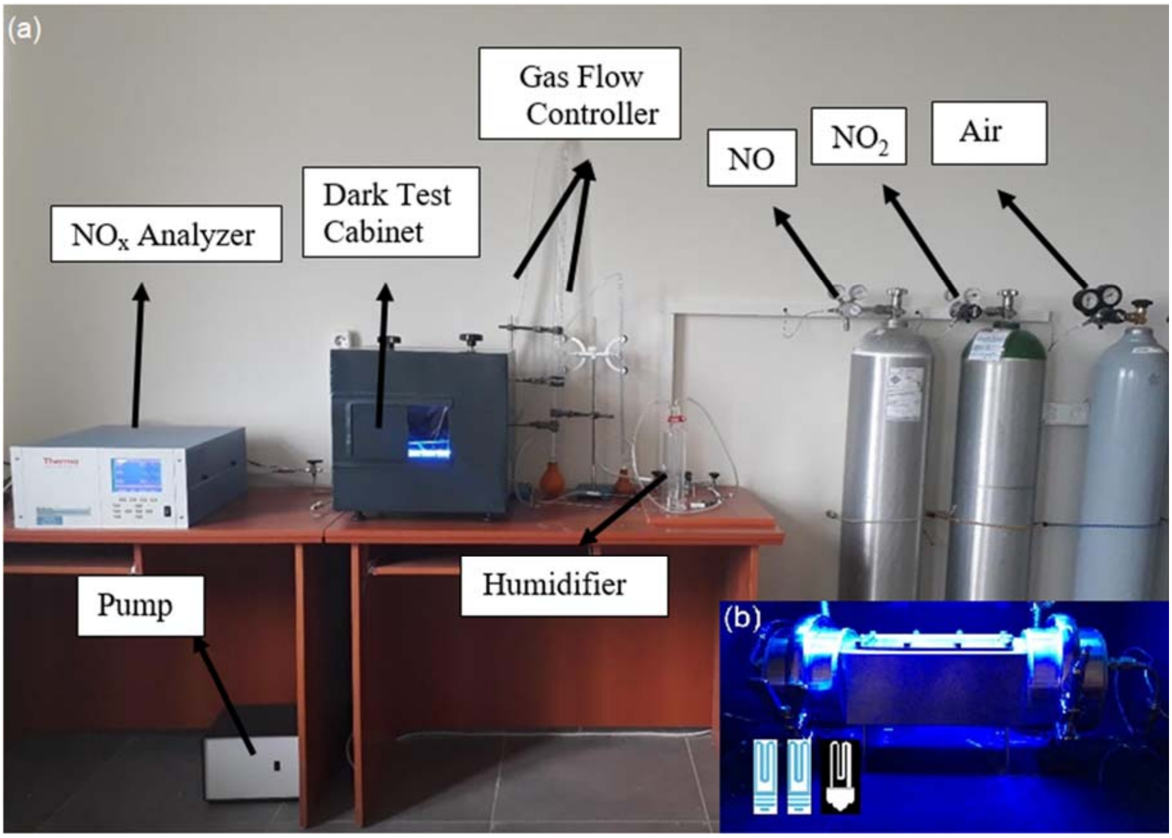

Figure 3.10 (a) The photocatalytic activity measurement system, (b) dark test cabinet detail

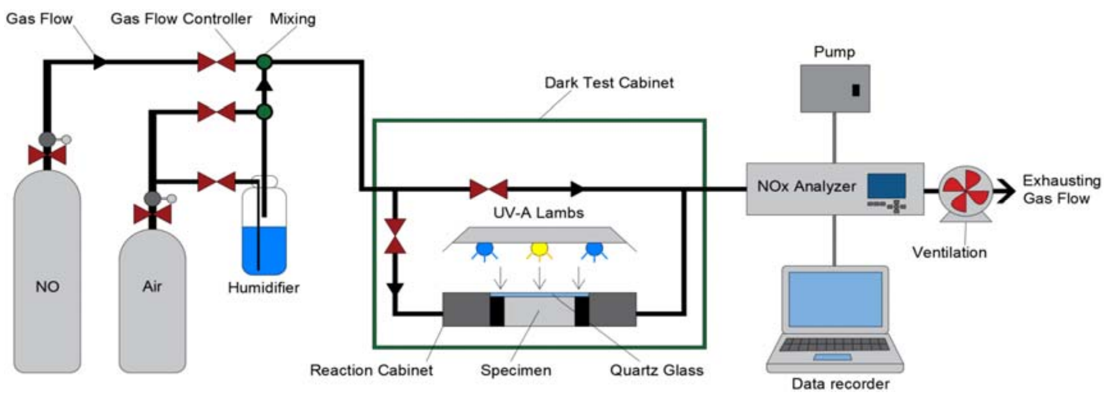

Figure 3.11 Schematic view of the photocatalytic activity measurement system

Since moisture content has a significant effect on photocatalytic activity (Cassar et al., 2007; Seo and Yun, 2015; Dylla et al., 2010), the specimens were dried in the oven at 45 °C for 24 hours before testing to prevent moisture-related variability. After that, the specimen's relevant surface was ground, and it was placed into the reactor cabinet under UV lamps without any gas flow for 3-4 hours to adapt it to the testing environment. The UV lamp was then switched off and gas flow was initiated throughout the system at the specified flow rate and concentration. At least 10 minutes after balancing the gas concentration passing through the system, the UV lamp was turned back on. This regulation and implementation method ensured that any measurement errors caused by the system were prevented or minimized and the testing procedure was optimized to examine NO degradation originating from the specimen. Testing was continued until NO degradation ceased, and gas flow become stable. After completing degradation measurement, the experiment was continued until the first gas concentration was achieved by turning off the UV sources while the gas flow continued. Changes in NO and NO_2 values can be observed in the test results. NO degradation capability of the specimens was calculated by using equation given below.

$$NO_{deg}(\%) = \frac{NO_i - NO_f}{NO_i} \times 100$$

where NO_{deg}, NO_i, NO_f are degradation percentage of the NO, initial concentration of NO and final (reduced) concentration of the NO.

4. EXPERIMENTAL STUDIES

4.1. Compressive Strength

The compressive strength test results of the specimens incorporating nano TiO_2 produced with five different mixing methods are shown in Table 4.1 at different curing ages. The effect of mixing methods on compressive strength was evident, especially for the 1st and 2nd mixing methods. The compressive strength results of NA-3, NA-4 and NA-5 were slightly different from each other, ranging between 75.80 MPa and 78.37 MPa at the age of 28 days. As shown in the table, the highest compressive strength values at 7 and 28 days were for the NA-1 prepared using the 1st mixing method: these values are 77.03 and 88.30 MPa, respectively. It can be also seen from Table 4.1 that the lowest strength values at 7 and 28 days were for NA-3 and NA-4. These values are 64.33 and 75.80 MPa, respectively.

Due to the fact that the relatively smaller particle size of nano-TiO_2 provides better particle size distribution, ensuring high-density matrices and optimized particle packing of constituents because of its filler effect and flaw-bridging effect at the nano level (Al-Dahawi et al., 2016; Mohseni et al., 2015; Li et al., 2017), the addition of nano TiO_2 reduced porosity and improved the microstructure of the specimens, as expected. On the other hand, nano-TiO_2 also acted as a nucleus due to the high surface areas of nano-scale materials, resulting in more nucleation sites, which provided the proper conditions for formation of hydration products. The logic behind this behavior is that small particles provide heterogeneous nucleation sites, which pull unhydrated cement particles and create more space for the formation of hydration products (Wang et al., 2014; Chen et al., 2012). In addition, nanoscale materials have hydration agitation and acceleration effect (Mohseni et al., 2015; Li et al., 2017; Chen et al., 2012; Han et al., 2017). However, homogenous dispersion of nano-TiO_2 in the cementitious systems prevents agglomeration problems and occurrences of weak points in the matrix and significantly increases compressive strength.

Table 4.1 Compressive strength, NO degradation and electrical impedance test results

Mixture ID.	Compressive strength (MPa)		NO degradation (%)			Electrical impedance (Ω)		
	7d	28d	7d	28d	90d	7d	28d	90d
NA-1	77.03 (8.56)	88.30 (6.38)	45.2 (18.55)	27.4 (16.58)	22.4 (15.50)	106.7 (12.73)	652.8 (10.11)	9015.0 (6.43)
NA-2	71.63 (4.15)	87.93 (6.03)	28.3 (12.13)	18.7 (17.95)	22.2 (15.23)	86.4 (13.41)	491.0 (6.88)	6016.0 (5.54)
NA-3	64.33 (5.19)	78.37 (2.13)	32.0 (20.11)	21.6 (23.10)	23.0 (19.32)	166.6 (29.06)	1073.0 (20.78)	9744.0 (12.14)
NA-4	65.73 (3.27)	75.80 (2.56)	40.6 (13.98)	39.9 (13.56)	30.8 (9.68)	67.0 (9.54)	250.8 (8.55)	3227.0 (3.54)
NA-5	66.00 (1.00)	77.63 (1.93)	55.3 (9.88)	46.5 (7.51)	44.8 (8.19)	47.7 (11.32)	162.1 (3.08)	1864.0 (3.37)

Note: Numbers in parentheses are coefficients of variation (COV).

To understand the relatively lower compressive strength results of NA-3 prepared with high speed mixing, it is also important to note that this process can lead to increases in agglomeration as a result of increased ionic concentration, causing decrements in the thickness of electrical double layers (Han and Ferron, 2016). As for the relatively low compressive strength performance of the NA-4 and NA-5 specimens, it can be attributed to the relatively high number of voids throughout the matrix caused by the presence of PAA (Negim et al., 2017; Tian et al., 2013). In addition, there are many studies in the literature that show PAA utilization rate negatively affects compressive strength beyond a certain level (Tian et al., 2013; Ma et al., 2011; Ma and Li, 2013; Alqedra et al., 2014). Alqedra et al., (2014) investigated the effects of different concentrations of PAA on the mechanical properties of concrete. The study concluded that compressive strength results of 3-day-old and 28-day-old concrete specimens increased up to a PAA utilization rate of 1%, beyond which decrements were noted. Compared to the current study, which is based on results from cement paste specimens, this limit value of 1% can be lower due to the use of concrete specimens. Therefore, the compressive strength values of NA-4 and NA-5 were affected negatively by incorporation of PAA. When compressive strength results are evaluated, it is evident that the 1st mixing method provided higher compressive strength results for each curing age. Although it is possible to state that the better dispersion of nano materials, the higher the strength; to only evaluate nano TiO_2 dispersion according to compressive strength results will cause misleading results because of due to the utilization of surfactants in this study, which have a lowering effect on compressive strength. Therefore, for this study, a more accurate evaluation for the dispersion capability of the mixing methods can be made by considering not only compressive strength but also photocatalytic performance, electrical properties and especially microstructural properties of specimens prepared with different mixing methods.

4.2. Electrical Impedance

The electrical impedance measurement results of the specimens incorporating nano-TiO_2 produced with five different mixing methods are shown in Table 4.1 for different curing ages. Electrical impedance values increased continuously with time for all mixing methods. It is well-known that electrical conductivity of concrete is generally associated with microstructural properties (Spragg et al., 2013). Therefore, one of the most important reasons for the increase in electrical impedance values with prolonged curing time is the time-varying microstructure of the composites. Due to ongoing hydration reactions, pore structure (decrease in volume, size, and connectivity of the pores) and pore solution (decrease in ion concentration) undergo changes, and the matrix will be denser, resulting in greater electrical resistivity (and electrical impedance). Higher electrical impedance value results were observed in the first three mixing methods compared to the last two. For specimens prepared with the 1st, 2nd, and 3rd mixing methods, impedance values at 28 days varied between 491 Ω and 1073 Ω. On the other hand, the impedance values at 28 days of the NA-4 and NA-5 specimens were 250.8 Ω and 162.1 Ω, respectively. This trend was also seen with the 90-day test results: impedance values at 90 days of specimens prepared with the 1st, 2nd, and 3rd mixing methods varied between 6016 Ω and 9774 Ω, and the NA-4 and NA-5 specimens were at 3227 Ω and 1864 Ω, respectively.

As mentioned earlier, electrical conductivity of cement-based composites largely depends on their pore structure and pore solution, and the addition of nano materials has a negligible effect on the compactness, porosity, and microstructure of the matrix. On the other hand, nano-TiO_2 as a semiconductor has an enhancement effect on electrical conductivity, which could also be obtained due to the occurrence of additional conductive paths (Jiang et al., 2018, Li et al., 2017; Xiong et al., 2006; Kannan et al., 2018; D'Alessandro et al., 2017). It should also be noted that both PCE and PAA have an enhancing effect on electrical conductivity (Ismail et al., 2019; Leonavičius et al., 2019; Li et al, 2018a). However, this situation was valid for all mixtures and the utilization rates of the surfactant materials in this study were low. Therefore, it is possible to state that the effect of surfactants on the electrical conductivity was too negligible to manipulate the results. It can also be stated that the electrical impedance measurements of specimens prepared with different mixing methods showed the same trend in results for each testing age, including 90 days, which is a sufficient time for almost completing the hydration process, which almost stops the change in specimen microstructure. This is, therefore, a determinative testing age for understanding the effects of the hydration process on electrical properties and observing the effects of nano-TiO_2 based on its existence and homogeneity in the matrix. Comparing the results shows that the nano-TiO_2 used in the NA-5 was distributed more homogeneously, enhancing electrical conductivity due to additional conductive paths with semiconductor TiO_2 particles, which can be regarded as the key factor in the better electrical conductivity of specimens prepared with the 5^{th} mixing method. The enhancing effect of incorporation of nano-TiO_2 on the electrical conductivity was more dominant than the electrical conductivity reducing effect due to a dense microstructure formed through the use of nano TiO_2 (Li et al., 2017). The microstructural analysis results discussed in the next sections support these results.

4.3. Photocatalytic Performance

Table 4.1 lists NO degradation values obtained from specimens incorporating nano-TiO_2. produced with five different mixing methods. Alteration graphs of the NO concentration in the reactor during each test (covering all testing periods for each test) are provided in Figure 4.1. When the 7-day NO degradation results are evaluated, specimens prepared with the 5^{th} mixing method showed a higher degradation value (55.3%) than those prepared with other methods. The 4^{th} mixing method showed the second-highest degradation rate, which was 40.6%. The lowest degradation results for the 7-day curing age were recorded from the specimens prepared using the 2^{nd} mixing method, with a value of 28.3%. The 3^{rd} mixing method resulted in similar photocatalytic performance as the 2^{nd} at 32.0%. It is worth noting that the photocatalytic performances of all specimens were higher at early curing ages. NO degradation results exhibited a decremental trend with further aging, most probably because TiO_2 particle surfaces were covered with hydration product due to ongoing hydration reactions, changing the matrix microstructure, which has a significant effect on electrical resistivity. This finding has also been reported by other researchers (Chen and Poon, 2009; Poon and Cheung, 2007; Lackoff et al., 2003). In regard to decrements in degradation results at 7- to 28- day curing ages, the highest decrement percentage was obtained from the NA-1 at 39.3%. NA-5 had the lowest decrement percentage at 19,0%. According to the 28-day

NO_x degradation results, the highest and lowest degradation values were again obtained from the 5th and 2nd mixing methods at 46.5% and 18.7%, respectively. At the end of the 90-day curing process, the NO degradation results of specimens prepared with the 5th mixing method was still the highest at 44.8%. NA-1, NA-2 and NA-3 showed similar photocatalytic performance with NO degradation values at 22-23%.

NO degradation results of specimens were given in Figure 4.1, 4.2, 4.3, 4.4, 4.5 for mixing methods from 1st to 5th, respectively. Table 4.1 and Figure 4.1 show that specimens prepared with the 5th mixing method clearly exhibited significantly higher photocatalytic degradation performance. The reason for better NO degradation results in the 5th mixing method can be related to its homogeneous dispersion capability, favoring uniformity of the nano-TiO_2 throughout the matrix. If nano particles were not dispersed homogeneously, photocatalytic performance could be lower because of the smaller number of photocatalyst particles on UV-reached surfaces due to agglomeration problems in the core or any point of specimens. It is also possible to state that the 5th mixing method, which resulted in uniform/homogeneous dispersion of the nano-TiO_2 throughout the matrix, contributed to photocatalytic performance, which is more stable and less variable over time. In terms of photocatalytic performance, it can be also concluded that in NA-4 and NA-5, the effect of PAA on nano-TiO_2 dispersion was significantly evident.

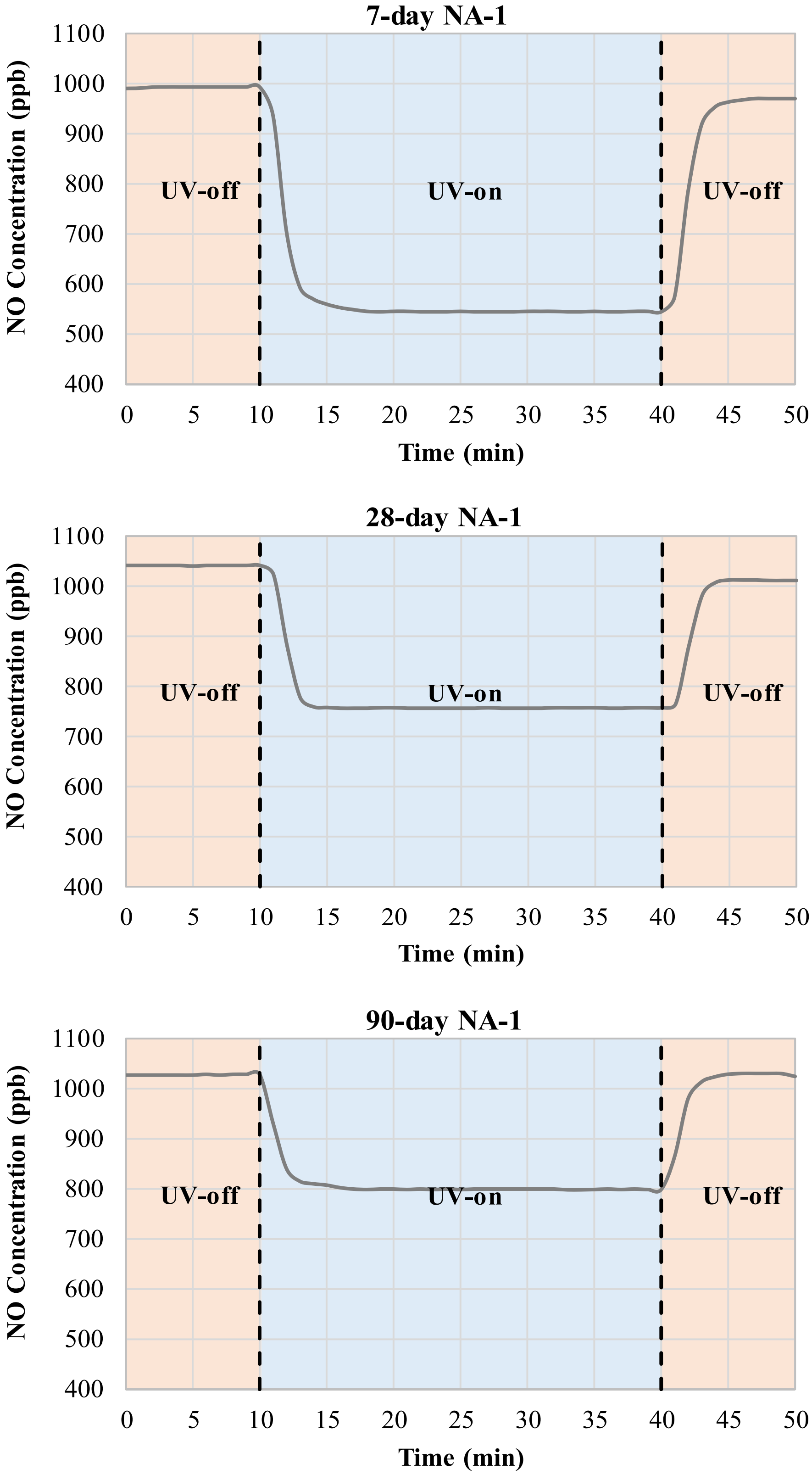

Figure 4.1 NO degradation variations at 7, 28, 90 days for 1st mixing method

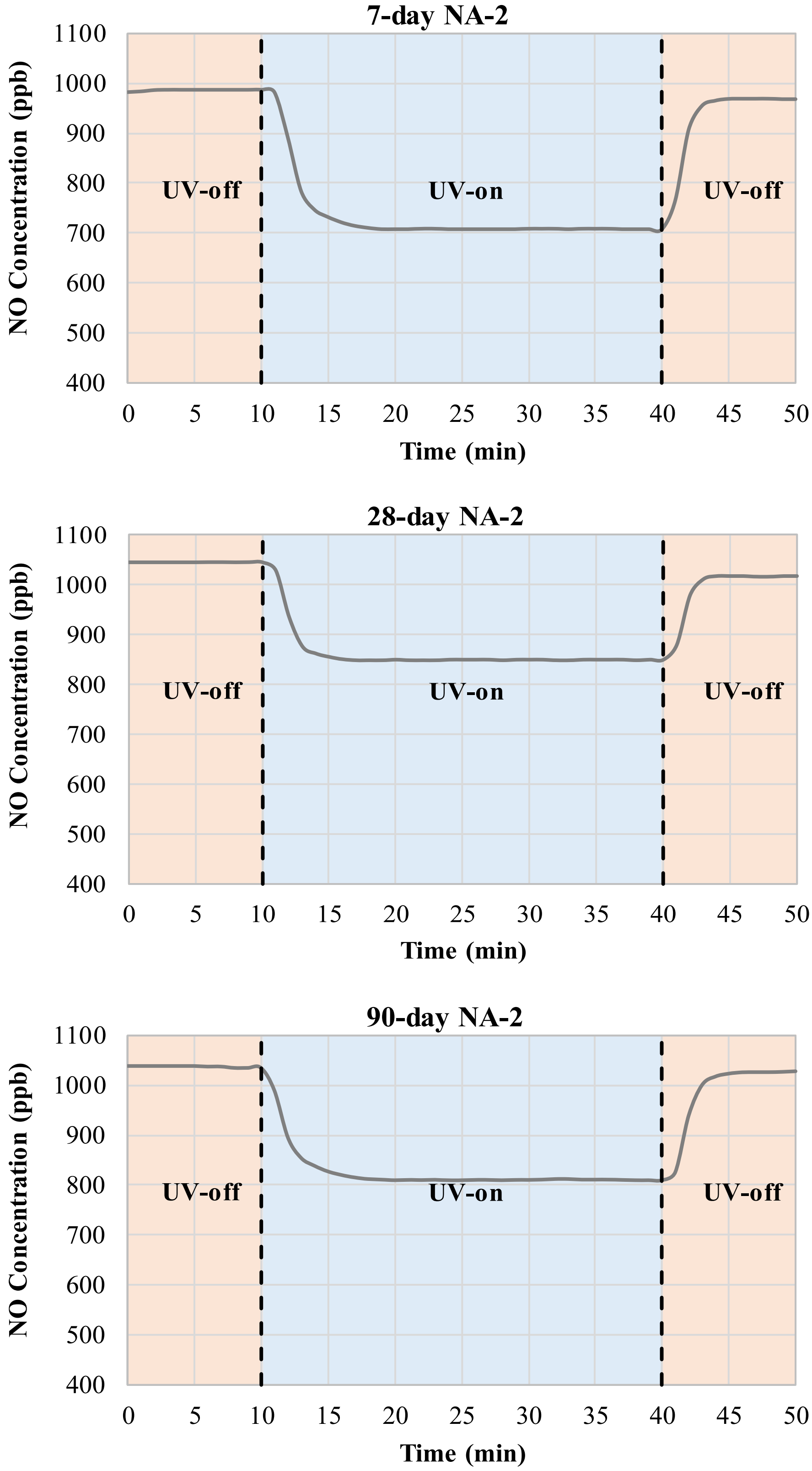

Figure 4.2 NO degradation variations at 7, 28, 90 days for 2nd mixing method

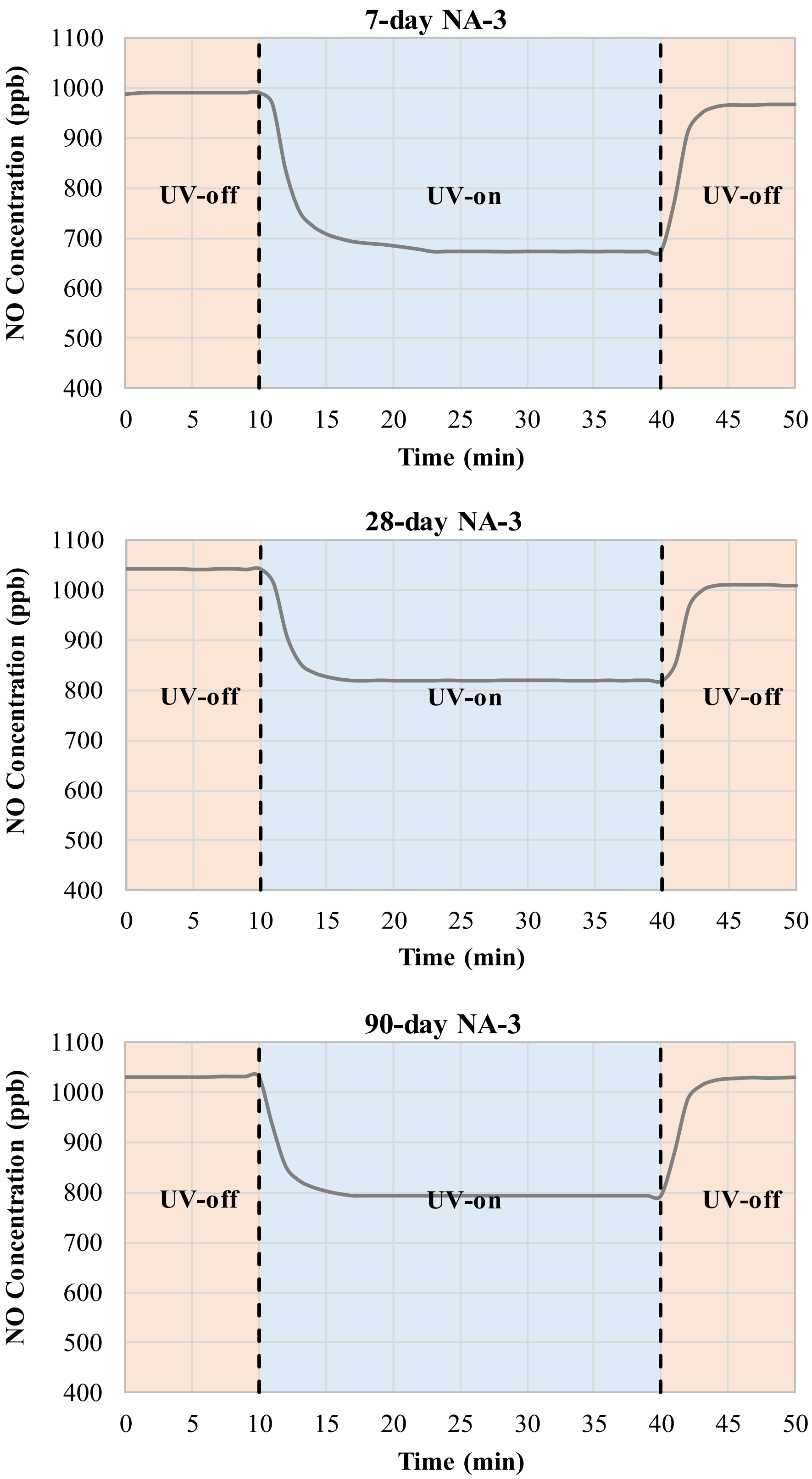

Figure 4.3 NO degradation variations at 7, 28, 90 days for 3rd mixing method

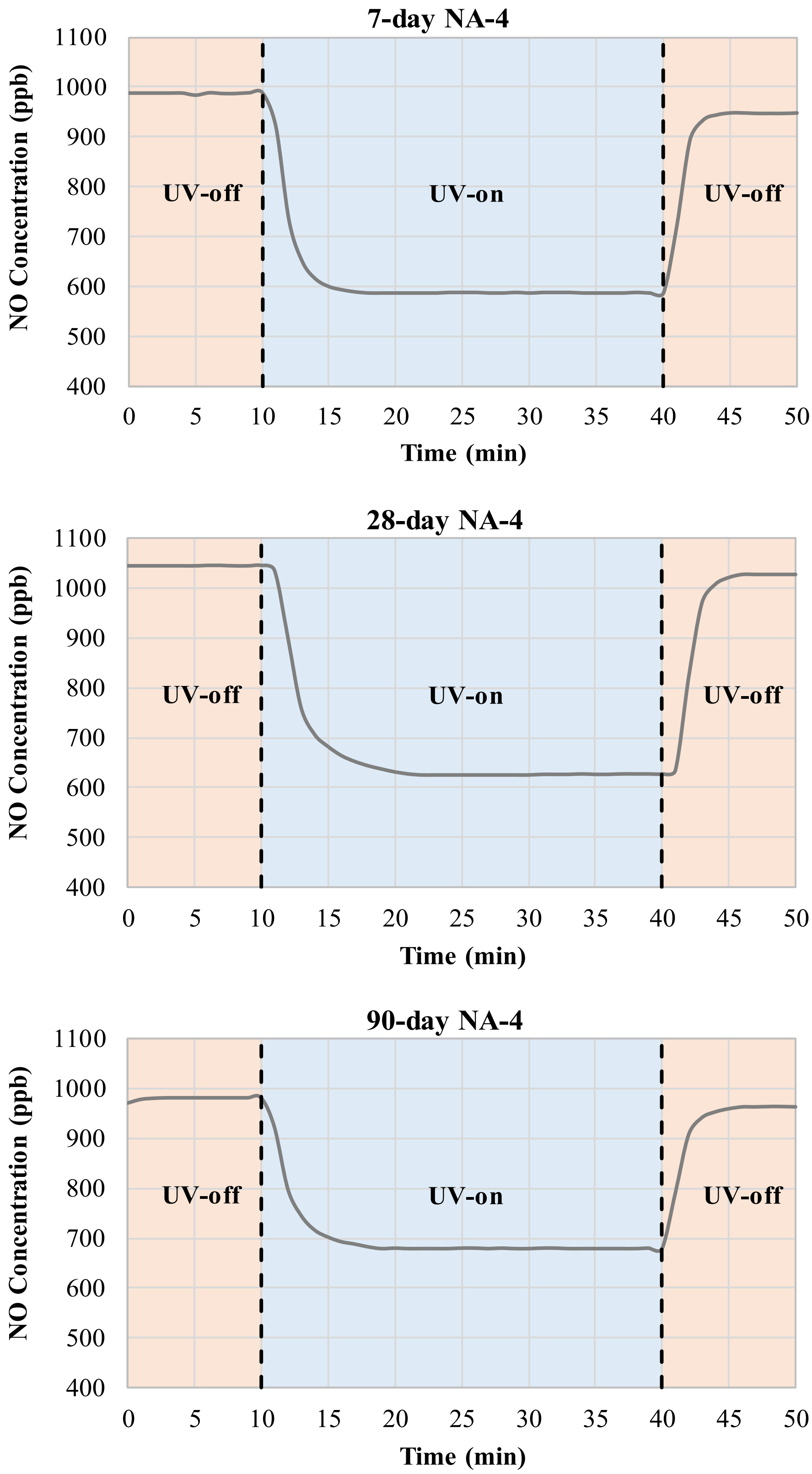

Figure 4.4 NO degradation variations at 7, 28, 90 days for 4th mixing method

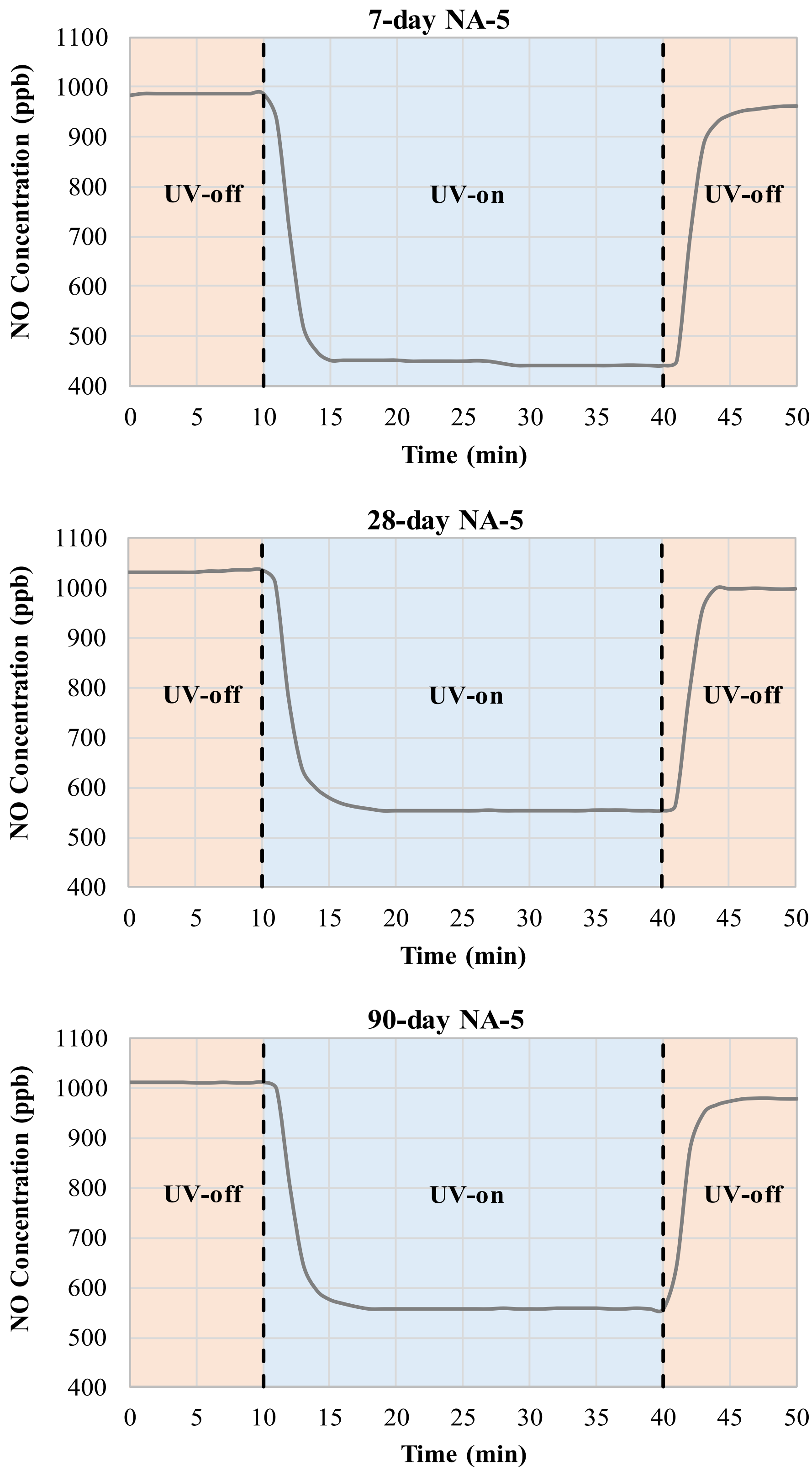

Figure 4.5 NO degradation variations at 7, 28, 90 days for 5th mixing method

4.4. Microstructural Characteristics

4.4.1. CT Imaging Characteristics

As for the microstructure of the specimens, cross-section views obtained by the computed tomography device are shown in Figure 4.6: the yellow dots indicate TiO_2 particles. Figures 4.6-d and 4.6-e show that the nano-TiO_2 particles have been well-dispersed and there is no sign of agglomeration throughout the cross-section of the matrix. The stable photocatalytic performances of these specimens can be attributed to the proper distribution of the nano-TiO_2 particles, in the case of the 4th and 5th mixing methods. The highest NO degradation result of NA-5 was also related to proper dispersion of the nano-TiO_2 particles, which ensured the presence of relatively high-TiO_2 particles on the specimen surface reached by UV light. On the other hand, NA-3 has been shown to have lower photocatalytic performance due to agglomeration problems related to nano-sized TiO_2, resulting in instability throughout the matrix that can be seen in Figure 4.6-c. Due to the agglomeration problem associated with the surface charge of particles due to nonhomogeneous dispersion, the vast majority of particles can remain at depths that prevent them from coming into contact with UV light. This is, therefore, a situation that prevents further photocatalytic reactions. Although this is also valid for the 1st and 2nd mixing methods, it is more evident for the 3rd method, which can be easily seen from Figure 4.6.

a)	b)
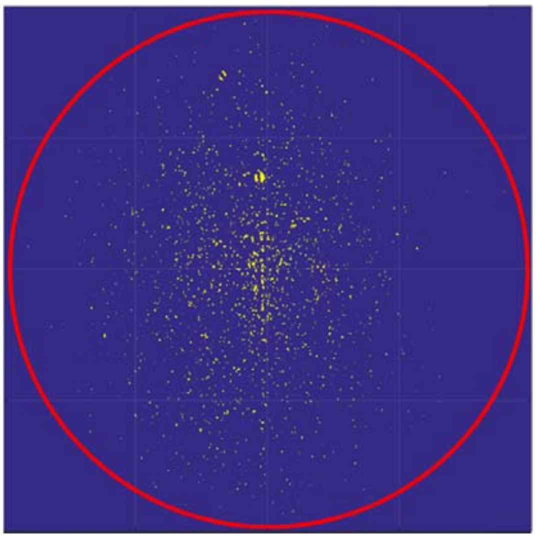	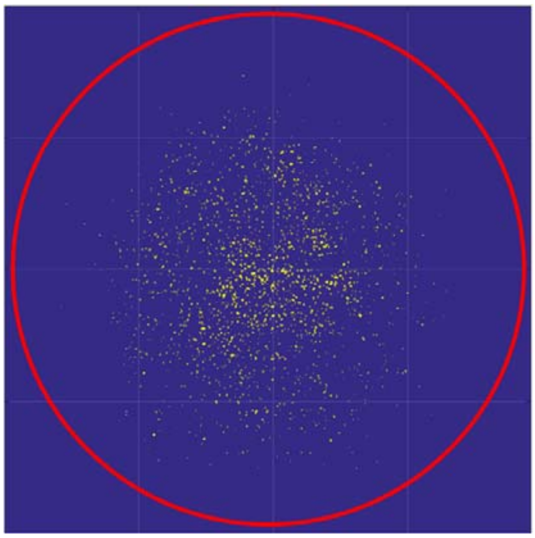

c)	d)
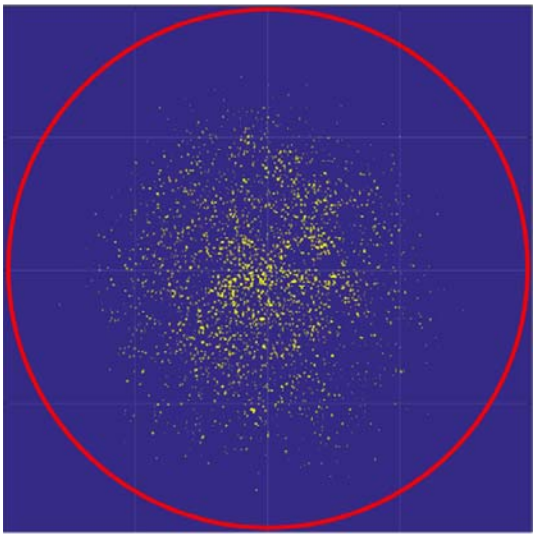	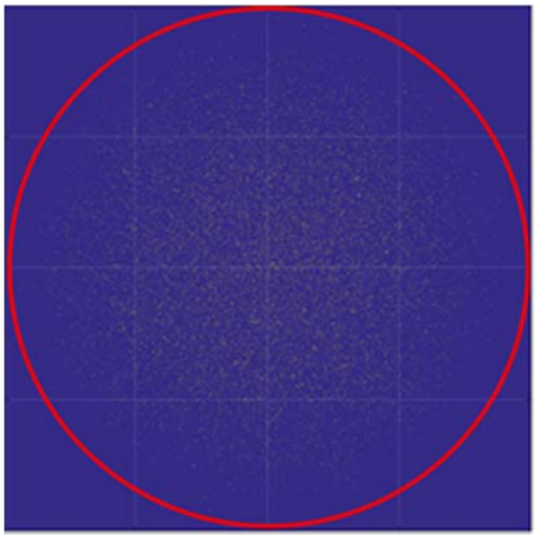

e)

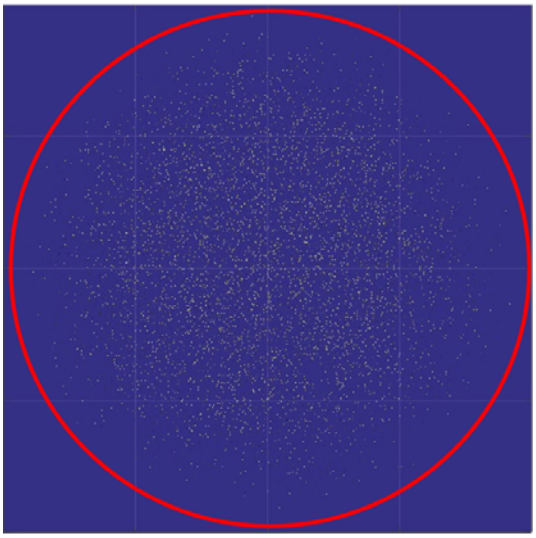

Figure 4.6 Tomography images of the specimens prepared with different mixing methods a) NA-1, b) NA-2, c) NA-3, d) NA-4 and e) NA-5

4.4.2. SEM/EDX Results

The dispersion of Ti elements in the mixtures for specimens prepared with different mixing methods is demonstrated in Figure 4.7 SEM/EDX mapping micrographs show that the dispersion of Ti elements was quite different between specimens. It is clear that the Ti particles (indicated in red) are distributed very homogeneously in the cross-section of NA-5 (Figure 4.7-e), which is also evidence of the good nano-TiO_2 dispersion capability of the 5^{th} mixing method. The significantly better NO degradation capability and higher electrical conductivity performance of NA-4 and NA-5 compared to the others allows us to conclude that PAA considerably contributes to homogeneous distribution of nano-sized TiO_2 particles throughout the matrix. The better dispersion of TiO_2 throughout NA-5 over NA-4 can be attributed to the presence of PCE as a surfactant, which is in addition to the PAA used for NA-5. It has been reported that the fluidity of specimens can affect their homogeneity (Jimenez-Relinque et al., 2015). It is therefore very likely that the higher fluidity of NA-5 (along with the presence of PAA) leads to relatively more homogeneous systems, further improving the microstructural properties of mixtures in favor of photocatalytic efficiency. As for the NA-3 specimen, it can be easily observed from Figure 4.7-c that the 3rd mixing method caused high-level agglomeration. Figure 4.7-a and 4.7-b show some agglomeration zones throughout NA-1 and NA-2.

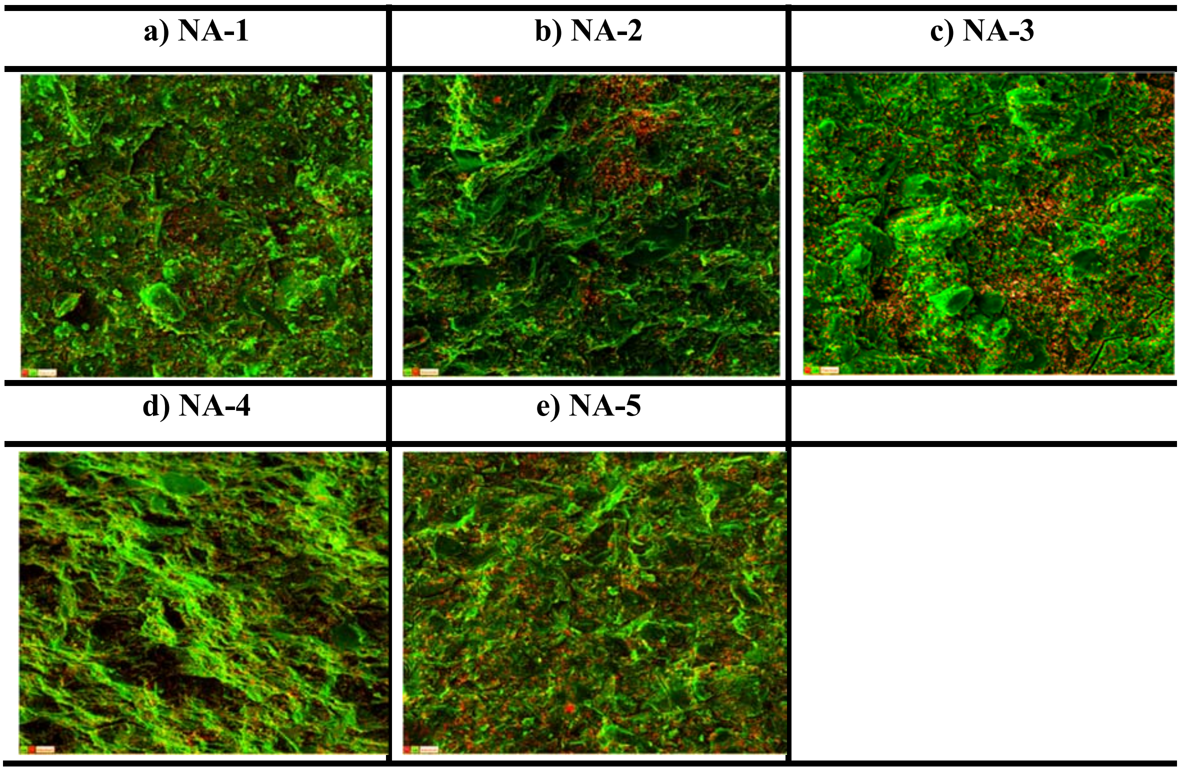

Figure 4.7 SEM micrographs taken from fractured specimens at age of 90 days

5. EXPERIMENTAL RESULTS AND DISCUSSION

5.1. Influence of the Mixing Method on Compressive Strength

Compressive strength tests showed an incremental trend for all mixtures, regardless of mixing methods, which can be attributed to ongoing hydration and further curing. Increments were more pronounced in NA-2 and NA-3 than in NA-1, NA-4 and NA-5. The increment rates in the compressive strength results of NA-1, NA-2, NA-3, NA-4, NA-5 specimens from 7 to 28 days were 14.6% (from 77.03 to 88.30 MPa), 22.76% (from 71.63 to 87.93 MPa), 21.82% (from 64.33 to 78.37 MPa), 15.32% (from 65.73 to 75.80 MPa) and 17.62% (from 66.00 to 77.63 MPa), respectively. When the COV (the ratio of the standard deviation of a number of measurements to the arithmetic mean) values in Table 4.1 are evaluated, the COV values of NA-5 were 1.0% and 1.93% for 7 days and 28 days curing age, respectively, the lowest ones for each age. Although the compressive strength results of NA-1 were the highest for all curing ages, the individual strength values of six different replicates varied significantly, with COV values of 8.56% for 7 days and 6.38% for 28 days as the highest ones. COV values of NA-2, NA-3 and N-4 were 4.15%, 5.19% and 3.27% for 7 days and 6.03%, 2.13% and 2.26% for 28 days respectively, which were higher than NA-5 results and lower than NA-1. Relatively low COV values of NA-5 specimens indicate that individual strength values of these specimens were concordant with each other, showing consistent results throughout the test. This low variability between the results can be attributed to the capability of the 5th mixing method to distribute nanoparticles homogeneously throughout the matrix. Consequently, homogeneously incorporating nano-sized TiO_2 particles into the matrix with a proper mixing process is believed to provide a stable and uniform microstructure and thereby obtaining reproducible products with more consistent performance.

5.2. Influence of the Mixing Method on NO Degradation

In mixtures containing nano-TiO_2 particles, the highest photocatalytic efficiency was obtained by using the 5th mixing methods, regardless of curing age. NO degradation rates were the most stable with prolonged curing ages compared to other mixtures. Degradation values at 7, 28 and 90 days were 55.3%, 46.5% and 44.8%, respectively. Several previous studies have measured photocatalytic efficiency of cement-based composites containing different types of photocatalysts with different properties arising from their production process and differing ingredients. However, many of those studies used standards related to measurement of photocatalytic efficiency that have since been revised. There are also many differences between the ingredients used in different studies. Therefore, it is not possible to make a direct comparison. Nonetheless, it is possible to look at those that used mixtures with minimum common characteristics with those of current study. Hüsken et al. (2009) investigated the effects of different parameters related to the production process. When they compared degradation rate results, they observed that pretreatment on surfaces where photocatalytic reactions occur (surface conditions), the technique used to incorporate TiO_2 into the composition (application technique), as well as the applied light source and pigments used for aesthetic concerns all have major influences on NO degradation capability. Their degradation rate results, in accordance with product-related parameters, ranged from 2.9 to 39.6%. All NO degradation results of NA-5 in the current study are significantly higher than those of the study conducted by Husken et al. For the specimen in their study, which has almost the same parameters as NA-5 (such as 5% TiO_2 content and incorporation of TiO_2 with a prepared suspension), the degradation value was 16.5%, which is significantly lower than that of NA-5. In another research study from the same authors (Hüsken and Brouwers, 2008), they reported a 30% degradation rate for the specimen containing 5% TiO_2. According to Ballari et al. (2011), 100×200 mm specimens (about twice the area of those used in the current study) were used and the maximum NO degradation value of specimens under almost the same conditions as NA-5 was 43.3%. Although its surface was wider than that of NA-5 and its TiO_2 content was 5.9%, their specimen showed almost the same photocatalytic efficiency performance as NA-5. Considering these comparisons, it can be stated that the incorporation technique of nano-materials, additives and additional ingredients used for homogenous distribution have an undeniable influence on specific performances of the final product, including photocatalytic efficiency. In this study, developing only the mixing method undeniably improved the mixture properties. One of the main goals was to investigate the effect of mixing procedure or technique on photocatalytic performance, and it has confirmed that the NO degradation capability of NA-5 can be improved by implementing different processes and parameters around measuring procedures, measurement process related parameters, and some product-related parameters or processes. For example, according to Hüsken et al., (2009), using the sand blasting process on the UV-reachable surface before NO degradation rates are measured significantly increases NO degradation capability compared to the grinding process, which was also used in the current study. Therefore, as mentioned above, the photocatalytic efficiency of NA-5 (which was the best one for the current study) can be advanced by different improvement techniques.

5.3. Influence of the Mixing Method on Electrical Impedance

To determine electrical conductivity performance, three different parts of the same specimen were used to monitor the conductivity behavior of the whole cast specimen (as mentioned earlier). The results obtained from different parts of two identical specimens for each mixing method is a more realistic parameter for revealing the overall microstructure of the matrix in terms of homogeneity and homogenous dispersion of semi-conductive nano-TiO_2 particles. In this study, individual EI results of six NA-5 replicates for late age were closest to each other, possessing very small COV values of 3.08% for 28-days and 3.37% for 90-day curing ages, compared to specimens prepared with other mixing methods. The low variability between EI results from the 5^{th} mixing method was expected, considering microstructural properties and NO degradation capability of NA-5. Thereby, it can be definitively stated that the variability between results found in this study reveals the effect of the mixing process on matrix microstructure. Additionally, considering that the COV value of the NA-4 at the 90-day curing age was relatively low compared to the others, therefore use of PAA has undeniable benefits for obtaining more reliable and uniform EI results due to the homogeneous microstructure of specimens. The highest COV values of EI results of NA-3 replicates for all curing ages have also proven that high-speed mixing leads to agglomeration problems, as mentioned in Section 4.1. Based on the abovementioned statements, the EI test is a more effective method for evaluating homogeneous distribution of conductive nanoparticles throughout the matrix. On the other hand, variable EI test results for all matrix specimens showed a decreasing trend with prolonged curing age, regardless of the mixing method. It should be noted that the effect of porosity, pore solution chemistry and tortuosity of the pore network on electrical conductivity is more pronounced, especially at early ages, due to the uncompleted hydration process. These are the main parameters influencing electrical conductivity of cement-based composites (Spragg et al 2013). Therefore, the pore structure of every replicate specimen prepared with different mixing methods is quite different at early age. Pores are gradually closed by ongoing hydration, and the majority of the pore solution is consumed by the ongoing hydration process. In addition, paths between pores disappear as they are covered by hydration products. Due to the effect of final hydration products on pore characteristics, the manipulative characteristics of these parameters in terms of EI values are eliminated at late curing ages. Consequently, the decremental trend in variability between EI results with prolonged curing age may be due to the occurrence of more stable and regular microstructure at the end of the hydration process. A similar trend was also observed for the correlation between NO degradation and EI test results. This correlation, directly associated with the presence of semi-conductive nano-TiO_2 particles and their homogeneous distribution throughout the matrix, tended to get stronger with prolonged curing age (Figure 5.1). At the end of 90-day curing, the correlation was strong, with a coefficient of correlation value of 0.89. Based on the above-mentioned explanations and Figure 5.1, there is a significant relationship between electrical conductivity and photocatalytic efficiency regardless of mixing method, although this relationship becomes more evident with prolonged curing time.

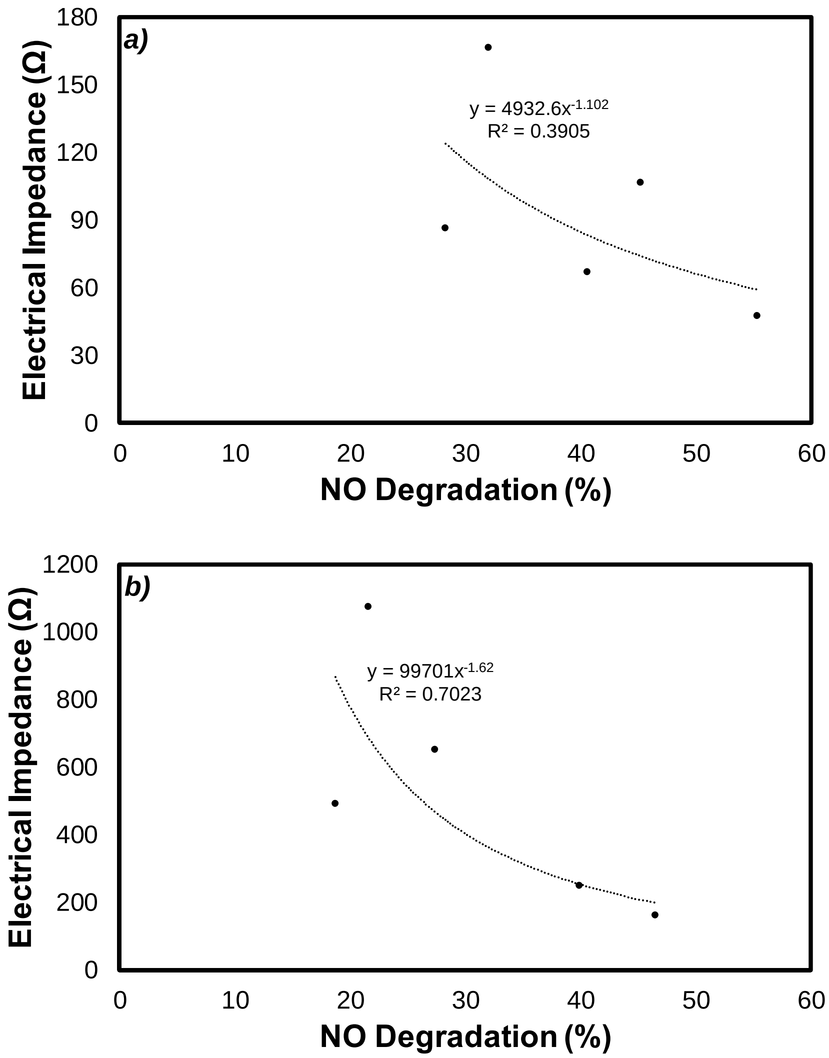

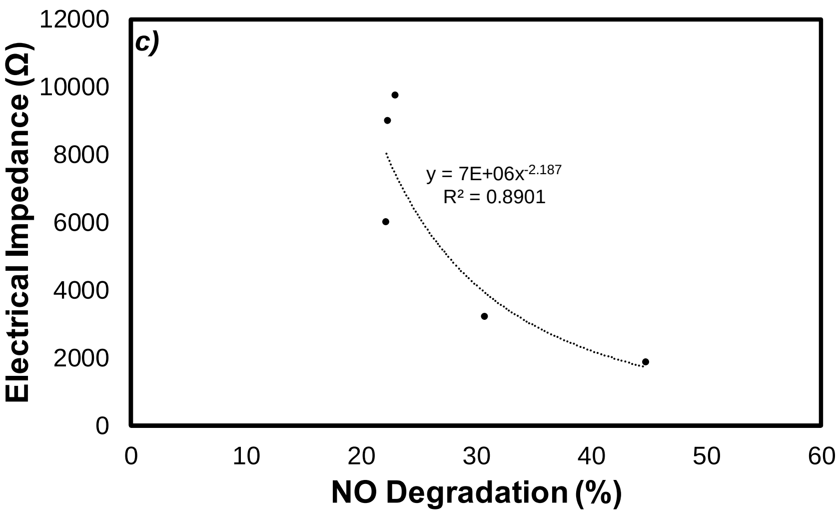

Figure 5.1 Electrical impedance versus NO degradation results of each specimen for a) 7 days b) 28 days c) 90 days

One of the main aims of this study was to obtain reliable, reproducible products with the same performances associated with microstructural property. This can be ensured by homogeneous and uniform distribution of ingredients throughout the matrix. The electrical property and NO degradation capability of cement-based composites are strongly associated with their microstructural properties. EI results and NO degradation rates both changed depending on curing age. This variation can be attributed to the changed microstructure of cement-based composites with prolonged curing ages. For the cement-based composites containing TiO_2 as a photocatalyst, the dispersion of semi-conductive TiO_2 throughout the entire volume of the specimens (which can be considered as the path of the electric current) is the main criteria for increasing electrical conductivity. On the other hand, NO degradation capability or photocatalytic efficiency depend on the presence and amount of TiO_2 in the UV-accessible surface of the specimen rather than its entire volume. To stimulate photocatalytic reactions and ensure satisfying photocatalytic efficiency, it is necessary to ensure there are sufficient photocatalysts on the surfaces where UV light can reach. Agglomeration of nano-TiO_2 on the surface where the photocatalytic reactions occur can contribute to the NO degradation capability of cement-based composites, but this type of agglomeration cannot be guaranteed. Therefore, the purpose of the uniform dispersion of nano-TiO_2 particles was to increase of number of TiO_2 particles distributed throughout the matrices as much as possible to obtain reliable reproducible products with the same performances. Homogeneous dispersion of nanoparticles in the mixtures eliminates embedded particles that remain lumpy in the dark depths of composites due to the agglomeration effects of nanoparticles and increases/guarantees the presence of photocatalyst particles on the specimen's surface illuminated by UV light. In a general sense, it is possible to state that factors associated with microstructural properties of cement-based composites influencing EI results are also generally effective on NO degradation results. However, NO degradation capability can be more easily affected because of its dependence on the conditions of a single surface, and accordingly, the possibility of surrounding the TiO_2 particles too close to the surface or on the surface with ongoing hydration products.

6. CONCLUSION

In the current study, to investigate and improve the dispersion capability of high-dosage TiO_2 in cement-based systems, five different mixing methods based on three mixing techniques: ultrasonication, hand blender, and conventional cement mixer, as well as two surfactant materials: polycarboxylate based superplasticizer (PCE) and polyacrylic acid (PAA) were used. All specimens created with these methods were evaluated in terms of nano-TiO_2 dispersion throughout the cement-based mixtures. The main aim was to ensure good dispersion of the nano-TiO_2 in the matrix to maximize NO degradation capability of the mixtures by using a large part of the nano-TiO_2 incorporated into the mixtures for photocatalytic activity. To evaluate dispersion, electrical impedance and compressive strength values were measured, photocatalytic performance of the specimens was determined, and microstructural analysis was performed. Conclusions are as follows:

The amplitude of the ultrasonication process was highly influential on zeta potential, which increased negatively with increasing amplitude value applied. The effect of using surfactant materials on the zeta potential was also evident. The zeta potential of the suspension increased negatively to a certain level with increased utilization rates of surfactant materials.

Use of PAA resulted in higher electrical conductivity due to the occurrence of additional conductive paths and owing to the better dispersion of semi-conductive nano-TiO_2 materials.

Irrespective of the test, the results obtained from specimens with higher NO degradation capability were largely concordant with each other. Therefore, uniform dispersion of nano-scale materials throughout cement-based matrix provides stable and uniform microstructure, and these specimens can be considered a reliable, reproducible product with the same performance.

Photocatalytic performances of the specimens decreased with time. The specimens prepared more homogenously showed the highest NO degradation rates. The degradation capability of these specimens was more stable with prolonged curing ages.

The correlation between NO degradation rates and EI results is directly associated with the presence of semi-conductive nano-TiO_2 particles and their homogeneous distribution throughout the matrix, which tended to get stronger with prolonged curing age. Regardless of mixing method, there is a significant relationship between electrical conductivity and photocatalytic efficiency, which becomes more evident with prolonged curing time.

In the presence of PAA, greater fluidity resulted from including PCE leads in relatively more homogeneous systems, providing mixtures with the ability to further improve their microstructural properties in favor of photocatalytic efficiency. Therefore, greater fluidity can contribute to homogeneous dispersion of ingredients throughout the matrix.

Finally, the results indicate that the 5^{th} mixing method has a higher capability to evenly disperse TiO_2 materials at the nano scale, without sacrificing any other properties. The effect of PAA was more pronounced for better dispersion of the nano TiO_2 in the matrix. Incorporating nano-TiO_2 into cement-based mixtures using the ultrasonication process and binary utilization of PCE and PAA can provide better dispersion of the nano-scale particles throughout the matrix.

REFERENCES

Al-Dahawi, A., Öztürk, O., Emami, F., Yıldırım, G., & Şahmaran, M. Effect of mixing methods on the electrical properties of cementitious composites incorporating different carbon-based materials. Construction and Building Materials, 104 **(2016)**, 160-168.

Almquist, C. B. ve Biswas, P. Role of Synthesis Method and Particle Size of Nanostructured TiO_2 on Its Photoactivity. Journal of Catalysis, 212(2), **(2002)**, 145-156.

Alqedra, M., Dabbour, B., & Arafa, M. Influence of Several Nano Minerals on The Mechanical Properties of Fresh and hardened Concrete. Scientific Cooperation's International Workshops on Engineering Branches, **(2014).** http://hdl.handle.net/20.500.12358/24552

Alrekabi, S., Cundy, A., Lampropoulos, A., & Savina, I. Experimental investigation on the effect of ultrasonication on dispersion and mechanical performance of multi-wall carbon nanotube-cement mortar composites. Studies, 9, **(2016)**, 11.

Anpo, M., Shima, T., Kodama, S. and Kubokawa, Y., "Photocatalytic hydrogenation of propyne with water on small-particle titania: size quantization effects and reaction intermediates", J. Phys. Chem., 91, **(1987)**, 4305-4310.

Ba-Abbad M, Kadhum AH, Mohamad A, Takriff MS, Sopian K. Synthesis and Catalytic Activity of TiO2 Nanoparticles for Photochemical Oxidation of Concentrated Chlorophenols under Direct Solar Radiation. International Journal of Electrochemical Science; 7.6, **(2012)**, 4871-4888.

Baglioni, P., Cassar, L., Hashimoto, K., Filippone, F., Mattioli, G., Bonapasta, A. A., ... & Ragaini, V.. International RILEM Symposium on Photocatalysis, Environment and Construction Materials-TDP 2007 (pp. 171-177). RILEM Publications, Bagneux, France, **(2007)**,.

Ballari, M. M., Yu, Q. L., & Brouwers, H. J. H. Experimental study of the NO and NO_2 degradation by photocatalytically active concrete. Catalysis Today, 161(1), **(2011)**, 175-180.

Bjornstrom, J., Martinelli, A., Matic, A., Börjesson, L. ve Panas, I. **(2004)**. Accelerating effects of colloidal nano-silica for beneficial calcium–silicate–hydrate formation in cement. Chemical Physics Letters, 392(1), **(2004)**, 242-248.

Campillo, I., A. Guerrero, J.S. Dolado, A. Porro, J.a. Ibáñez, and S. Goñi. Improvement of Initial Mechanical Strength by Nanoalumina in Belite Cements. Materials Letters, 61(8-9), **(2007)**,1889-1892.

Çamurlu, H. E., Kesmez, Ö., Burunkaya, E., Kiraz, N., Yeşil, Z., Asiltürk, M., & Arpaç, E. Sol-gel thin films with anti-reflective and self-cleaning properties. Chemical Papers, 66(5), **(2012)**, 461-471.

Cao, L., Gao, Z., Suib, S. L., Obee, T. N., Hay, S. O., and Freihaut, J. D.. Photocatalytic Oxidation of Toluene on Nanoscale TiO2 Catalysts: Studies of Deactivation and Regeneration. Journal of Catalysis, 196(2), **(2000)**, 253–261.

Cao, L., Huang, A., Spiess, F.-J., & Suib, S. L.. Gas-Phase Oxidation of 1-Butene Using Nanoscale TiO2 Photocatalysts. Journal of Catalysis, 188(1), **(1999)**, 48–57.

Carp, O., Huisman, C. L., & Reller, A.. Photoinduced reactivity of titanium dioxide. Progress in solid state chemistry, 32(1-2), **(2004)**, 33-177.

Cassar, L. Nanotechnology and photocatalysis in cementitious materials. In Proceedings of the 2nd International Symposium on Nanotechnology in Construction (pp. 277-683). NANOC, **(2005)**

Chen, H., Namdeo, A. and Bell, M.. Classification of road traffic and roadside pollution concentrations for assessment of personal exposure. Environmental Modelling and Software, 23(3), **(2008)**, 282-287.

Chen, J., & Poon, C. S.. Photocatalytic activity of titanium dioxide modified concrete materials–Influence of utilizing recycled glass cullets as aggregates. Journal of environmental management, 90(11), **(2009)**, 3436-3442.

Chen, J., & Poon, C. S.. Photocatalytic construction and building materials: from fundamentals to applications. Building and environment, 44(9), **(2009)**, 1899-1906.

Chen, J., Kou, S. and Poon, C.. Hydration and properties of nano-TiO_2 blended cement composites. Cement and Concrete Composites, 34(5), **(2012)**, 642-649.

D'Alessandro, A., Fabiani, C., Pisello, A. L., Ubertini, F., Materazzi, A. L., Cotana, F.. Innovative concretes for low-carbon constructions: A review. International Journal of Low-Carbon Technologies, 12(3), **(2017)**, 289-309.

Demeestere, K., Dewulf, J., Witte, B. D., Beeldens, A. ve Langenhove, H. V.. Heterogeneous photocatalytic removal of toluene from air on building materials enriched with TiO_2. Building and Environment, 43(4), **(2008)**, 406-414.

Diamanti, M. V., Ormellese, M. ve Pedeferri, M.. Characterization of photocatalytic and superhydrophilic properties of mortars containing titanium dioxide. Cement and Concrete Research, 38(11), **(2008)**, 1349-1353.

Diebold, U.. The surface science of titanium dioxide. Surface Science Reports, 48, **(2003)**, 53-229.

Dr. S. U. Kannan Jebin Raj Jerom Antony Manoj Mujahid "Study on the Properties of Self-Cleaning Concrete Using Titanium Dioxide" Published in International Journal of

Trend in Scientific Research and Development, ISSN: 2456-6470, Volume-2 Issue-5, August 2018,

Dylla, H., Hassan, M. M., Mohammad, L. N., Rupnow, T., & Wright, E.. Evaluation of environmental effectiveness of titanium dioxide photocatalyst coating for concrete pavement. Transportation research record, 2164(1), **(2010)**, 46-51.

EPA,. Review of the Primary National Ambient Air Quality Standards for Oxides of Nitrogen. U.S. EPA, Office of Air Quality Planning and Standards. Research Triangle Park, NC. EPA. **(2018)**

Fazio, S., Guzman, J., Colomer, M. T., Salomoni, A., & Moreno, R.. Colloidal stability of nanosized titania aqueous suspensions. Journal of the European Ceramic Society, 28(11), **(2008)**, 2171-2176.

Fei, P., Xiong, H., Cai, J., Liu, C., Zia-Ud-Din, ve Yu, Y.. Enhanced the weatherability of bamboo fiber-based outdoor building decoration materials by rutil nano-TiO_2. Construction and Building Materials, 114, **(2016)**, 307-316.

Feng, L. C., Gong, C. W., Wu, Y. P., Feng, D. C. ve Xie, N.. The Study on Mechanical Properties and Microstructure of Cement Paste with Nano-TiO_2. Advanced Materials Research, 629, **(2013)**, 477-481.

Folli, A., Jakobsen, U. H., Guerrini, G. L., & Macphee, D. E. **(2009)**. Rhodamine B discolouration on TiO2 in the cement environment: a look at fundamental aspects of the self-cleaning effect in concretes. Journal of Advanced Oxidation Technologies, 12(1), 126-133.

Folli, A., Pochard, I., Nonat, A., Jakobsen, U. H., Shepherd, A. M., & Macphee, D. E.. Engineering photocatalytic cements: understanding TiO_2 surface chemistry to control and modulate photocatalytic performances. Journal of the American Ceramic Society, 93(10), **(2010)**, 3360-3369.

Fujishima, A., and Zhang, X.. Titanium dioxide photocatalysis: present situation and future approaches. Comptes Rendus Chimie, 9(5-6), **(2006)**, 750–760. doi:10.1016/j.crci.2005.02.055

Greenwood, R., & Kendall, K.. Selection of suitable dispersants for aqueous suspensions of zirconia and titania powders using acoustophoresis. Journal of the European Ceramic Society, 19(4), **(1999)**, 479-488.

Habert, G., Billard, C., Rossi, P., Chen, C. ve Roussel, N.. Cement production technology improvement compared to factor 4 objectives. Cement and Concrete Research, 40(5), **(2010)**, 820-826.

Hager, S., Bauer, R., & Kudielka, G.. Photocatalytic oxidation of gaseous chlorinated organics over titanium dioxide. Chemosphere, 41(8), **(2000)**, 1219-1225.

Han, B., Li, Z., Zhang, L., Zeng, S., Yu, X., Han, B. ve Ou, J.. Reactive powder concrete reinforced with nano SiO_2-coated TiO_2. Construction and Building Materials, 148, **(2017)**, 104-112.

Han, B., Zhang, L., Zeng, S., Dong, S., Yu, X., Yang, R., & Ou, J.. Nano-core effect in nano-engineered cementitious composites. Composites Part A: Applied Science and Manufacturing, 95, **(2017)**, 100-109.

Han, D., & Ferron, R. D.. Influence of high mixing intensity on rheology, hydration, and microstructure of fresh state cement paste. Cement and Concrete Research, 84, **(2016)**, 95-106.

Hanaor, D. A., & Sorrell, C. C.. Review of the anatase to rutile phase transformation. Journal of Materials science, 46(4), **(2011)**, 855-874.

Hanson, S. ve Tikalsky, P.. Influence of Ultraviolet Light on Photocatalytic TiO_2 Materials. Journal of Materials in Civil Engineering, 25(7), **(2013)**, 893-898.

He, H.-Y., and Chen, P.. Recent Advances in Property Enhancement of Nano Tio2ın Photodegradatıon of Organıc Pollutants. Chemical Engineering Communications, 199(12), **(2012)**, 1543–1574.

Hou, T. C.. Wireless and electromechanical approaches for strain sensing and crack detection in FRC materials. PhD dissertation, Civil and Environmental Engineering, University of Michigan, Ann Arbor, MI., **(2008)**.

Hung, W., Fu, S., Tseng, J., Chu, H. ve Ko, T.. Study on photocatalytic degradation of gaseous dichloromethane using pure and iron ion-doped TiO_2 prepared by the sol–gel method. Chemosphere, 66(11), **(2007)**, 2142-2151.

Hüsken, G., & Brouwers, H. J. H.. Air purification by cementitious materials: Evaluation of air purifying properties. In International Conference on Construction and Building Technology, Kuala Lumpur, Malaysia, 304, **(2008)**, 263 - 274.

Hüsken, G., Hunger, M., & Brouwers, H. J. H.. Experimental study of photocatalytic concrete products for air purification. Building and environment, 44(12), **(2009)**, 2463-2474.

Internet: Cembureau. URL: https://cembureau.eu/media/1716/activity-report-2017.pdf/, (Erişim Tarihi: **10 Temmuz 2018)**

Internet: T.C. Çevre ve Şehircilik Bakanlığı. Hava kalitesi izleme istasyonları. URL: https://www.havaizleme.gov.tr// , **(01 Mayıs 2020)**

Ismail, I., Bakar, N. F. A., Ling, T. H., Ideris, N., Zain, Z. H. M., & Radacsi, N.. Morphology and Conductivity Evaluation of Electrospun Polyacrylic Acid (PAA) Microfiber. Materials Today: Proceedings, 17, **(2019)**, 574-583.

Iwasaki, M., Hara, M., Kawada, H., Tada, H. ve Ito, S.. Cobalt Ion-Doped TiO_2 Photocatalyst Response to Visible Light. Journal of Colloid and Interface Science, 224(1), **(2000)**, 202-204.

Jalal, M., Fathi, M., ve Farzad, M.. Effects of fly ash and TiO_2 nanoparticles on rheological, mechanical, microstructural and thermal properties of high strength self compacting concrete. Mechanics of Materials, 61, **(2013)**, 11-27.

Jayapalan, A. R., Lee, B. Y. ve Kurtis, K. E.. Effect of nano-sized titanium dioxide on early age hydration of Portland cement in nanotechnology in construction. Berlin: Springer, 3, **(2009)**, 267-273.

Jayapalan, A. R., Lee, B. Y., Land, E. M., Bergin, M. H., & Kurtis, K. E.. Photocatalytic efficiency of cement-based materials: Demonstration of proposed test method. ACI Materials Journal, 112(2), **(2015)**, 219.

Jayapalan, A., Lee, B., Fredrich, S. ve Kurtis, K.. Influence of additions of anataz TiO_2 nanoparticles on early-age properties of cement-based materials. Transportation Research Record. Journal of the Transportation Research Board, 2141, **(2010)**, 41-46

Jiang, S., Zhou, D., Zhang, L., Ouyang, J., Yu, X., Cui, X., & Han, B.. Comparison of compressive strength and electrical resistivity of cementitious composites with different nano-and micro-fillers. Archives of Civil and Mechanical Engineering, 18(1), **(2018)**, 60-68.

Jimenez-Relinque, E., Rodriguez-Garcia, J. R., Castillo, A., & Castellote, M.. Characteristics and efficiency of photocatalytic cementitious materials: Type of binder, roughness and microstructure. Cement and Concrete Research, 71, **(2015)**, 124-131.

Jo, B. W., Im, C. H., Tae, G. H. ve Park, J. B.. Characteristics of cement mortar with nano-SiO_2 particles. Construction and Building Materials, 21(6), **(2007)**, 1351-1355.

Jun, J., Dhayal, M., Shin, J., Kim, J. ve Getoff, N.. Surface properties and photoactivity of TiO_2 treated with electron beam. Radiation Physics and Chemistry, 75(5), **(2006)**, 583-589.

Kabra, K., Chaudhary, R. ve Sawhney, R. L.. Treatment of Hazardous Organic and Inorganic Compounds through Aqueous-Phase Photocatalysis: A Review. Industrial and Engineering Chemistry Research,43(24), **(2004)**, 7683-7696.

Kapur, A., Oss, H. G., Keoleian, G., Kesler, S. E. ve Kendall, A.. The contemporary cement cycle of the United States. Journal of Material Cycles and Waste Management, 11(2), **(2009)**, 155-165

Karunakaran, C. ve Senthilvelan, S.. Photooxidation of aniline on alumina with sunlight and artificial UV light. Catalysis Communications, 6(2), **(2005)**, 159-165.

Kawashima, S., Hou, P., Corr, D. J., & Shah, S. P.. Modification of cement-based materials with nanoparticles. Cement and Concrete Composites, 36, **(2013)**, 8-15.

Kawashima, S., Seo, J. W. T., Corr, D., Hersam, M. C., & Shah, S. P.. Dispersion of $CaCO_3$ nanoparticles by sonication and surfactant treatment for application in fly ash–cement systems. Materials and Structures, 47(6), **(2014)**, 1011-1023.

Kemp, T. J. ve Mcintyre, R. A.. Influence of transition metal-doped titanium(IV) dioxide on the photodegradation of polystyrene. Polymer Degradation and Stability, 91(12), **(2006)**, 3010-3019.

Kim, B. M., Yadav, H. M., & Kim, J. S.. Self-cleaning performance of sol–gel-derived TiO2/SiO2 double-layer thin films. Journal of Coatings Technology and Research, 13(5), **(2016)**, 905-910.

Kim, H. K., Nam, I. W., & Lee, H. K.. Enhanced effect of carbon nanotube on mechanical and electrical properties of cement composites by incorporation of silica fume. Composite Structures, 107, **(2014)**, 60-69.

Kim, Y. J., Hu, J., Lee, S. J., & You, B. H.. Mechanical properties of fiber reinforced lightweight concrete containing surfactant. Advances in Civil Engineering, **(2010)**.

Kong, L., Yin, X., Yuan, X., Zhang, Y., Liu, X., Cheng, L., & Zhang, L.. Electromagnetic wave absorption properties of graphene modified with carbon nanotube/poly (dimethyl siloxane) composites. Carbon, 73, **(2014)**, 185-193.

Lackhoff, M., Prieto, X., Nestle, N., Dehn, F., Niessner, R.. Photocatalytic activity of semiconductor-modified cement—influence of semiconductor type and cement ageing. Applied Catalysis B: Environmental, 43(3), **(2003)**, 205-216.

Lakshminarasimhan, N., Kim, W., & Choi, W.. Effect of the agglomerated state on the photocatalytic hydrogen production with in situ agglomeration of colloidal TiO2 nanoparticles. The Journal of Physical Chemistry C, 112(51), **(2008)**, 20451-20457.

Lee, B. Y., Jayapalan, A. R. ve Kurtis, K. E.. Effects of nano-TiO_2 on properties of cement-based materials. Magazine of Concrete Research, 65(21), **(2013)**, 1293-1302.

Leonavičius, D., Pundienė, I., Pranckevičienė, J., Girskas, G., & Kligys, M.. The Effect of The Electrical Conductivity of Superplasticizers on The Fluidity and Early Hydration Parameters of Cement Paste. Ceramics–Silikáty, 63(4), **(2019)**, 390-398.

Li, G. Y., Wang, P. M., & Zhao, X.. Pressure-sensitive properties and microstructure of carbon nanotube reinforced cement composites. Cement and Concrete Composites, 29(5), **(2007)**, 377-382.

Li, H., Zhang, M. H. & Ou, J. P.. Flexural fatigue performance of concrete containing nano-particles for pavement. International Journal of Fatigue, 29(7), **(2007)**, 1292-1301.

Li, H., Zhang, M. H. and Ou, J. P.. Abrasion resistance of concrete containing nanoparticles for pavement. Wear, 260(11), **(2006)**, 1262-1266.

Li, H., Zhang, M. H. and Ou, J. P.. Flexural fatigue performance of concrete containing nano-particles for pavement. International Journal of Fatigue, 29(7), **(2007)**, 1292-1301.

Li, L., Liu, L., Qing, Y., Zhang, Z., Yan, N., Wu, Y., & Tian, C.. Stretchable alkaline poly (acrylic acid) electrolyte with high ionic conductivity enhanced by cellulose nanofibrils. Electrochimica Acta, 270, **(2018)**, 302-309.

Li, X., Li, F., Yang, C. ve Ge, W.. Photocatalytic activity of WOx-TiO_2 under visible light irradiation. Journal of Photochemistry and Photobiology A: Chemistry, 141(2-3), **(2001)**, 209-217.

Li, Z., Han, B., Yu, X., Dong, S., Zhang, L., Dong, X., Ou, J.. Effect of nano-titanium dioxide on mechanical and electrical properties and microstructure of reactive powder concrete. Materials Research Express, 4(9), **(2017)**, 095008.

Ma, B., Li, H., Li, X., Mei, J. ve Lv, Y.. Influence of nano-TiO_2 on physical and hydration characteristics of fly ash–cement systems. Construction and Building Materials, 122, **(2016)**, 242-253.

Ma, B., Li, H., Mei, J., Li, X. ve Chen, F.. Effects of Nano-TiO_2 on the Toughness and Durability of Cement-Based Material. Advances in Materials Science and Engineering, vol., 1-10, **(2015)**.

Ma, H., & Li, Z.. Microstructures and mechanical properties of polymer modified mortars under distinct mechanisms. Construction and Building Materials, 47, **(2013)**, 579-587.

Ma, H., Tian, Y., & Li, Z.. Interactions between organic and inorganic phases in PA-and PU/PA-modified-cement-based materials. Journal of materials in civil engineering, 23(10), **(2011)**, 1412-1421.

Maggos, T., Bartzis, J., Leva, P. ve Kotzias, D.. Application of photocatalytic technology for NOx removal. Applied Physics A, 89(1), **(2007)**, 81-84.

Martyanov, I. N. and Klabunde, K. J.. Photocatalytic Oxidation of Gaseous 2-Chloroethyl Ethyl Sulfide over TiO_2. Environmental Science and Technology,37(15), **(2003)**, 3448-3453.

Melo, J. V., Trichês, G., Gleize, P. J. ve Villena, J.. Development and evaluation of the efficiency of photocatalytic pavement blocks in the laboratory and after one year in the field. Construction and Building Materials, 37, **(2012)**, 310-319.

Mendoza, O., Sierra, G., & Tobón, J. I.. Influence of super plasticizer and $Ca(OH)_2$ on the stability of functionalized multi-walled carbon nanotubes dispersions for cement composites applications. Construction and Building Materials, 47, **(2013)**, 771-778.

Mohseni, E., Miyandehi, B. M., Yang, J., & Yazdi, M. A.. Single and combined effects of nano-SiO2, nano-Al_2O_3 and nano-TiO2 on the mechanical, rheological and durability properties of self-compacting mortar containing fly ash. Construction and Building Materials, 84, **(2015)**, 331-340.

Moore, V. C., Strano, M. S., Haroz, E. H., Hauge, R. H., Smalley, R. E., Schmidt, J., & Talmon, Y.. Individually suspended single-walled carbon nanotubes in various surfactants. Nano letters, 3(10), **(2003)**, 1379-1382.

Musso, S., Tulliani, J. M., Ferro, G., & Tagliaferro, A.. Influence of carbon nanotubes structure on the mechanical behavior of cement composites. Composites Science and Technology, 69(11-12), **(2009)**, 1985-1990.

Nazari, A. and Riahi, S.. Abrasion resistance of concrete containing SiO_2 and Al_2O_3 nanoparticles in different curing media. Energy and Buildings, 43(10), **(2011a)**, 2939-2946.

Nazari, A. and Riahi, S.. Corrigendum to "The effect of TiO_2 nanoparticles on water permeability and thermal and mechanical properties of high strength self compacting concrete". Materials Science and Engineering: A, 528(9), **(2011b)**, 3526.

Nazari, A. and Riahi, S.. The Effects of TiO_2 Nanoparticles on Flexural Damage of Self-compacting Concrete. International Journal of Damage Mechanics, 20(7), **(2011d)**, 1049-1072.

Nazari, A. and Riahi, S.. TiO_2 nanoparticles effects on physical, thermal and mechanical properties of self-compacting concrete with ground granulated blast furnace slag as binder. Energy and Buildings,43(4), **(2011c)**, 995-1002.

Negim, E. S. R., Bekbayeva, N., Akmaral, L., Herki, U., Merey, B. M., Rinat, N., & I Yeligbayeva, G.. Effect of methyl cellulose/poly (acrylic acid) blends on physico-mechanical properties of Portland cement pastes. Oriental Journal of Chemistry, 33(1), **(2017)**, 450-457.

Nishikawa, H. ve Takahara, Y.. Adsorption and photocatalytic decomposition of odor compounds containing sulfur using TiO2/SiO2 bead. Journal of Molecular Catalysis A: Chemical, 172(1-2), **(2001)**, 247-251.

Nochaiya, T., and Chaipanich, A.. Behavior of multi-walled carbon nanotubes on the porosity and microstructure of cement-based materials. Applied Surface Science, 257(6), **(2011)**, 1941-1945.

Noorvand, H., Ali, A. A., Demirboga, R., Farzadnia, N. ve Noorvand, H.. Incorporation of nano TiO_2 in black rice husk ash mortars. Construction and Building Materials, 47, **(2013)**, 1350-1361.

Ohama, Y. and Van Gemert, D.. Applications of Titanium Dioxide Photocatalysis to Construction Materials: State-of-the-Art Report of the RILEM Technical Committee 194-TDP. **(2011)**

Ohtani, B., Prieto-Mahaney, O., Li, D. ve Abe, R.. What is Degussa (Evonik) P25? Crystalline composition analysis, reconstruction from isolated pure particles and photocatalytic activity test. Journal of Photochemistry and Photobiology A: Chemistry, 216(2-3), **(2010)**, 179-182.

Othman, S. H., Rashid, S. A., Ghazi, T. I. M., & Abdullah, N.. Dispersion and stabilization of photocatalytic TiO_2 nanoparticles in aqueous suspension for coatings applications. Journal of Nanomaterials, 2, **(2012)**.

Poon, C. S., and Cheung, E.. NO removal efficiency of photocatalytic paving blocks prepared with recycled materials. Construction and Building Materials, 21(8), **(2007)**, 1746-1753.

Qamar, M., Muneer, M. ve Bahnemann, D.. Heterogeneous photocatalysed degradation of two selected pesticide derivatives, triclopyr and daminozid in aqueous suspensions of titanium dioxide. Journal of Environmental Management, 80, **(2006)**, 99-106.

Rahim, A. and Nair, S. R.. Influence of nano-materials in high strength concrete. Journal of Chemical and Pharmaceutical Sciences, 974, **(2016)**, 15–21.

Ren, H., Koshy, P., Chen, W. F., Qi, S., & Sorrell, C. C.. Photocatalytic materials and technologies for air purification. Journal of Hazardous Materials, 325, **(2017)**, 340-366.

Ruot, B., Plassais, A., Olive, F., Guillot, L. Bonafous, L.. TiO_2-containing cement pastes and mortars: Measurements of the photocatalytic efficiency using a rhodamine B-based colourimetric test. Solar Energy, 83(10), **(2009)**, 1794-1801.

Saafi, M., Andrew, K., Tang, P. L., McGhon, D., Taylor, S., Rahman, M., Zhou, X.. Multifunctional properties of carbon nanotube/fly ash geopolymeric nanocomposites. Construction and Building Materials, 49, **(2013)**, 46-55.

Salemi, N., Behfarnia, K. ve Zaree, S.A.. Effect of nanoparticles on frost durability of concrete. Asian Journal of Civil Engineering, 15(3), **(2014)**, 411–20.

Salman, M., Eweed, K.M. ve Hameed, M.. Influence of partial replacement TiO_2 nanoparticles on the compressive and flexural strength of ordinary cement mortar. Al-Nahrain Journal for Engineering Sciences, 19(2), **(2017)**, 265–70.

Saquib, M.. TiO_2-mediated photocatalytic degradation of a triphenylmethane dye (gentian violet), in aqueous suspensions. Dyes and Pigments, 56(1), **(2003)**, 37-49.

Sarker, P. K., Haque, R. ve Ramgolam, K. V.. Fracture behaviour of heat cured fly ash based geopolymer concrete. Materials and Design, 44, **(2013)**, 580-586.

Sato, K., Li, J. G., Kamiya, H., & Ishigaki, T.. Ultrasonic dispersion of TiO_2 nanoparticles in aqueous suspension. Journal of the American Ceramic Society, 91(8), **(2008)**, 2481-2487.

Sayılkan, F., Asiltürk, M., Tatar, P., Kiraz, N., Arpaç, E. ve Sayılkan, H.. Photocatalytic performance of Sn-doped TiO_2 nanostructured mono and double layer thin films for

Malachite Green dye degradation under UV and vis-lights. Journal of Hazardous Materials, 144(1-2), **(2007)**, 140-146.

Schindler, K. M. and Kunst, M.. Charge-Carrier Dynamics in TiO_2 Powders. Journal of Physical Chemistry, 94(21), **(1990)**, 8222-8226.

Schokker, A. J.. The Sustainable Concrete Guide - Strategies and Examples. Farmington Hills, MI: U.S. Green Concrete Council. **(2010)**

Seo, D., & Yun, T. S.. NOx removal rate of photocatalytic cementitious materials with TiO2 in wet condition. Building and Environment, 112, **(2017)**, 233-240.

Shekari, A. H. and Razzaghi, M. S.. Influence of nano particles on durability and mechanical properties of high performance concrete, Procedia Engineering, 14, **(2011)**, 3036–3041.

Sobolkina, A., Mechtcherine, V., Khavrus, V., Maier, D., Mende, M., Ritschel, M., & Leonhardt, A.. Dispersion of carbon nanotubes and its influence on the mechanical properties of the cement matrix. Cement and Concrete Composites, 34(10), **(2012)**, 1104-1113.

Spragg, R., Bu, Y., Snyder, K., Bentz, D., & Weiss, J.. Electrical testing of cement-based materials: role of testing techniques, sample conditioning, and accelerated curing, Publication FHWA/IN/JTRP-2013/28. Joint Transportation Research Program, Indiana Department of Transportation and Purdue University, West Lafayette, Indiana, **(2013)**. http://dx.doi.org/10.5703/1288284315230.

Su, R., Bechstein, R., Sø, L., Vang, R. T., Sillassen, M., Esbjörnsson, B. ve Besenbacher, F. **(2011)**. How the Anataz-to-Rutil Ratio Influences the Photoreactivity of TiO_2. The Journal of Physical Chemistry C, 115(49), 24287-24292.

Sugrañez, R., Álvarez, J. I., Cruz-Yusta, M., Mármol, I., Morales, J., Vila, J., & Sánchez, L. **(2013)**. Enhanced photocatalytic degradation of NOx gases by regulating the microstructure of mortar cement modified with titanium dioxide. Building and Environment, 69, 55-63.

Teizer, J., Venugopal, M., Teizer, W. ve Felkl, J.. Nanotechnology and its impact on construction: bridging the gap between researchers and industry professionals. Journal of Construction Engineering and Management, 138(5), **(2011)**, 594-604.

Theivasanthi, T., and Alagar, M.. Titanium dioxide (TiO_2) nanoparticles XRD analyses: an insight. arXiv preprint arXiv:1307.1091, **(2013).**

Tian, Y., Jin, X. Y., Jin, N. G., Zhao, R., Li, Z. J., & Ma, H. Y.. Research on the microstructure formation of polyacrylate latex modified mortars. Construction and Building Materials, 47, **(2013)**, 1381-1394.

Tristantini, D., and Mustikasari, R.. Modification of TiO2 nanoparticle with PEG and SiO_2 for anti-fogging and self-cleaning application. International Journal of Engineering & Technology, 11(2), **(2011)**, 73-78.

Tyson, B. M., Al-Rub, R. K. A., Yazdanbakhsh, A., Grasley, Z.. A quantitative method for analyzing the dispersion and agglomeration of nano-particles in composite materials. Composites Part B: Engineering, 42(6), **(2011)**, 1395-1403.

Tyson, B. M., Al-Rub, R. K. A., Yazdanbakhsh, A., Grasley, Z.. A quantitative method for analyzing the dispersion and agglomeration of nano-particles in composite materials. Composites Part B: Engineering, 42(6), **(2011)**, 1395-1403.

Wang, C., Zhang, Z., Ying, J. Y.. Photocatalytic decomposition of halogenated organics over nanocrystalline titania. Nanostructured Materials, 9(1-8), **(1997)**, 583-586.

Wang, F., Sun, G., Zhang, W., Yang, L. and Liu, P.. Performance of photocatalytic cementitious material: Influence of substrate surface microstructure. Construction and Building Materials, 110, **(2016)**, 175-181.

Wang, S., Ang, H., Tade, M. O.. Volatile organic compounds in indoor environment and photocatalytic oxidation: State of the art. Environment International, 33(5), **(2007)**, 694-705.

Wang, S., Chen, T., Chen, R., Hu, Y., Chen, M., & Wang, Y.. Emodin loaded solid lipid nanoparticles: preparation, characterization and antitumor activity studies. International journal of pharmaceutics, 430(1-2), **(2012)**, 238-246.

Wang, X., Wang, K., Tanesi, J., & Ardani, A.. Effects of nanomaterials on the hydration kinetics and rheology of Portland cement pastes. Advances in Civil Engineering Materials, 3(2), **(2014)**, 142-159.

Xie, Y., Yuan, C.. Photocatalysis of neodymium ion modified TiO_2 sol under visible light irradiation. Applied Surface Science, 221(1-4), **(2004)**, 17-24.

Xiong, G., Deng, M., Xu, L., Tang, M.. Properties of Cement-Based Composites by Doping Nano-TiO2. Journal-Chinese Ceramic Society, 34(9), **(2006)**, 1158.

Xu, M., Clack, H., Xia, T., Bao, Y., Wu, K., Shi, H., & Li, V.. Effect of TiO_2 and fly ash on photocatalytic NOx abatement of engineered cementitious composites. Construction and Building Materials, 236, **(2020)**, 117559.

Yang, L., Jia, Z., Zhang, Y., Dai, J.. Effects of nano-TiO_2 on strength, shrinkage and microstructure of alkali activated slag pastes. Cement and Concrete Composites, 57, **(2015)**, 1-7.

Yang, R., Wang, M., Shen, Z., Wang, W., Ma, H. ve Gu, J.. The degradation and mineralization of 4-chlorophenol in aqueous solutions by electron beam irradiation in the presence of TiO_2 nanoparticles. Radiation Physics and Chemistry, 76(7), **(2007)**, 1122-1125.

Yazdanbakhsh, A., Grasley, Z., Tyson, B., & Al-Rub, R. K. A.. Dispersion quantification of inclusions in composites. Composites Part A: Applied Science and Manufacturing, 42(1), **(2011)**, 75-83.

Yousefi, A., Allahverdi, A., Hejazi, P.. Effective dispersion of nano-TiO_2 powder for enhancement of photocatalytic properties in cement mixes. Construction and Building Materials, 41, **(2013)**, 224-230

Yousefi, A., Muhamad Bunnori, N., Khavarian, M., & Majid, T. A.. Dispersion of Multi-Walled Carbon Nanotubes in Portland Cement Concrete Using Ultra-Sonication and Polycarboxylic Based Superplasticizer. In Applied Mechanics and Materials (Vol. 802, pp. 112-117). Trans Tech Publications Ltd. **(2015)**

Yuan, Z., Li, B., Zhang, J., Xu, C., Ke, J.. Synthesis of TiO_2 thin film by a modified sol-gel method and properties of the prepared films for photocatalyst. Journal of sol-gel science and technology, 39(3), **(2006)**, 249-253.

Zhang, M. H., & Islam, J.. Use of nano-silica to reduce setting time and increase early strength of concretes with high volumes of fly ash or slag. Construction and Building Materials, 29, **(2012)**, 573-580.

Zhang, M. H., Islam, J., & Peethamparan, S.. Use of nano-silica to increase early strength and reduce setting time of concretes with high volumes of slag. Cement and Concrete Composites, 34(5), **(2012)**, 650-662.

Zhang, Q. , Gao, L. and Guo, J.. Effects of Calcination on the Photocatalytic Properties of Nanosized TiO2 Powders Prepared by TiCl4 Hydrolysis. Applied Catalysis B: Environmental. 26., **(2000)**, 207-215.

Zhang, Q., Joo, J. B., Lu, Z., Dahl, M., Oliveira, D. Q., Ye, M., & Yin, Y.. Self-assembly and photocatalysis of mesoporous TiO_2 nanocrystal clusters. Nano Research, 4(1), **(2011)**, 103-114.

Zhang, R., Cheng, X., Hou, P. ve Ye, Z.. Influences of nano-TiO_2 on the properties of cement-based materials: Hydration and drying shrinkage. Construction and Building Materials, 81, **(2015)**, 35-41.

Zhao, J., & Yang, X.. Photocatalytic oxidation for indoor air purification: a literature review. Building and environment, 38(5), **(2003)**, 645-654.

Zhao, Y., Li, C., Liu, X., Gu, F.. Highly enhanced degradation of dye with well-dispersed TiO_2 nanoparticles under visible irradiation. Journal of Alloys and Compounds, 440(1-2), **(2007)**, 281-286.

Zivica, V. and Bajza, A.. Acidic attack of cement-based materials - a review. Construction and Building Materials,15(8), **(2001)**, 331-340.

Znaidi, L., Seraphimova, R., Bocquet, J., Colbeau-Justin, C. ve Pommier, C.. Continuous process for the synthesis of nano-size TiO_2 powders and their use as photocatalysts Materials Reearch. Bulletin, 36(5–6), **(2001)**, 811–825.